121

M.O. 682

AIR MINISTRY

METEOROLOGICAL OFFICE

Scientific Paper No. 5

An Experiment in Numerical Forecasting

by E. KNIGHTING, B.Sc., G. A. CORBY, B.Sc.,
F. H. BUSHBY, B.Sc., and C. E. WALLINGTON, M.Sc.

LONDON: HER MAJESTY'S STATIONERY OFFICE
FIVE SHILLINGS NET

M.O. 682

AIR MINISTRY
METEOROLOGICAL OFFICE

Scientific Paper No. 5

An Experiment in Numerical Forecasting

by E. KNIGHTING, B.Sc., G. A. CORBY, B.Sc.,
F. H. BUSHBY, B.Sc. and C. E. WALLINGTON, M.Sc.

LONDON
HER MAJESTY'S STATIONERY OFFICE
1961

U.D.C. 551·509·313:
551·509: 681·14

Contents

An Experiment in Numerical Forecasting

by E. Knighting, B.Sc., G. A. Corby, B.Sc., F. H. Bushby, B.Sc., and C. E. Wallington, M.Sc.

INTRODUCTION

The Meteorological Office electronic computer, a Ferranti Mercury machine, known as METEOR, was installed at the Napier Shaw Laboratory during the winter 1958–1959 and became available for regular use as from 12 January 1959. Experience on a similar machine at Manchester University had been gained previously and programmes had been developed in readiness for experiments in numerical forecasting, using the Sawyer–Bushby two-level model. Methods of automatic data extraction and analysis by the machine had also been developed but as these methods had only been tested superficially it was decided to compute each forecast twice, once based on the analysis carried out within the computer and once based on the subjective analysis prepared conventionally in the Forecast Division. The aims of the experiment were twofold:

(i) To establish the standard of forecasting which could be achieved with the two-level model, for comparison with the standard of conventional forecasts and that of other numerical forecasting models, and

(ii) To provide a trial of the technique of data extraction and objective analysis.

Forecasts were made daily from Tuesday to Friday, based on the 0000 GMT data, analysed both within the machine and conventionally. Additionally a 24-hour forecast based on subjective initial data was made on Mondays to provide preliminary estimates of the fields for Tuesday's machine analysis, and also a machine analysis was carried out for Saturday to permit verification of the forecast made on Friday. This first experiment commenced on 20 January 1959 and was terminated on 12 May 1959 by which time complete results had been obtained for 42 cases. A further series of analyses and forecasts were computed during the period 27 July to 13 November 1959. This second experiment yielded 50 cases with complete results.

Computing commenced at 0830 GMT and the complete experiment for one day, comprising a 36-hour forecast based on subjective initial fields, also the machine extraction and analysis of data followed by a 36-hour forecast based on the machine analysis, was usually completed by about 1100 GMT. The experiments and the results obtained are described in the following sections of this report.

THE MODEL ATMOSPHERE USED IN THE EXPERIMENTS

Basic assumptions

The model used was basically that described by Sawyer and Bushby[1]*. It consists of a baroclinic fluid in which the thermal wind is constant in direction in any vertical column,

* Superscript figures refer to Bibliography on p. 53.

but not necessarily parallel to the wind direction at any particular level. The thermal wind speed is proportional to the pressure difference through the layer concerned. The atmosphere is considered to be bounded by two pressure surfaces, one $p = p_o$ near the ground and one $p = p_1$ near the tropopause, across which the flow of air is assumed to be negligible. The geostrophic approximation is used and a parabolic relationship is assumed between vertical motion and pressure. The vertical motion is denoted by $\varpi = dp/dt$, the maximum value being ϖ_m. Furthermore, in our experiments the non-adiabatic effect of heating of cold air over a warm sea was incorporated as suggested by Bushby and Hinds[2], but the vertical advection of vorticity was neglected in the equation for the mean motion of the atmosphere, since this term has been shown by Jones[3] and Arnason and Carstensen[4] to produce spurious cyclogenesis in the model.

The equations

It is convenient to represent the surface of the northern hemisphere by a stereographic projection from the south pole on to a plane perpendicular to the earth's axis and passing through the north pole. The prognostic equations which are used can then be written:

$$\nabla^2 \frac{\partial h_m}{\partial t} + J(h_m, \beta^2 g f^{-1} \nabla^2 h_m + f) + \tfrac{1}{4} J(h', \beta^2 g f^{-1} \nabla^2 h') = 0 \qquad (1)$$

$$\nabla^2 \frac{\partial h'}{\partial t} + J(h_m, \beta^2 g f^{-1} \nabla^2 h') + J(h', \beta^2 g f^{-1} \nabla^2 h_m + f) + \frac{4g(\nabla^2 h_m + f^2 \beta^{-2} g^{-1})\{\beta^2 g f^{-1} J(h_m, h') - Q + \partial h'/\partial t\}}{R A \Gamma_p (p_o - p_1)} = 0 \qquad (2)$$

$$\frac{\partial h'}{\partial t} = \beta^2 g f^{-1} J(h', h_m) - \frac{R A \Gamma_p \varpi_m}{g} + Q = 0 \qquad (3)$$

$$H_1 = H_o + \left(\frac{\partial H}{\partial t}\right)_o \delta t \qquad (4)$$

$$H_{r+1} = H_{r-1} + 2\left(\frac{\partial H}{\partial t}\right)_r \delta t \qquad (5)$$

where

h_m = the height of the central level of our model

h' = the thickness of the layer from the bottom to the central pressure level

∇^2 = the two-dimensional Laplacian operator referred to rectangular Cartesian coordinates

J = the Jacobian operator referred to the same coordinates

β = the magnification factor of the chart $= \sec^2\left(\frac{\pi}{4} - \frac{\theta}{2}\right)$, θ being the geographical latitude

f = Coriolis parameter

g = acceleration due to gravity

Q = the non-adiabatic rate of heating due to cold air over warm sea

R = gas constant

Γ_p = a measure of the departure of the lapse rate from the adiabatic given by $\Gamma_p = \frac{\partial T}{\partial p} - \frac{\gamma}{g\rho}$, T being the temperature, γ the appropriate wet or dry adiabatic lapse rate and ρ the density

$$A = \frac{p_o + 3p_1}{2(p_o - p_1)} - \frac{4p_o p_1}{(p_o - p_1)^2} \log_e \frac{2p_o}{p_o + p_1}$$

H_r = h' or h_m at time $t + r\delta t$

$$\left(\frac{\partial H}{\partial t}\right)_r = \frac{\partial h'}{\partial t} \text{ or } \frac{\partial h_m}{\partial t} \text{ at time } t + r\delta t.$$

In the experiments we made $p_o = 1000$ and $p_1 = 200$ millibars. Thus h_m and h' represented the height of the 600-millibar contour surface and the 1000–600 millibar thickness respectively. Since information is more readily available for the height of the 500-millibar surface (h_{500}) and the thickness of the 1000–500 millibar layer (h'_{500}), it was decided to derive the initial values of h' and h_m from those of h'_{500} and h_{500} from the equations:

$$h' = \tfrac{4}{5} h'_{500} \quad . \quad . \quad . \quad (6)$$

$$\text{and } h_m = h_{500} - \tfrac{1}{5} h'_{500} \quad . \quad . \quad . \quad (7)$$

At the end of the forecast h'_{500} and h_{500} were obtained from h' and h_m through the same equations.

The empirical relationship for the non-adiabatic heating of the air over the sea took the form used by Bushby and Hinds[2], that is

$$Q = 2{\cdot}068 \times 10^{-2}\{129(T_s + 282{\cdot}5) - h'\}\text{m hr}^{-1}, \quad . \quad . \quad . \quad (8)$$

for computed positive values of Q; negative values of Q were treated as zero. Here T_s is the monthly mean surface temperature (°F), and h' is in metres. No heating term was applied over the land areas.

Method of solution

The above set of equations was solved for a rectangular grid of 24 × 20 points (see Figure 1), the grid length being approximately 200 statute miles at the north pole. The grid is not quite rectangular in Figure 1 since the working charts at present in use are not based on a stereographic projection.

The finite difference approximations used were as follows:

$$\nabla^2 z = \frac{1}{a^2}\left(\sum_1^4 z_i - 4z_o\right) \quad . \quad . \quad . \quad (9)$$

$$J(u, v) = \frac{1}{4a^2}\Big\{(u_1 - u_3)(v_2 - v_4) - (u_2 - u_4)(v_1 - v_3)\Big\}, \quad . \quad . \quad . \quad (10)$$

where a is the grid length and the suffixes refer to the points indicated in Figure 2.

In order to obtain a solution of equations (1), (2), (4) and (5) for h_m and h' at any time $t + r\delta t$, it is sufficient to know h_m and h' at all grid points at time t, and at the two outer rings of points for all time from t to $t + r\delta t$. Values at the latter two rings of points were assumed to remain constant during the forecast period.

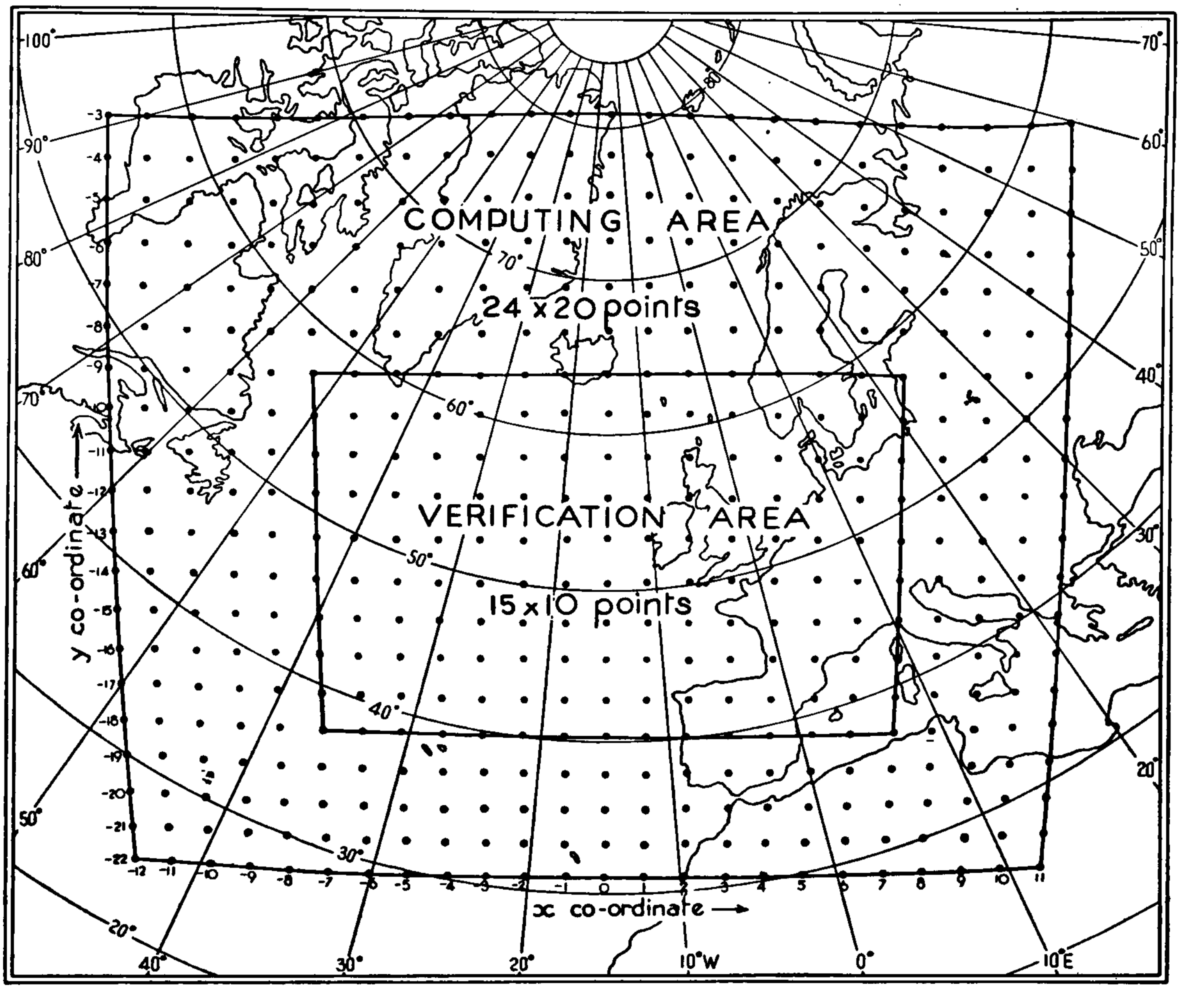

FIGURE 1. Computing grid for numerical forecasting experiment.

The grid points form a square network on a stereographic projection from the south pole on to a plane perpendicular to the earth's axis.

Grid length $=88{\cdot}1412\ (1+\sin\phi)$ nautical miles, where ϕ is the latitude
$=176$ n.m. (325 km) at north pole
$=164$ n.m. (303 km) at 60°N
$=132$ n.m. (244 km) at 30°N.

The initial values of h_m and h' at time t can be obtained by interpolating by eye from a set of isopleths representing the fields of those quantities. Since both conventional analysis and interpolation by eye are subjective processes, this method of obtaining the data will be referred to as the subjective method. An alternative objective method is described later (page 5). These values have to be written down and then punched on to paper tape ready to be fed to the computer. There are obviously sources of error in this process, and therefore the following smoothness check was imposed on both sets of data before commencing the calculation:

$$4z_0 - 2\sum_{1}^{4} z_i + \sum_{5}^{8} z_i \leqslant 128\text{m}. \qquad (11)$$

If this criterion was not satisfied at any point, the data were checked in the vicinity of that point, and any necessary corrections made.

Equations (1) and (2) were solved for $\partial h_m/\partial t$ and $\partial h'/\partial t$ respectively by the Liebmann iterative process using over-relaxation. This process starts from a preliminary guess at the solution. For the first time-step no good guess was available and, using zero at all the grid points as the guess, about 30 iterations were commonly required to achieve a solution of equation (1). At subsequent time-steps a good estimate of the solution was available in the form of the solution derived for the previous time-step and then three iterations were usually sufficient.

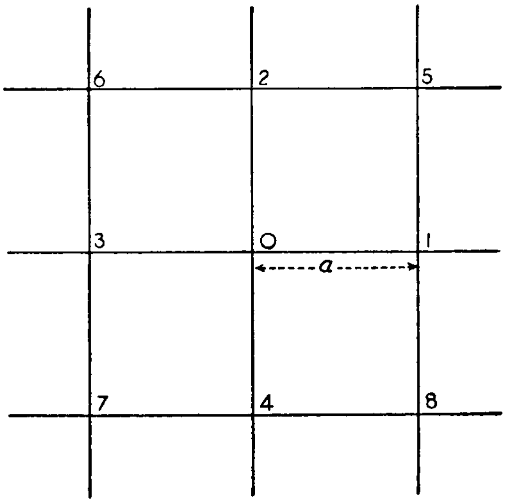

FIGURE 2. Suffix notation relative to origin, O

The length of the time-step was initially chosen as one hour, but as this occasionally led to computational instability, it was shortened to $\frac{3}{4}$ hour. Thus a 36-hour forecast consisted of 48 time-steps and the total computing time per forecast was 35–40 minutes including the input of instructions and data to the computer and the output of results.

THE OBJECTIVE ANALYSIS

The basic method

To carry out a numerical forecast with the model adopted for the experiment, the computer required as initial data the 500-millibar contour and 1000–500 millibar thickness fields, expressed in the form of values at the grid points (numbering 480 in our case). When the fields were analysed objectively within the machine, these values were obtained by interpolation between the observations. Assuming that the observations had been placed in the computer's memory (see *Automatic data extraction*, page 8), the method used was essentially that described by Bushby and Huckle[5]. Briefly, each grid point was dealt with individually and a quadric surface of the form

$$h_s = ax^2 + by^2 + 2hxy + 2gx + 2fy + c \qquad (12)$$

was fitted by least squares to the observations within the vicinity of each grid point. Here h_s is identified with the 500-millibar height or 1000–500 millibar thickness and x, y are position coordinates on the grid. By means of the geostrophic approximation we can obtain an estimate of the slope of the surface in the vicinity of each wind observation and it was therefore possible to arrange for wind as well as height observations to play a part in determining the quadric of best fit to the observations. Furthermore, in order to introduce an element of time continuity into the analysis and to ensure a solution in regions of sparse data, a forecast field also contributed to the quadric surface. On this basis the expression which was minimized to determine the quadric took the form:

$$E = \Sigma p(h_s - h_o)^2 + T^2 \Sigma p(\mathbf{V}_s - \mathbf{V}_o)^2 + \Sigma q(h_s - h_f)^2 \quad . \quad . \quad . \ (13)$$

where p, q are distance weighting functions of the form $a/(1+br^4)$, r being the distance between observation and grid point,

h_s, $\mathbf{V}_s$ are the height and geostrophic wind given by the quadric, equation (12),

h_o, $\mathbf{V}_o$ are observed values of height and wind,

h_f is a forecast height at a grid point,

T^2 is a parameter chosen to give a suitable weight to the wind observations relative to the heights.

Values of p, q, T^2 as determined previously from experiments described by Bushby and Huckle[5] were used in the present work. The quadric of best fit was found by forming and solving the six linear equations

$$\frac{\partial E}{\partial a} = \frac{\partial E}{\partial b} = \frac{\partial E}{\partial h} = \frac{\partial E}{\partial g} = \frac{\partial E}{\partial f} = \frac{\partial E}{\partial c} = 0$$

obtained by partial differentiation of equation (13).

The elimination of erroneous observations

The observations inevitably contained errors of transmission, coding, etc., and for the first experiment the machine was programmed so that before the computation of the analysis commenced, certain tests of the data were applied by the computer. The tests comprised a simple comparison between the observed heights and winds and values at the same positions interpolated from the forecast field, using the geostrophic approximation to obtain estimates of the wind. The computer was programmed to print out particulars of those observations which differed from the forecast field by more than some specified limit. Such doubtful observations were then examined, and an opinion formed as to their correctness or otherwise. The facilities of the programme were then exploited to erase, or if possible correct, the erroneous observations in the computer's memory.

Experience with this procedure suggested that gross errors in the observations were successfully detected in the majority of cases. However, the forecast field used for the purpose was normally the 24-hour numerical forecast computed on the previous day and in regions where this forecast was substantially in error, the procedure necessitated the examination of many observations most of which were then wrongly indicated by the computer as suspect. Furthermore, the method could not be applied to observations outside the boundary of the grid.

In order to overcome at least some of these disadvantages and to avoid human intervention in a machine computation, which is generally inefficient, an attempt was made during the second experiment to render the treatment of erroneous observations automatic. In the scheme adopted an analysis was carried out within the machine using all the observations without any checks of the data being applied except for those carried out during the automatic extraction of the data (see page 8). On completion of this stage the computer was made to test the observations against this first analysis and to suppress those observations of 500-millibar height, 1000–500 millibar thickness, 500-millibar wind or 1000–500 millibar thermal wind which differed by more than specified criteria from those implicit in the first analysis. The computer was then made to repeat the analysis without using the bad observations. This technique for detecting spurious data relies on the fact that the analysis in the vicinity of a bad observation leans heavily towards good observations in the same area. If, however, the bad observation was an isolated one the process would only detect this if the error were a very gross one. For this reason the process was not used to deal with observations from ocean weather ships, these being subjected to careful (human) scrutiny before input to the computer. The process was found to be satisfactory in practice.

The analysis computation (upper air data)

In the machine analysis of the upper air data, the observations from upwards of 200 stations were used including a selection of those within six grid lengths outside the boundary of the grid. Subject to the elimination of erroneous observations as indicated above, the analysis computation proceeded as follows. Each grid point was dealt with individually, commencing with the top left point and working systematically through the grid. The six nearest observations within six grid lengths of each grid point were selected, and the coefficients of the equations determining the quadrics of best fit to these 500-millibar contour and 1000–500 millibar thickness observations were formed. The equations were solved and the values given by the quadrics at the grid point in question were taken to be the contour height and thickness at the point. Sometimes there were, naturally, less than six observations within six grid lengths of the point, especially over the ocean, but the inclusion of a forecast field in the fitting process ensured a solution however sparse the data.

One analysis computation of the two fields over 480 grid points occupied the computer for about 11 minutes. This included the output of results but not the variable time taken during the first experiment for the (human) examination of the suspect observations.

During the second experiment, the time taken to test for erroneous observations within the computer was less than one minute but if any were detected and suppressed a second analysis occupying an additional 11 minutes was computed. This extra time was, however, usually considerably less than that required for human examination of suspect observations.

The analysis of surface observations

The analyses produced by the method as so far described were based only on upper air observations. Accordingly where the upper air network was sparse, for example over the Atlantic Ocean, the analyses were unduly smooth and lacking in detail. The human analyst overcomes this difficulty to a considerable extent by exploiting surface observations from ships; about 150 such observations are received for the main synoptic hours. When constructing charts at several levels the human analyst ensures by a graphical technique that his charts have vertical consistency and do not contravene the hydrostatic approximation. This has the effect of improving both the accuracy and the representation of detail in the upper charts over sparse networks. It was clearly desirable that this gridding technique should be simulated in the machine analysis, and this was attempted as follows.

Although too smooth for the reasons given, the difference between the 500-millibar contour and 1000–500 millibar thickness analyses yields a good first guess for the surface

(1000-millibar) field. A machine analysis of the surface observations was therefore carried out by the same technique except that instead of a forecast preliminary field this first guess was used. Thus to obtain a fit for each grid point the expression of equation (13) was minimized for the surface observations using for each forecast value the corresponding value of $(h_{500} - h'_{500})$. The observations comprised all available ship reports of surface pressure and wind for the region, the surface pressures being converted to 1000-millibar heights and the winds being veered and increased empirically to give values appropriate to the top of the friction layer. Furthermore, 1000-millibar heights for a selection of land stations around the Atlantic seaboard were included. The surface analysis was carried out only for the westernmost 18 columns of the grid, the analysis over the remainder of the 24×20 grid, viz. the European sector, having been found to be defined satisfactorily by the upper air data alone. Procedures for the elimination of spurious observations, similar to those described on page 6 for the upper air data, were included in both experiments.

Having determined a revised surface analysis in this way it was next necessary to modify the previously found 500-millibar and thickness analyses so as to achieve vertical consistency with the new and more detailed surface analysis. In the nature of the problem there is no unique procedure for making these adjustments which must necessarily be on a somewhat arbitrary basis. Essentially, the result of the 1000-millibar analysis indicated what changes in the field of $(h_{500} - h'_{500})$ were necessary in order to fit the available surface observations, and the problem was to decide what consequential adjustments should be made to the fields of h_{500} and h'_{500}. It was decided to assign half the change so determined to h_{500} and half to h'_{500}. Thus at a grid point where the new 1000-millibar height was found to be h_o, $\frac{1}{2}\{h_o - (h_{500} - h'_{500})\}$ was added to h_{500} and subtracted from h'_{500}. The adjusted fields so obtained were treated as the final analysis for the numerical forecasts.

AUTOMATIC DATA EXTRACTION

Extraction of upper air information

In order to save time and labour in preparing the necessary data tapes for the machine to carry out the objective analysis of the upper air charts, it was decided to use original telecommunication tapes. The Frankfurt meteorological broadcast was the most suitable since the ABTOP collectives which that broadcast contains provided the basic information necessary for the objective analyses, namely the 500-millibar and 1000-millibar heights and the 500-millibar and 850-millibar winds, $\mathbf{V}_{500}$ and $\mathbf{V}_{850}$. The 1000–500 millibar thickness was easily evaluated, and the 1000–500 millibar thermal wind $\mathbf{V}'$ was evaluated from the relation

$$\mathbf{V}' = 1{\cdot}14(\mathbf{V}_{500} - \mathbf{V}_{850}) \quad . \quad . \quad . \quad (14)$$

The tape was scanned until the heading ABTOP 0000n YYGG was encountered, where n is the highest level in hundreds of millibars in the message, YY is the day of the month and GG is the time of observation. The first five-figure group on each line of the collective was examined to see if it was the block and station number of an observing station. If so, the required information from that station was stored in the machine for use in the objective analysis programme.

Various checks on the data were made; for instance it was clear that if the reported wind direction was greater than 360 degrees an error had occurred and that report was ignored.

Nevertheless, after the experiment had been progressing for a few weeks it was clear that some erroneous data were still being extracted (see page 6) and it was decided to introduce some additional checks at this stage. Each piece of information extracted was checked to see that it was between reasonable limits, and in addition the following hydrostatic check was introduced. An approximation to the thickness was computed from the relationship:

$$h'_{500} = 0{\cdot}73\theta + 561, \qquad (15)$$

where θ is the mean of the 850, 750 and 500-millibar temperatures in degrees Celsius. Any observation where the reported thickness did not lie within seven decametres of this computed value was ignored. These additional checks proved quite satisfactory.

When all the data tapes available for any given day had been scanned by the computer, the computer printed out a list of stations for which no information had been found. This enabled other sources of information to be looked through, and a special tape could then be prepared containing any additional data that was available. The computer took approximately 20 minutes to scan through all the data received via the Frankfurt broadcast from 0000 GMT to 0830 GMT. The computer was then diverted to other work for about half an hour whilst the additional tape was being prepared, before proceeding to the upper air analysis programme described on page 5.

Extraction of surface reports from ships

Reports of temperature, surface pressure and wind, together with latitude and longitude were required from ships on the Atlantic in order to calculate the 1000-millibar analysis (see page 7). A tape containing all available ship collective reports was prepared for us by the Meteorological Communications Centre, Dunstable. The tape was scanned by the machine and the relevant information was extracted. Each report was checked for correct day of the week and time. The wind direction was also checked for feasibility.

THE ACCURACY OF THE ANALYSES

An example of a typical objective analysis, that for 0000 GMT on 28 January 1959, is given in Figure 3(*a*) (1000–500 millibar thickness), Figure 4(*a*) (500-millibar contour height) and Figure 5(*a*) (1000-millibar contour height). For comparison, the corresponding charts as analysed by hand in the Central Forecast Office (CFO) are given in Figures 3(*b*), 4(*b*) and 5(*b*). On these charts isopleths are drawn at intervals of 60 metres on the upper charts and 30 metres on the surface (1000-millibar) charts.

Considering first the thickness chart, Figures 3(*a*) and 3(*b*), it will be seen that there was close agreement between the objective and subjective analyses as regards the placing of the isopleths over Europe and North America. The cold trough over the western Atlantic was also well represented, although both the intensity of the thermal jet and the distortion of the thickness lines in the vicinity of south Greenland were somewhat smoothed out on the objective charts.

On the 500-millibar chart, Figures 4(*a*) and 4(*b*), the most obvious differences occurred near south Greenland where the well marked vortex on the CFO chart appeared only as a trough on the objective analysis, the contour height difference in the centre being about 80 metres. There were also other smaller differences especially in areas of weak gradient, but apart from these the main trough–ridge pattern was well represented.

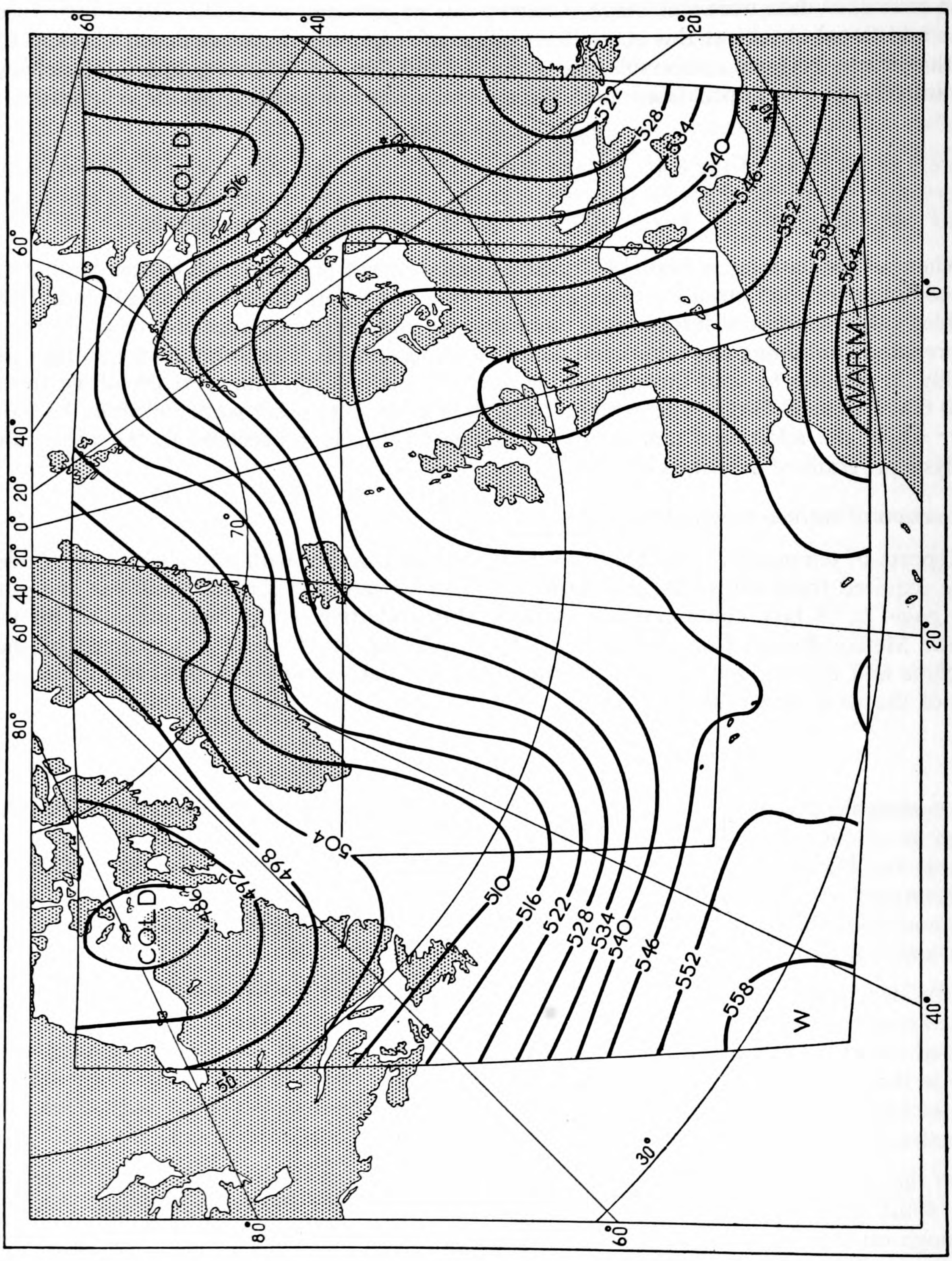

FIGURE 3(*a*). Objective analysis for 0000 GMT, 28 January 1959: 500–1000 millibar thickness in decametres.

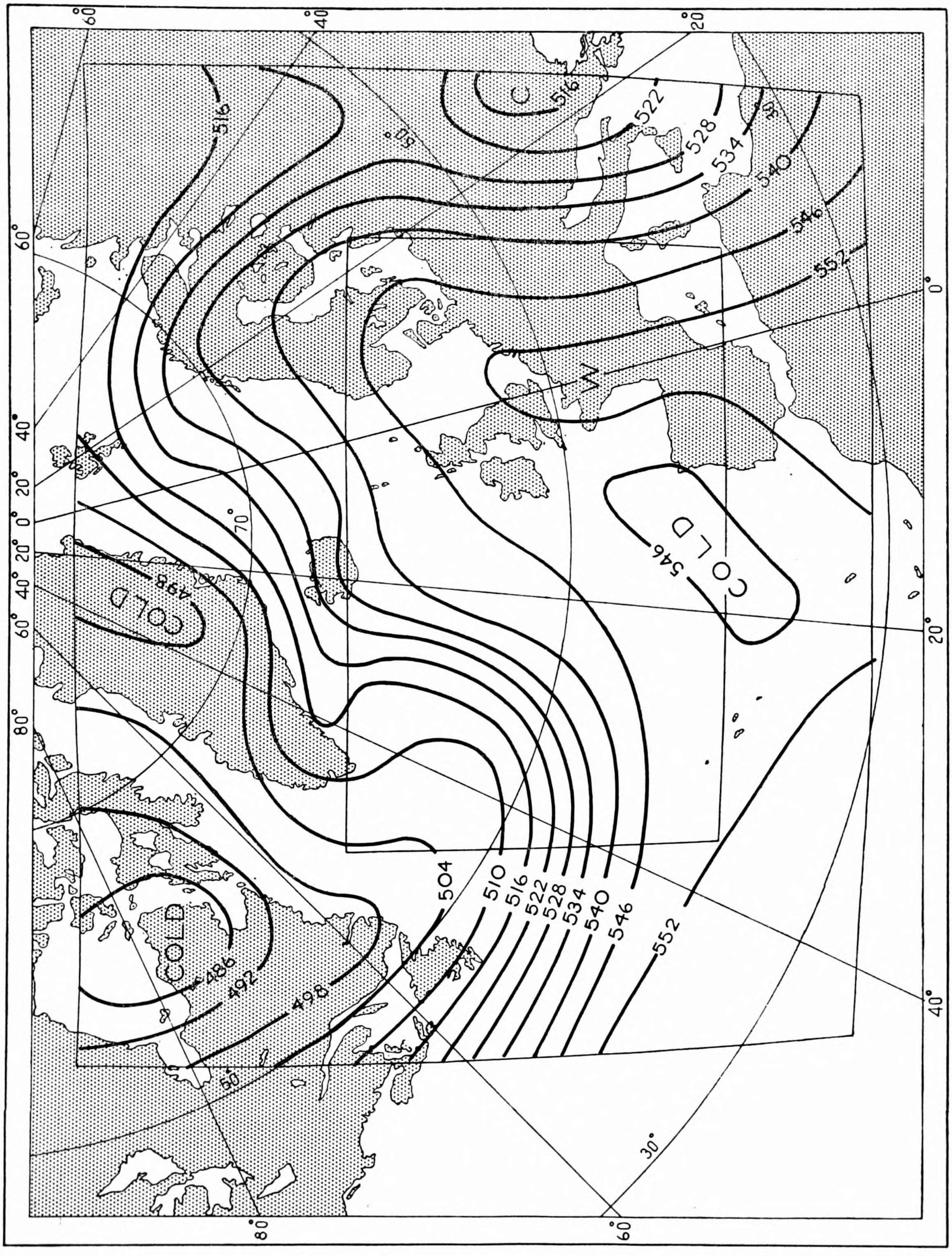

FIGURE 3(*b*). CFO analysis for 0000 GMT, 28 January 1959: 500–1000 millibar thickness in decametres.

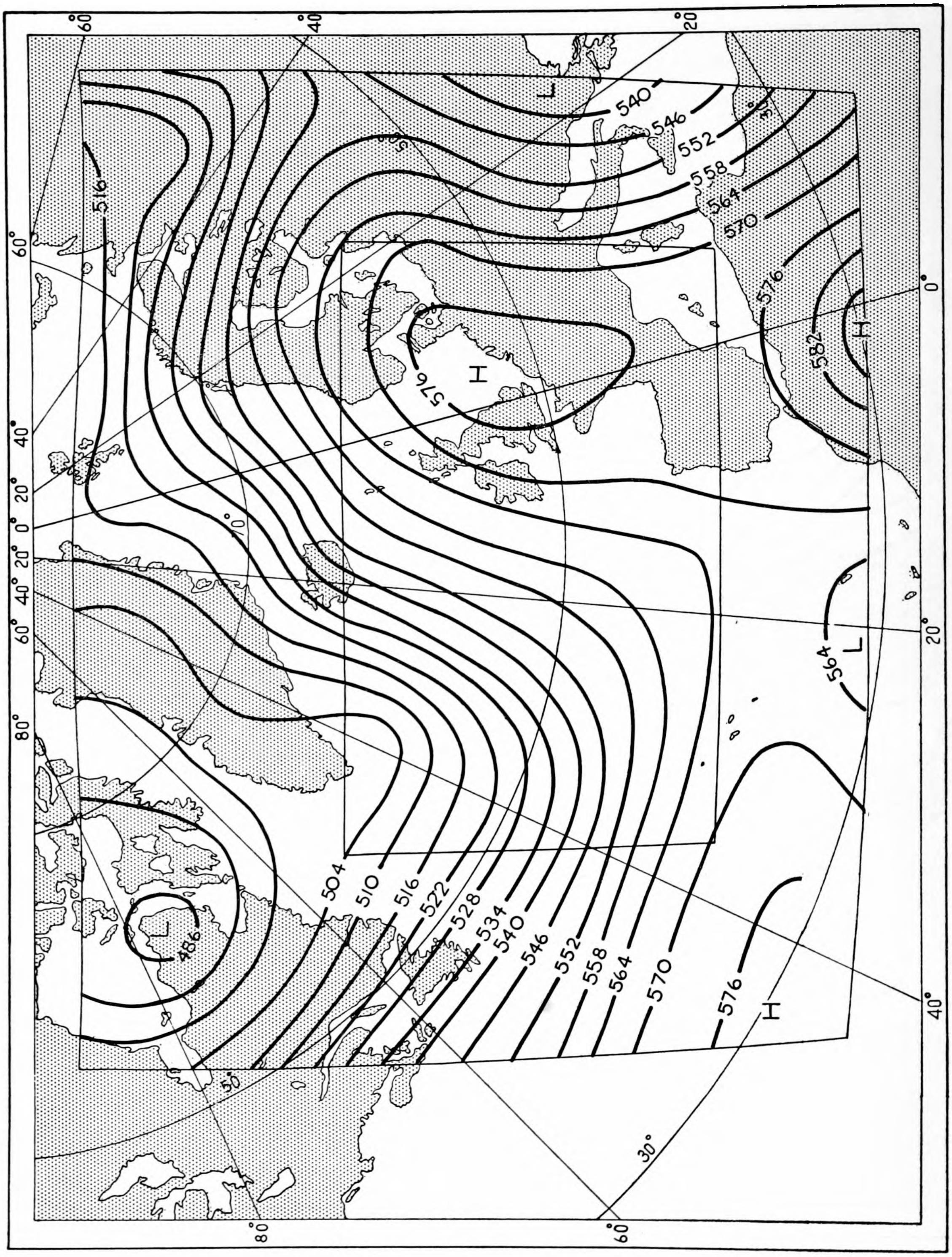

FIGURE 4(*a*). Objective analysis for 0000 GMT, 28 January 1959: 500-millibar contours in decametres.

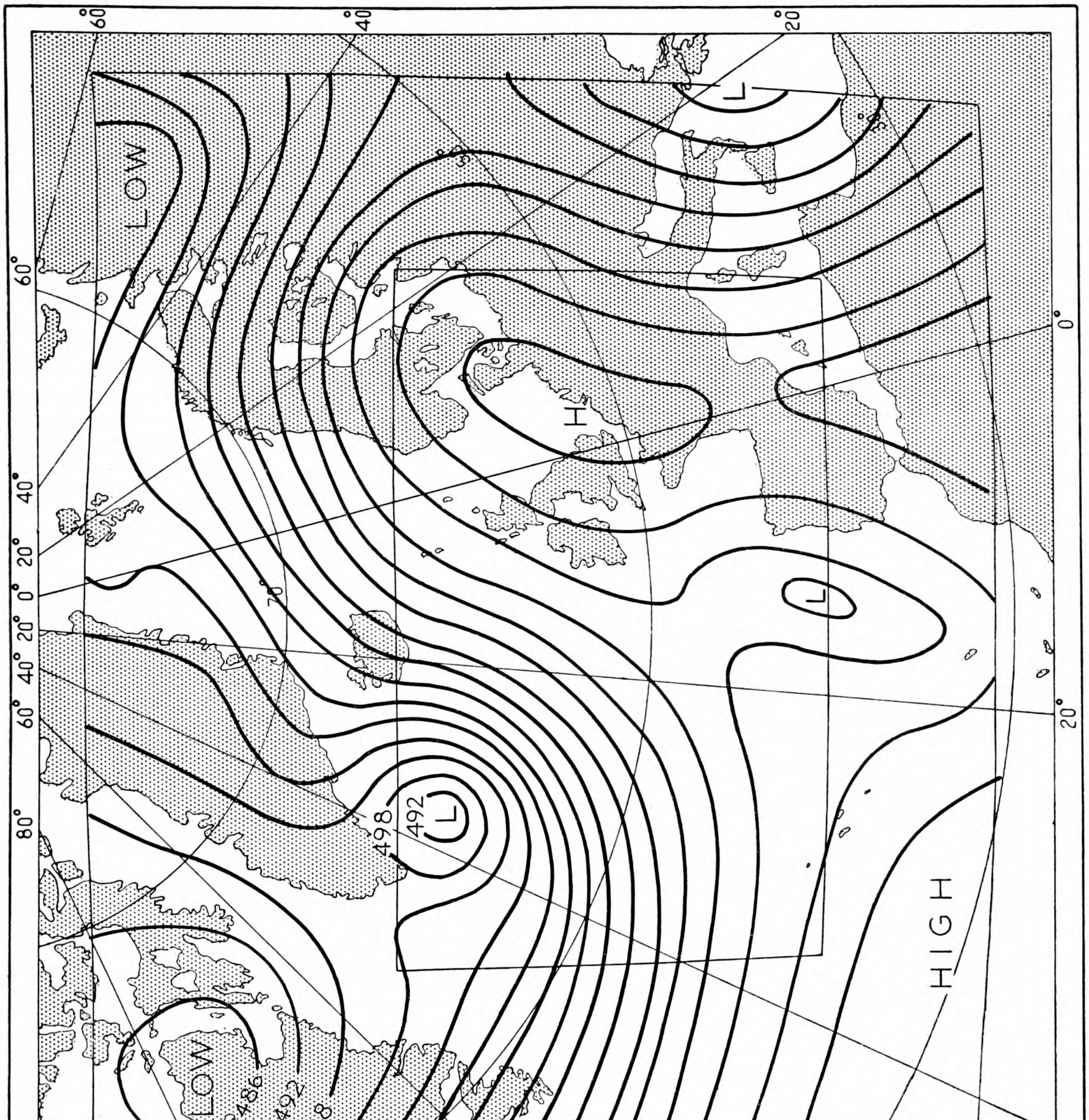

FIGURE 4(*b*). CFO analysis for 0000 GMT, 28 January 1959: 500-millibar contours in decametres.

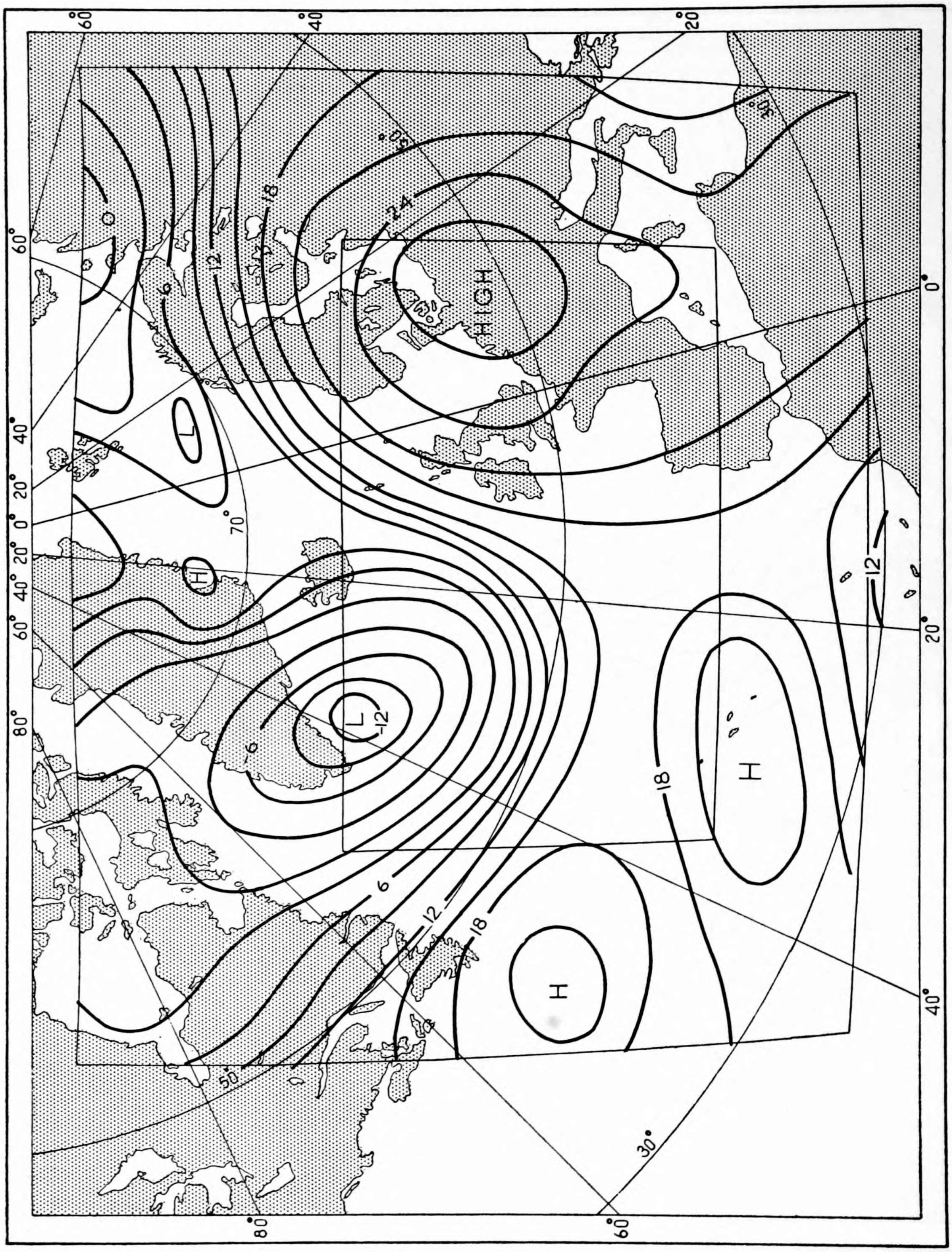

FIGURE 5(*a*). Objective analysis for 0000 GMT, 28 January 1959: 1000-millibar contours in decametres.

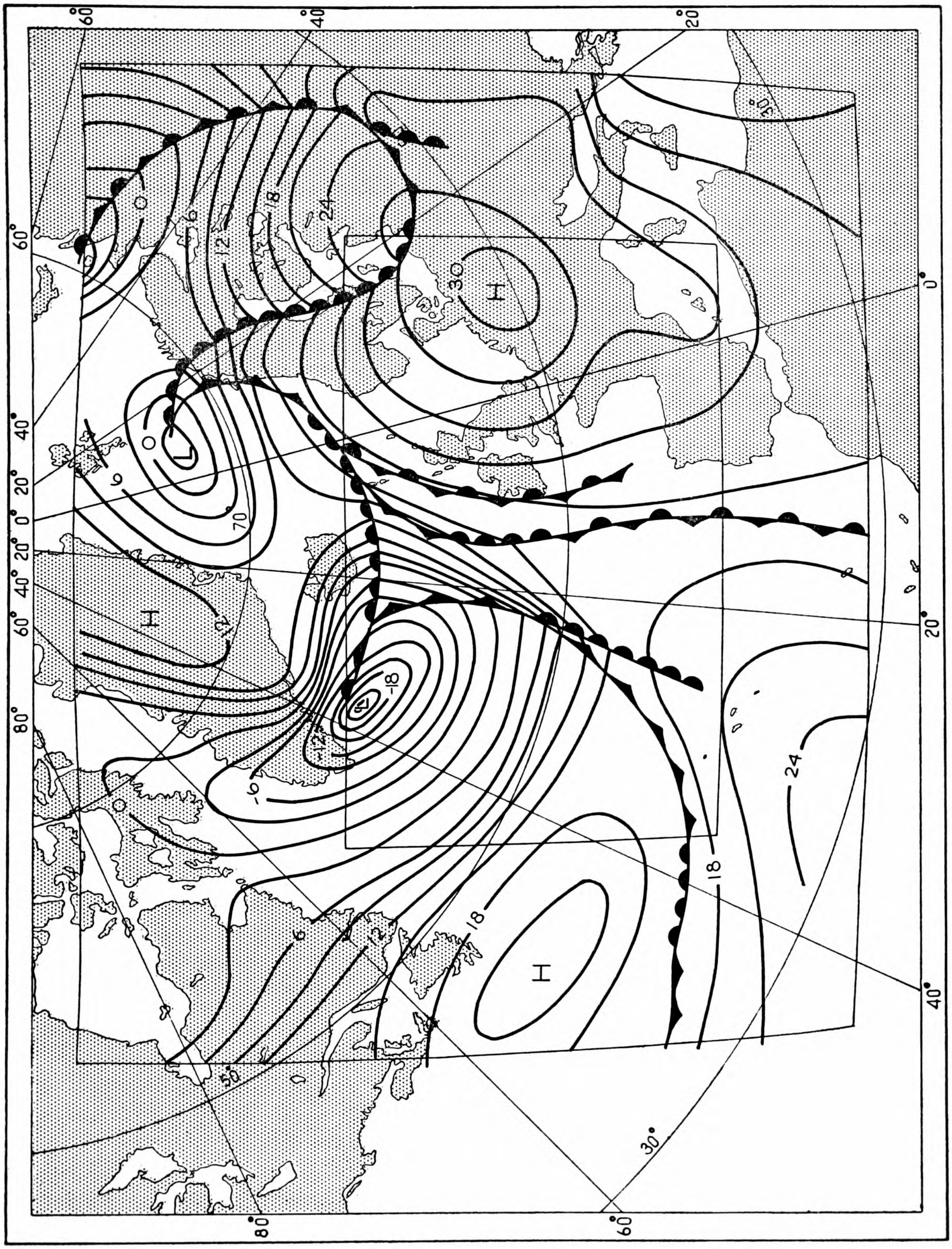

FIGURE 5(*b*). CFO analysis for 0000 GMT, 28 January 1959: 1000-millibar contours in decametres.

The surface (1000-millibar) chart as drawn in CFO, Figure 5(*b*), showed a deep depression a little south-east of the tip of Greenland, but the corresponding system on the objective analysis, Figure 5(*a*), was too shallow to the extent of about 110 metres. Similarly the depth of the depression in the north Norwegian Sea was underestimated. It is to be noted that similar errors in the intensity of the anticyclones did not occur.

Generally speaking over the land areas all the machine analyses were almost indistinguishable from those drawn by hand, especially over Europe where the station network is the most dense, or at least the differences were unimportant and confined mostly to areas of weak gradient. This is to be expected, as the network of observations over most of the land areas within our grid is adequate to define synoptic-scale systems with very little latitude. A much greater degree of uncertainty is inevitable over the oceans, however, and we can no more expect precise agreement between the machine and conventional analyses than we could between those produced independently by different human analysts.

Some statistics were evaluated expressing the difference between the machine and conventional analyses and these are reproduced in Table I.

TABLE I. *Analysis comparisons*

	h_e m	r	V_e kt
1000 mb	21/19	0·98/0·97	13/13
Total thickness	25/21	0·97/0·98	13/12
500 mb	27/24	0·99/0·99	14/12

r = correlation coefficients.

h_e = r.m.s. height differences and V_e = r.m.s. wind differences between machine and conventional analyses, evaluated over the 15 × 10 grid (see Figure 1).

The first figure in each case refers to the 42 cases of the first experiment and the second figure to the 50 cases of the second experiment.

The aim in a machine analysis system must presumably be to achieve results which differ from the human product by no more than the analyses produced independently by different analysts differ from each other. Precise figures expressing this aim and applicable to our grid are not available, but we may note that Berggren[6] found, from 29 analyses of a 500-millibar chart by different individuals, a standard deviation of 15 metres for 500-millibar height. The latter figure was determined for a somewhat larger grid but it represents differences of the same order of magnitude as those of Table I. We conclude that our machine analyses must in most respects be reasonably good. That this was not so in all respects was made abundantly clear by an examination of the individual analyses over the ocean.

As in the analysis for 28 January 1959 already discussed, the examination revealed that the depth of depressions on the Atlantic was systematically underestimated by the objective method, particularly for intense systems. Indeed, the root mean square difference between the machine and subjective values of pressure at the centre of depressions over the Atlantic was 66 metres (8·1 millibars), evaluated over 71 depressions. Furthermore the error was always in the same sense, viz. an under-estimation of depth in the machine analysis. Undoubtedly the inherent smoothing of the objective technique, which is necessary if spurious short-wave irregularities in the vicinity of isolated observations are to be avoided, was a contributory factor. Nevertheless the magnitude of these errors suggested some more fundamental short-coming of the objective method.

To isolate the causes of this failing, the method was applied to the analysis of artificial observations invented to fit intense lows having pressure profiles of various shapes. It became clear from these experiments that the errors arose from two causes:

(i) The quadric surfaces which can be represented by equation (1) are limited to elliptic or hyperbolic paraboloids having a vertical axis. In particular, hyperboloids are excluded and all vertical sections are necessarily parabolae with vertical axes. The characteristic rounded shape near the axis of a parabola had the effect of truncating the profiles of intense depressions unless observations near the centre were available.

(ii) Estimates of the slope of the pressure surface were used in the fitting process, these being obtained from the observed winds by means of the geostrophic approximation. It is well known, however, that observed winds may be considerably less than the geostrophic values in regions of large cyclonic curvature. Accordingly, under-estimates of the slope contributed to the quadric surfaces fitted to the data in the region of depressions.

It is not easy to avoid these two limitations of the objective analysis scheme without making the analysis computation unreasonably lengthy and it has been decided to undertake further work which will be the subject of a later report. In the meantime, for the purposes of the present experiment in numerical forecasting it must be admitted that the machine analyses cannot be regarded as adequate, at least for verification purposes.

VERIFICATION OF THE FORECAST CHARTS

During the course of the routine experiments a computer programme was available for calculating a number of verification statistics over a 150-point central area of the 24×20 network. (Figure 1 shows the verification area.) Statistics relating to the 24-hour forecasts were computed for the 1,000 and 500-millibar contour heights and the 500–1000 millibar thicknesses and included:

(i) The correlation coefficient between the forecast and actual contour height changes.

(ii) The root mean square error in the forecast contour heights.

(iii) The correlation coefficient between the forecast and actual contour heights.

(iv) The root mean square vector error in the forecast geostrophic winds measured over a single grid length.

(v) The stretch vector correlation between the forecast and actual geostrophic winds measured over a single grid length.

Verification statistics were calculated for various combinations of charts, namely:

(*a*) Forecasts based on objective analyses and verified against objective analyses.

(*b*) Forecasts based on subjective analyses and verified against objective analyses.

(*c*) Forecasts based on objective analyses and verified against subjective analyses.

(*d*) Forecasts based on subjective anaylses and verified against subjective analyses.

The 42 days of the first experiment (most Tuesdays, Wednesdays and Thursdays in the experimental period) already mentioned were those days on which information was readily available for dealing with all four combinations of forecast and verification charts. To provide a rough yardstick against which to gauge the significance of the tabulated statistics, corresponding values for the CFO 24-hour forecast charts and for persistence were also obtained for the 42 days. The complete statistics are reproduced in the Appendices but an overall assessment of the quality of the 24-hour numerical forecasts may be obtained from the mean correlations and root mean square errors listed in Tables II(*a*) and (*b*).

Although the differences between verification against objective and subjective analyses are not large, they are noticeable enough to show that the objective analyses, being somewhat smoother than the subjective fields, provide less stringent tests of the forecast fields. The overall impression given by Table II is that the numerical forecasts are comparable in quality with the CFO forecasts—and much better than persistence forecasts. At the 1000-millibar level, however, the unfavourable comparison between the root mean square height errors for the numerical forecasts and those for the CFO forecasts reflects the spurious anticyclogenesis in a number of the numerical predictions.

Verification of the 24-hour 500–1000 millibar thickness forecasts produced encouragingly low values of the root mean square height and vector wind errors, while the correlation

TABLE II(*a*). *Mean correlations and root mean square errors for numerical forecasts, CFO forecasts and persistence in the first experiment* (42 *cases*)

	24 hr numerical forecasts						24 hr persistence
	Based on objective analyses		Based on subjective analyses		CFO prebaratics		
	Compared with objective analyses	Compared with subjective analyses	Compared with objective analyses	Compared with subjective analyses	Compared with objective analyses	Compared with subjective analyses	Compared with subjective analyses
			1000 mb contours				
1	0·66	0·66	0·66	0·66	0·67	0·67	..
2	76	83	74	80	60	63	75
3	0·87	0·84	0·86	0·86	0·84	0·84	0·75
4	22	25	27	29	22	24	31
5	0·68	0·62	0·65	0·60	0·65	0·61	0·41
			500–1000 mb thicknesses				
1	0·81	0·76	0·81	0·78	0·67	0·68	..
2	43	53	49	54	61	64	78
3	0·93	0·89	0·92	0·90	0·87	0·87	0·76
4	21	24	25	26	25	26	32
5	0·70	0·62	0·65	0·61	0·60	0·58	0·31
			500 mb contours				
1	0·76	0·70	0·77	0·73	0·66	0·69	..
2	72	89	75	86	75	79	100
3	0·96	0·93	0·95	0·94	0·93	0·92	0·85
4	21	26	26	29	25	27	37
5	0·84	0·77	0·80	0·78	0·78	0·75	0·52

Row number 1 = Correlation coefficient between actual and forecast 24 hr changes
2 = Root mean square height error in metres
3 = Correlation coefficient between actual and forecast heights
4 = Root mean square vector wind error in knots
5 = Stretch vector correlation between actual and forecast winds.

coefficients suggest that the shape of the thickness field and the 24-hour changes were forecast moderately well.

At the 500-millibar level it appears that the shape of the fields is often forecast with moderate success but verification against the subjective analyses again produces rather high root mean square height errors associated with spurious anticyclogenesis.

Some additional forecasts were computed which could not be used in compiling Table II because they were for days when all four combinations of charts were not available. This arose because, for example, a numerical forecast proceeding from a subjective analysis was made on Mondays, principally in order to provide a basis for the objective analysis of Tuesday's chart, and no corresponding forecast proceeding from an objective analysis was made on Mondays. Nevertheless the additional forecasts enable us to assess the stability of the statistics and in Table III(*a*) statistics for certain comparisons over 59 cases are given, together with the corresponding values for the 42 cases of the first experiment; Table III(*b*) gives similar statistics for the second experiment. It will be seen that the statistics for the

TABLE II(*b*). *Mean correlations and root mean square errors for numerical forecasts, CFO forecasts and persistence in the second experiment* (50 *cases*)

	24 hr numerical forecasts				CFO prebaratics		24 hr persistence
	Based on objective analyses		Based on subjective analyses				
	Compared with objective analyses	Compared with subjective analyses	Compared with objective analyses	Compared with subjective analyses	Compared with objective analyses	Compared with subjective analyses	Compared with subjective analyses
			1000 mb contours				
1	0·65	0·65	0·61	0·61	0·69	0·70	..
2	50	55	53	57	40	42	57
3	0·88	0·86	0·87	0·85	0·88	0·86	0·77
4	16	19	21	23	15	18	23
5	0·69	0·60	0·63	0·58	0·68	0·60	0·43
			500–1000 mb thicknesses				
1	0·81	0·75	0·78	0·76	0·68	0·68	..
2	32	39	39	42	52	52	63
3	0·94	0·93	0·92	0·92	0·90	0·90	0·80
4	15	19	21	22	22	23	25
5	0·77	0·69	0·70	0·67	0·65	0·63	0·44
			500 mb contours				
1	0·75	0·73	0·73	0·74	0·65	0·68	..
2	53	66	57	63	56	58	78
3	0·97	0·95	0·96	0·95	0·95	0·94	0·88
4	15	20	21	23	21	23	29
5	0·86	0·81	0·82	0·80	0·78	0·76	0·61

Row number 1 = Correlation coefficient between actual and forecast 24 hr changes
2 = Root mean square height error in metres
3 = Correlation coefficient between actual and forecast heights
4 = Root mean square vector wind error in knots
5 = Stretch vector correlation between actual and forecast winds.

TABLE III(*a*). *Some statistics relating to numerical forecasts, CFO forecasts and persistence in the first experiment (for both* 42 *and* 59 *cases)*

	24 hr numerical forecasts									
	Based on objective analyses		Based on subjective analyses				CFO forecasts		24 hr persistence	
	Compared with objective analyses		Compared with objective analyses		Compared with subjective analyses		Compared with objective analyses		Compared with subjective analyses	
	Number of cases									
	42	59	42	59	42	59	42	59	42	59
	1000 mb contours									
1	0·66	0·67	0·66	0·66	0·66	0·65	0·67	0·68	..	..
2	76	75	74	75	75	80	60	60	75	75
3	0·87	0·87	0·86	0·86	0·86	0·86	0·84	0·85	0·74	0·75
4	22	22	27	27	29	30	22	21	32	31
5	0·68	0·68	0·65	0·64	0·60	0·59	0·65	0·67	0·41	0·41
	1000–500 mb thickness									
1	0·81	0·82	0·81	0·80	0·78	0·76	0·67	0·72	..	..
2	43	44	49	52	54	56	61	58	78	77
3	0·93	0·93	0·92	0·91	0·90	0·90	0·87	0·89	0·76	0·77
4	21	21	25	26	26	29	25	24	32	32
5	0·70	0·71	0·65	0·65	0·61	0·59	0·60	0·62	0·31	0·33
	500 mb contours									
1	0·76	0·74	0·77	0·77	0·73	0·73	0·66	0·68	..	..
2	72	73	75	77	86	89	75	75	99	99
3	0·96	0·96	0·95	0·95	0·94	0·94	0·93	0·94	0·85	0·86
4	21	22	26	26	29	30	25	25	37	36
5	0·84	0·83	0·80	0·80	0·78	0·77	0·78	0·79	0·52	0·52

Row number 1 = Correlation coefficient between actual and forecast 24 hr changes
2 = Root mean square height error in metres
3 = Correlation coefficient between actual and forecast heights
4 = Root mean square vector wind error in knots
5 = Stretch vector correlation between actual and forecast winds.

larger number of cases are in close concord with those for the smaller number, indicating that the figures are representative. In fact the statistics are more stable than might have been expected.

The most obvious result indicated by Table II is that the success of numerical forecasting as measured by these statistics is roughly equal to that of forecasting by conventional methods. This is perhaps surprising since the two methods are really quite different. However, the numerical forecast probably gains by handling the dynamical considerations more successfully than can possibly be achieved by the human forecaster, but loses because the numerical method makes no systematic use of extrapolation and lacks the subtle indications of experience which contribute substantially to the human forecaster's prediction. Whatever the explanation, it is gratifying to find that numerical forecasting at this early

TABLE III(*b*). *Some statistics relating to numerical forecasts, CFO forecasts and persistence in the second experiment (for both* 50 *and* 65 *cases)*

	24 hr numerical forecasts									
	Based on objective analyses		Based on subjective analyses				CFO forecasts		24 hr persistence	
	Compared with objective analyses		Compared with objective analyses		Compared with subjective analyses		Compared with objective analyses		Compared with subjective analyses	
	Number of cases									
	50	65	50	65	50	65	50	65	50	65
	1000 mb contours									
1	0·65	0·65	0·61	0·62	0·61	0·63	0·69	0·69	..	..
2	50	50	53	52	57	57	40	39	57	58
3	0·88	0·88	0·87	0·87	0·85	0·86	0·88	0·88	0·77	0·77
4	16	16	21	20	23	22	15	15	23	23
5	0·69	0·69	0·63	0·64	0·58	0·60	0·68	0·69	0·43	0·43
	1000–500 mb thickness									
1	0·81	0·81	0·78	0·78	0·76	0·77	0·68	0·68	..	..
2	32	32	39	39	42	42	52	51	63	63
3	0·94	0·94	0·92	0·92	0·92	0·92	0·90	0·90	0·80	0·80
4	15	15	21	21	22	21	22	21	25	25
5	0·77	0·76	0·70	0·69	0·67	0·68	0·65	0·64	0·44	0·43
	500 mb contours									
1	0·75	0·75	0·73	0·73	0·74	0·76	0·65	0·65	..	..
2	53	52	57	55	63	61	56	55	78	78
3	0·97	0·97	0·96	0·96	0·95	0·95	0·95	0·95	0·88	0·88
4	15	15	21	21	23	22	21	21	29	29
5	0·86	0·86	0·82	0·82	0·80	0·81	0·78	0·77	0·61	0·60

Row number 1 = Correlation coefficient between actual and forecast 24 hr changes
2 = Root mean square height error in metres
3 = Correlation coefficient between actual and forecast heights
4 = Root mean square vector wind error in knots
5 = Stretch vector correlation between actual and forecast winds.

stage is as successful as conventional forecasting, and this confirms the results found for the mid-tropospheric levels at other numerical weather prediction centres.

Table II indicates that the CFO forecasts yield much the same statistics whether a subjective or an objective analysis is used as the verifying chart. The numerical forecasts, however, give slightly better verification figures when compared with objective analyses. This may be because the scale of the motions forecast on the one hand and analysed on the other depends upon the same parameter, namely the grid length, whereas the grid-point values obtained from a subjective analysis do not so intimately depend on this parameter. It is considered that more weight should be given to the comparisons with subjective analyses because, as has been indicated on pages 9–17, there are problems concerning objective analysis which have not yet been solved. Unless specifically stated, therefore, subsequent discussion refers to verifications against subjective analyses.

Apart from their use as a basis for verification, both subjective and objective analyses were used to provide the initial data for carrying out the numerical forecasts. The verification of these two kinds of forecasts (Table II) showed that generally it does not matter upon which analysis a forecast is based. It follows that, in the mean, small-scale differences in the initial data do not lead within 24 hours to large amplitude differences in the forecast fields, although this may not be true on a particular occasion.

The 24-hour contour height changes at 500 millibars are forecast about as well by numerical methods as by conventional methods, and the mean wind errors are almost the same. The root mean square height error is significantly less for conventional forecasts than for the numerical forecasts and examination of the charts shows that in many cases the large height errors made at 500 millibars in the numerical forecast were due to over-estimation of the development in anticyclonic areas; the mean height error was 24 metres in the first experiment and 13 metres in the second, showing a systematic over-estimate of contour height. This over-development is known as "spurious anticyclogenesis"; it has been discussed by Shuman[7] for forecasts made using a barotropic model and it is known that the effect may be reduced by treating the motion at the mid-level as truly non-divergent. If a similar method can be used in the present baroclinic model to reduce the root mean square error in height to no more than that given by the conventional forecasts, then there will be nothing to choose between forecasts made by either method at mid-tropospheric levels.

The statistics referring to the thickness forecasts show that the 24-hour changes in thickness are better forecast by numerical methods than by conventional methods and that the root mean square thickness error is significantly less when numerical methods are used; the mean thickness error is only −3 metres in the first experiment and −1 metre in the second. There is certainly no loss incurred by using numerical methods in the accuracy of thermal wind forecasts. The mean temperature field is better forecast by numerical than by conventional methods; it is also better forecast than are the 500 or 1000-millibar contours.

The forecast at 1000 millibars is derived from that at 500 millibars and the thickness forecast. As far as wind is concerned the numerical forecast proceeding from an objective analysis is superior to that proceeding from a subjective analysis and as successful as a conventionally prepared forecast. The errors in the wind at 500 millibars and in the thermal wind are positively correlated, the stretch vector correlation being about 0·5. The root mean square height errors are considerably greater for the numerical forecasts than for the conventional forecasts. Examination of the surface forecasts made by numerical methods shows that anticyclonic development is often greatly over-estimated, and that cyclonic development is also over-estimated on some occasions. The excessive development of anticyclones occurs mainly with spurious anticyclogenesis at the mid-troposphere level associated with quite reasonable forecasts of the thickness, and the mean height error at 1000 millibars was 27 metres in the first experiment and 11 metres in the second. It follows that a model which reduces the spurious development in the mid-troposphere will also reduce the spurious development at the surface. There is a high correlation of about 0·8 between the height errors at 500 millibars and the thickness errors, so that the errors in the 1000-millibar forecast are not greater than those at 500 millibars or those in the thickness.

Table II also gives statistics relating to persistence forecasts, assuming that there has been no change in the 24 hours. Every statistic, except the root mean square height error, found in verifying the 1000-millibar forecasts, shows that a persistence forecast is poorer than the other forecasts.

THE ERRORS IN THE NUMERICAL FORECASTS

The errors which may arise in the numerical forecasts are of four main types:

(i) Errors due to the deficiencies of the model.

(ii) Errors due to the errors in the specification of the initial fields.

(iii) Errors due to the assumption of incorrect boundary conditions.

(iv) Errors due to the finite difference scheme adopted in the numerical integration of the equations.

The model which has been used is crude. No account is taken of non-adiabatic processes, with the exception of the addition of heat to relatively cold air passing over the ocean and it is remarkable that the forecasts of thicknesses are as good as they are, viz. better than those made by conventional methods. No account is taken of the underlying topography. The resolution in the vertical is extremely simple, as is the assumed-constant mean stability and the vertical profile of divergence. The wind is taken to be geostrophic except in computations of the divergence which proceed from the continuity equation. Each of these physical factors, which is omitted in constructing the model, must lead to errors in the forecasts. The errors which are apparent from inspection of the chart are those due to the geostrophic assumption leading to spurious anticyclogenesis, and those due to the neglect of the underlying topographical features.

There are errors which arise because the analyses from which the forecasts proceed are incorrect or not sufficiently detailed. These errors arose more frequently in the objectively analysed charts than in the subjectively analysed ones, but even on the latter the detail, particularly in the upper air charts, may not be sufficiently well defined for use either as a basis of forecasting or as a verifying chart. It is known from Berggren's work[6] that surprising differences occur between the analyses made by different analysts using the same data. The numerical forecasts have been verified accepting the CFO analyses as exact.

In order to solve the Poisson and Helmholtz equations for tendencies it is necessary to assume a knowledge of the tendencies at the boundaries of the area over which the forecast is computed; the assumption made is that the boundary values are zero. If the actual boundary values differ markedly from zero, for example if at the initial time a depression has just entered or is about to leave the area with corresponding large values of the tendency, the error in the forecast may become very large indeed. In the first example there will be a spurious source of positive vorticity near the boundary which will lead to an excessively deep depression; in the second the positive vorticity which is being transported to the boundary cannot be transported across the boundary and must accumulate, again leading to a deep depression, whose influence spreads backwards towards the centre of the chart. Another manifestation of the effect of the boundary assumptions is the movement of an anticyclone towards and then back from the boundary; this was noted on several occasions. But even apart from such extreme cases, there is an error field in the computed tendencies at all points due to incorrectly assigned boundary conditions.

It is known that the choice of finite difference approximation to the differential equations will lead to differences in the forecast fields; for example the forecast fields depend upon the grid length used in the computations (Knighting, Jones and Hinds[8]). The series of experiments which was carried out was not designed to reveal such differences, and such errors are not considered here.

SPURIOUS DEVELOPMENT

The vorticity equation may be written in pressure coordinates as

$$\frac{\partial\zeta}{\partial t}+\text{div}\left\{(\zeta+f)\mathbf{V}+\varpi\frac{\partial\mathbf{V}}{\partial p}\wedge\mathbf{k}\right\} = 0, \quad . \quad . \quad . \; (16)$$

where $\mathbf{V}$ is the velocity within a pressure surface, ζ the vorticity associated with $\mathbf{V}$, $\varpi = \frac{dp}{dt}$ and $\mathbf{k}$ is a unit vertical vector. The rate of change of the total vorticity within the area is given by

$$\iint\frac{\partial\zeta}{\partial t}dA = \oint\left\{(\zeta+f)\mathbf{V}+\varpi\frac{\partial\mathbf{V}}{\partial p}\wedge\mathbf{k}\right\}_n dS, \quad . \quad . \quad . \; (17)$$

where the second integral is taken around the boundary of the area and the suffix n denotes the component normal to the boundary; clearly the imposition of arbitrary boundary values in place of the true values affects the total computed vorticity within the area. The model which has been used assumes that $\mathbf{V}$ and $\partial\mathbf{V}/\partial p$ remain constant in time around the boundaries and allows of little change there in the sign of ζ, certainly ensuring that $(\zeta+f)$ remains positive. The value of ϖ is computed from the thermodynamic equation and does vary in sign, but the contribution from the term containing ϖ is not systematically of one sign, whereas that from the vorticity term is. There is therefore a systematic increase or decrease in the total vorticity within the area due to the arbitrary assumptions made concerning boundary values. Generally this must lead to an error in the mean height field within the area and spurious development, either cyclonic or anticyclonic.

At the mid-tropospheric level, assumed to be at 600 millibars, the model used ignores the effect of including ϖ, because these terms were found to make very little contribution to the equation for determining the height tendency at this level. Jones[3] had shown the necessity for including or excluding all the terms involving ϖ, demonstrating that the inclusion of only some terms led to very poor forecasts. In the model, equation (16) has been used in the form

$$\frac{\partial\zeta}{\partial t} = -\mathbf{V}.\nabla(\zeta+f)-(\zeta+f)\text{div}\,\mathbf{V}, \quad . \quad . \quad . \; (18)$$

and furthermore the computation of div $\mathbf{V}$ has been carried out in an entirely different manner from that of $\mathbf{V}$ and ζ. Div $\mathbf{V}$ was computed from the continuity equation, whereas $\mathbf{V}$ and ζ were computed from the geostrophic relation. The two terms on the right-hand side of equation (18) can no longer be represented by a divergence and equation (17), even with the correct boundary conditions, can no longer hold. The use of the geostrophic assumption has therefore led to a lack of balance, the rate of change of vorticity over an area being given by:

$$\iint\frac{\partial\zeta}{\partial t}dA = -\iint\mathbf{V}_g.\nabla(\zeta_g+f)dA+\iint(\zeta_g+f)\frac{\partial\varpi}{\partial p}dA. \quad . \quad . \quad . \; (19)$$

Computations show that the second integral on the right-hand side is negative and therefore leads to anticyclonic development. It is usually a rather small term compared with the first integral, especially over areas in which the latter is systematically of one sign. For example, long fetches with a southerly component of wind and anticyclonic curvature lead to anticyclogenesis which is essentially spurious. The corresponding effect of spurious cyclogenesis is not so frequently observed, partly because of the effect of the second integral and partly because systems in northern latitudes are more mobile than those in the south, so that the advection of positive vorticity towards the south is not directed to the same area throughout the 24 hours.

SOME EXAMPLES OF NUMERICAL FORECASTS

Some examples are given here of the numerical forecasts, mainly with reference to their short-comings. In considering the criticisms of the results it should not be forgotten that the numerical forecasts are, generally, on a par with those made by conventional means and, judged by this standard, are successful.

Figure 6 comprises all the forecast charts in chronological order, the associated actual charts being grouped as Figure 7, also in chronological order.

24-*hour forecast commencing from* 0000 *GMT*, 17 *February* 1959

The synoptic charts for 0000 GMT on 17 and 18 February 1959 and also the numerical forecasts based on an objective analysis are given. At 0000 GMT, 17 February, the 500-millibar chart shows a strong south-south-westerly flow between the anticyclone centred over the English Channel and the low south of Greenland; additionally, there was a light southerly flow to the west of Great Britain. The forecast chart shows considerable anti-cyclogenesis within this flow with a southerly component, for example at 55°N 25°W the actual contour height at 0000 GMT, 18 February, was 542 decametres, the forecast contour height being 560 decametres, while at ocean weather station "Juliett" the corresponding values were 556 and 582 decametres. The centre of low pressure was moved correctly and was not affected by the spurious anticyclogenesis. The result of the spurious anticyclogenesis was to give winds far in excess of those which occurred and the thickness chart shows how the warm air was carried too far north and then around the depression. The corresponding effect at 1000 millibars was to show marked spurious anticyclogenesis over a large area of the chart, south of about 57°N; the excessively warm air forecast in the region of the depression, allied to an almost correct forecast of the 500-millibar contour height in this region, led to apparent surface cyclogenesis and a surface pressure in the centre of the low about 20 millibars too low.

24-*hour forecast commencing from* 0000 *GMT*, 19 *March* 1959

A surface depression situated at 0000 GMT, 19 March 1959, at 39°N 55°W veered rapidly in the next 24 hours to a position 45°N 42°W with rapidly falling central pressure and with winds rising to gale force. The numerical forecast failed to predict the rapid movement and deepening; the failure occurred because at 0000 GMT, 19 March, the 500-millibar trough and the baroclinic zone associated with the development lay outside the western boundary of the computational area and were not accounted for in the calculations.

The depression to the south-west of Greenland, centred at the surface at 57°N 51°W, was forecast to move over Greenland; the actual surface charts show that the depression split into two parts, one part remaining almost stationary and the other moving along the eastern Greenland coast. This topographical modification could not be forecast with the use of the model, which does not take topography into account.

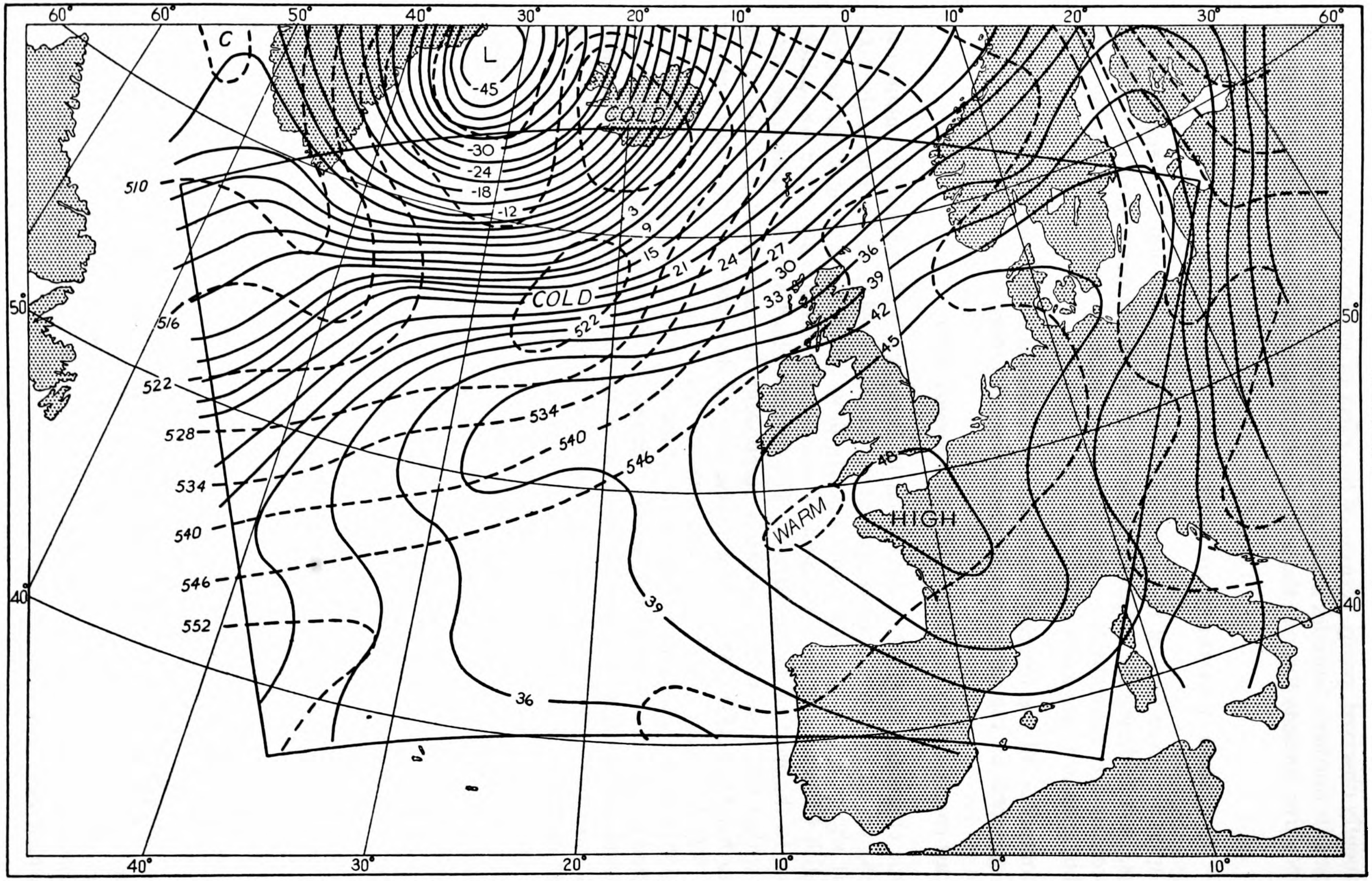

FIGURE 6(*a*). Numerical forecast for 0000 GMT, 18 February 1959, based on objective analysis for 0000 GMT, 17 February 1959: 1000-millibar contours and 500–1000 millibar thickness (broken lines) in decametres.

Verification data

	1000 mb	500–1000 mb
Root mean square height error	126 m ..	68 m
Root mean square vector wind error	32 kt ..	32 kt
Actual and forecast height change correlation coefficient..	0·86 ..	0·78

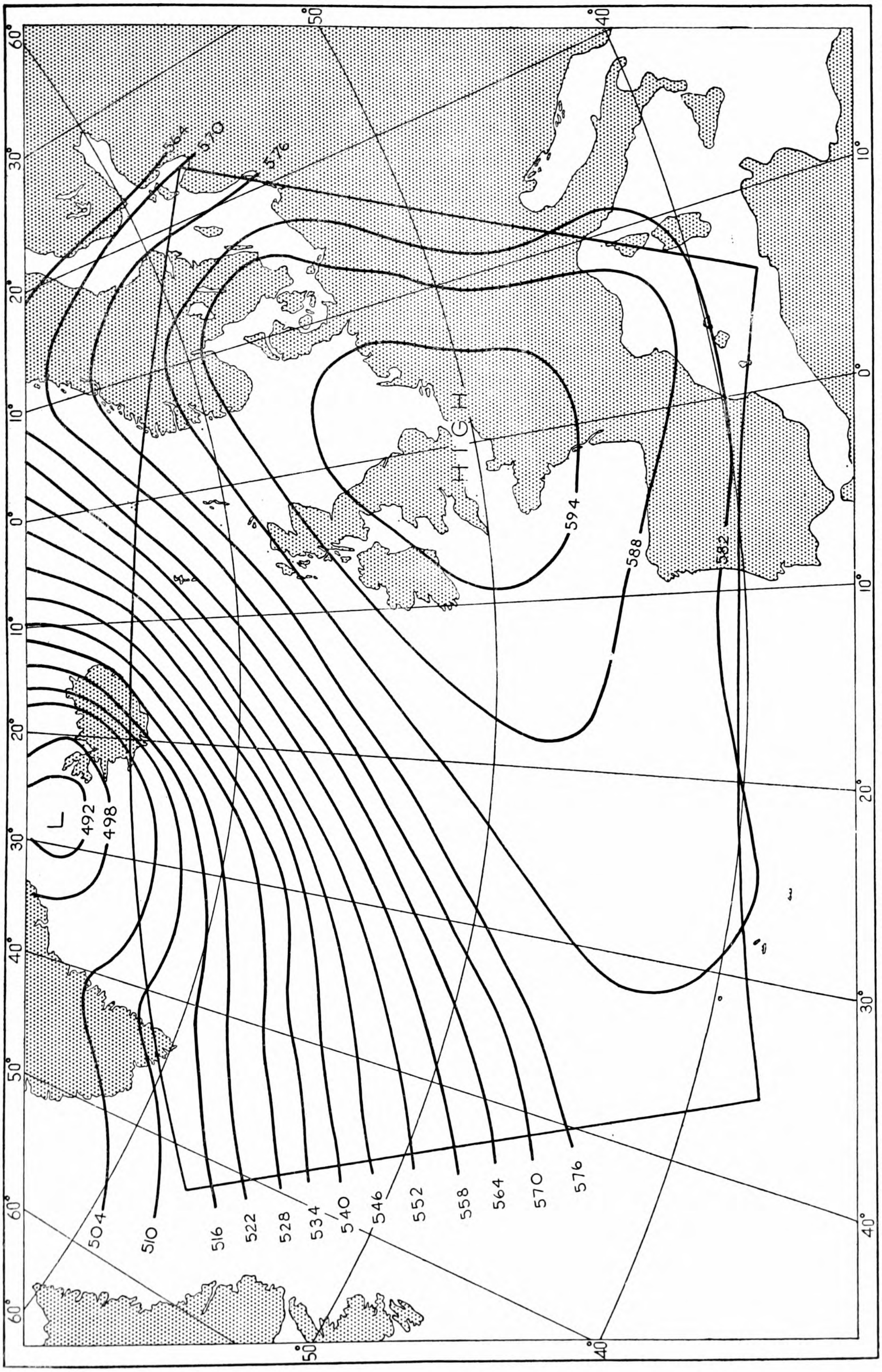

FIGURE 6(*b*). Numerical forecast for 0000 GMT, 18 February 1959, based on objective analysis of data for 0000 GMT, 17 February 1959: 500-millibar contours in decametres.

Verification data

Root mean square height error	143 m
Root mean square vector wind error	30 kt
Actual and forecast height change correlation coefficient..	0·87

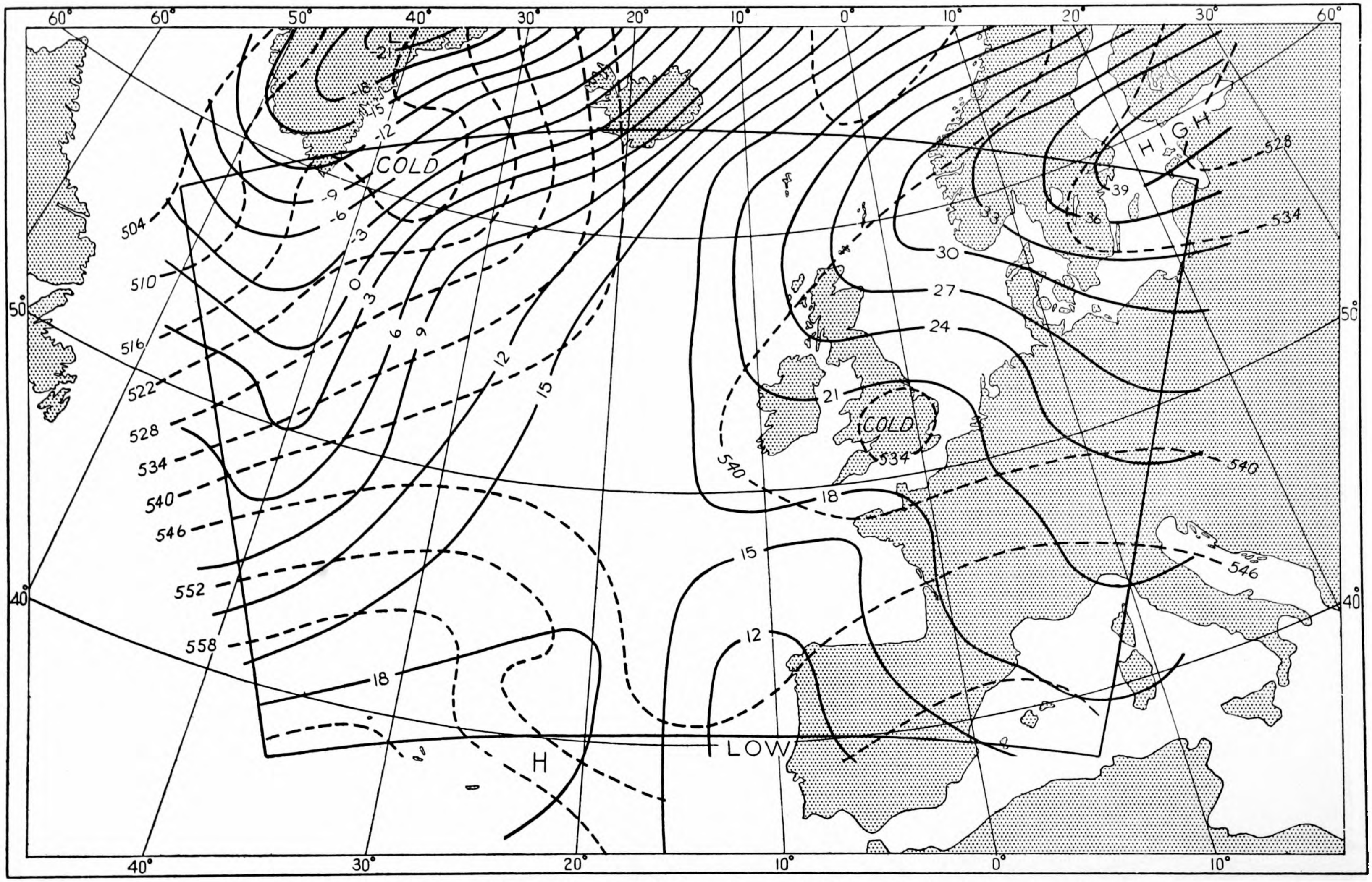

FIGURE 6(*c*). Numerical forecast for 0000 GMT, 20 March 1959, based on objective analysis of data for 0000 GMT, 19 March 1959: 1000-millibar contours and 500–1000 millibar thickness (broken lines) in decametres

Verification data

	1000 mb	500–1000 mb
Root mean square height error	105 m . .	58 m
Root mean square vector wind error	26 kt . .	26 kt
Actual and forecast height change correlation coefficient . .	0·27 . .	0·61

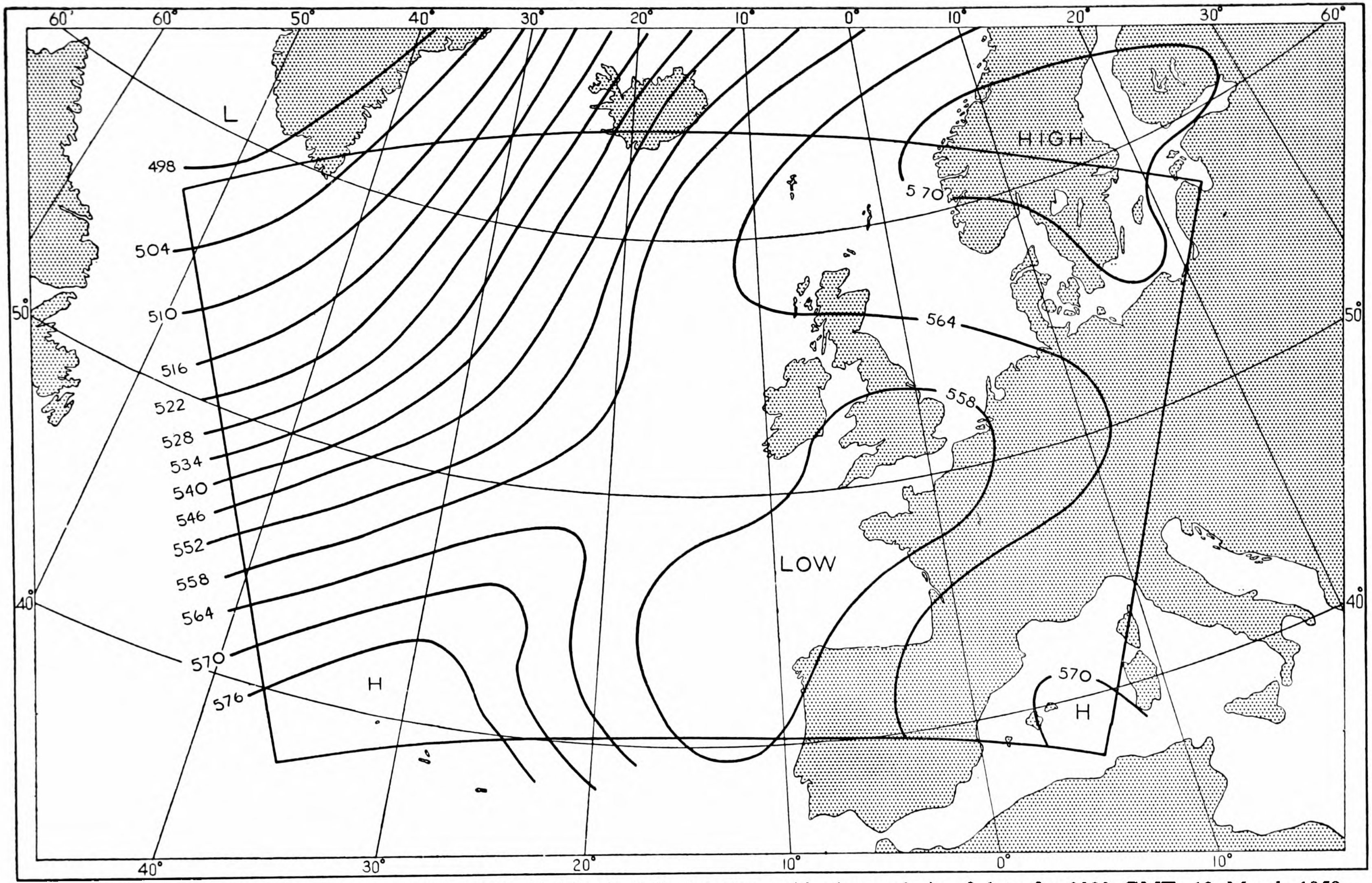

FIGURE 6(*d*). Numerical forecast for 0000 GMT, 20 March 1959, based on objective analysis of data for 0000 GMT, 19 March 1959: 500-millibar contours in decametres.

Verification data

Root mean square height error	145 m
Root mean square vector wind error	37 kt
Actual and forecast height change correlation coefficient . .	0·30

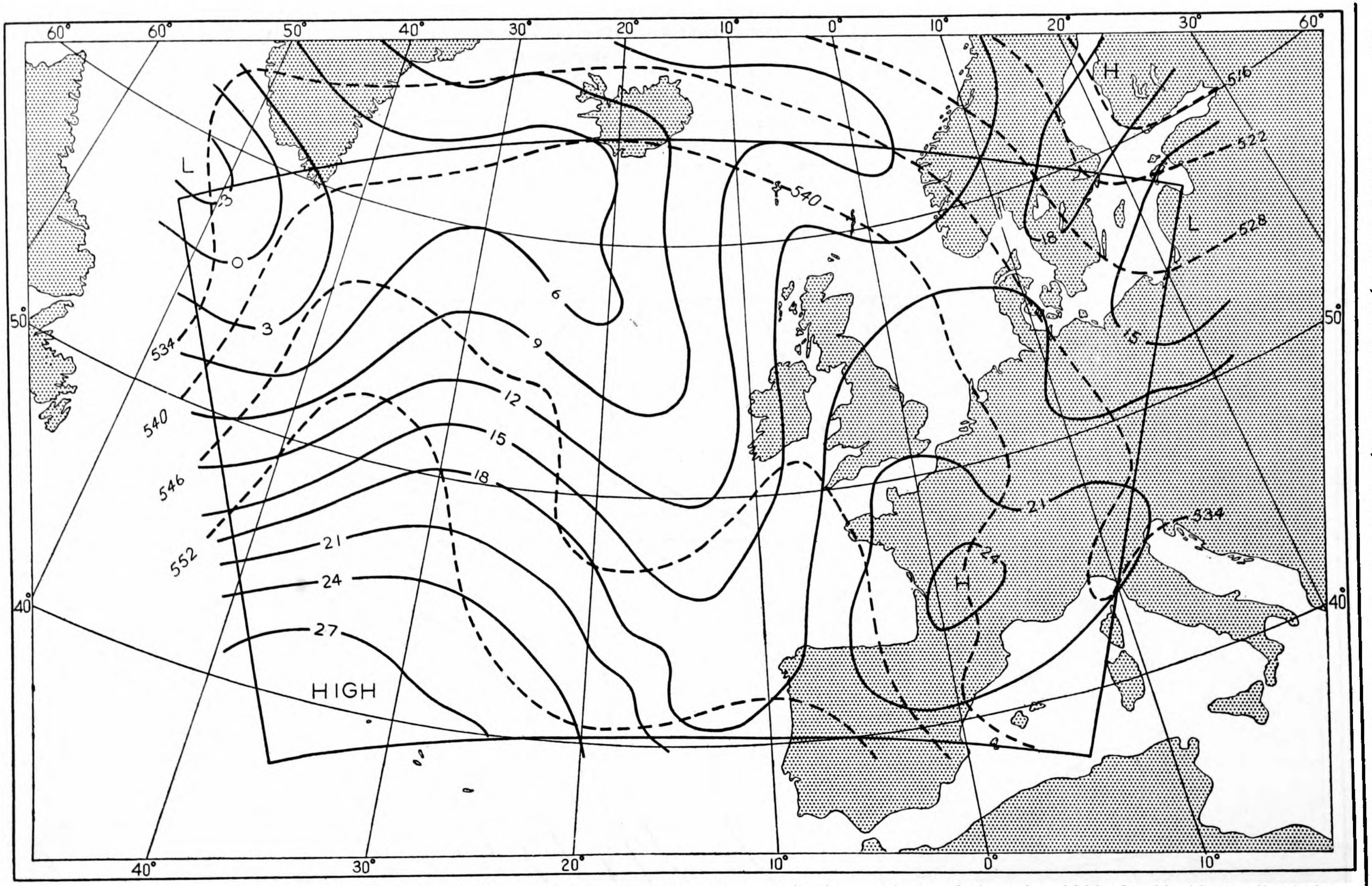

FIGURE 6(*e*). Numerical forecast for 0000 GMT, 23 April 1959, based on objective analysis of data for 0000 GMT, 22 April 1959: 1000-millibar contours and 500–1000 millibar thickness (broken lines) in decametres.

Verification data

	1000 mb	500–1000 mb
Root mean square height error	44 m ..	43 m
Root mean square vector wind error	17 kt ..	19 kt
Actual and forecast height change correlation coefficient..	0·78 ..	0·61

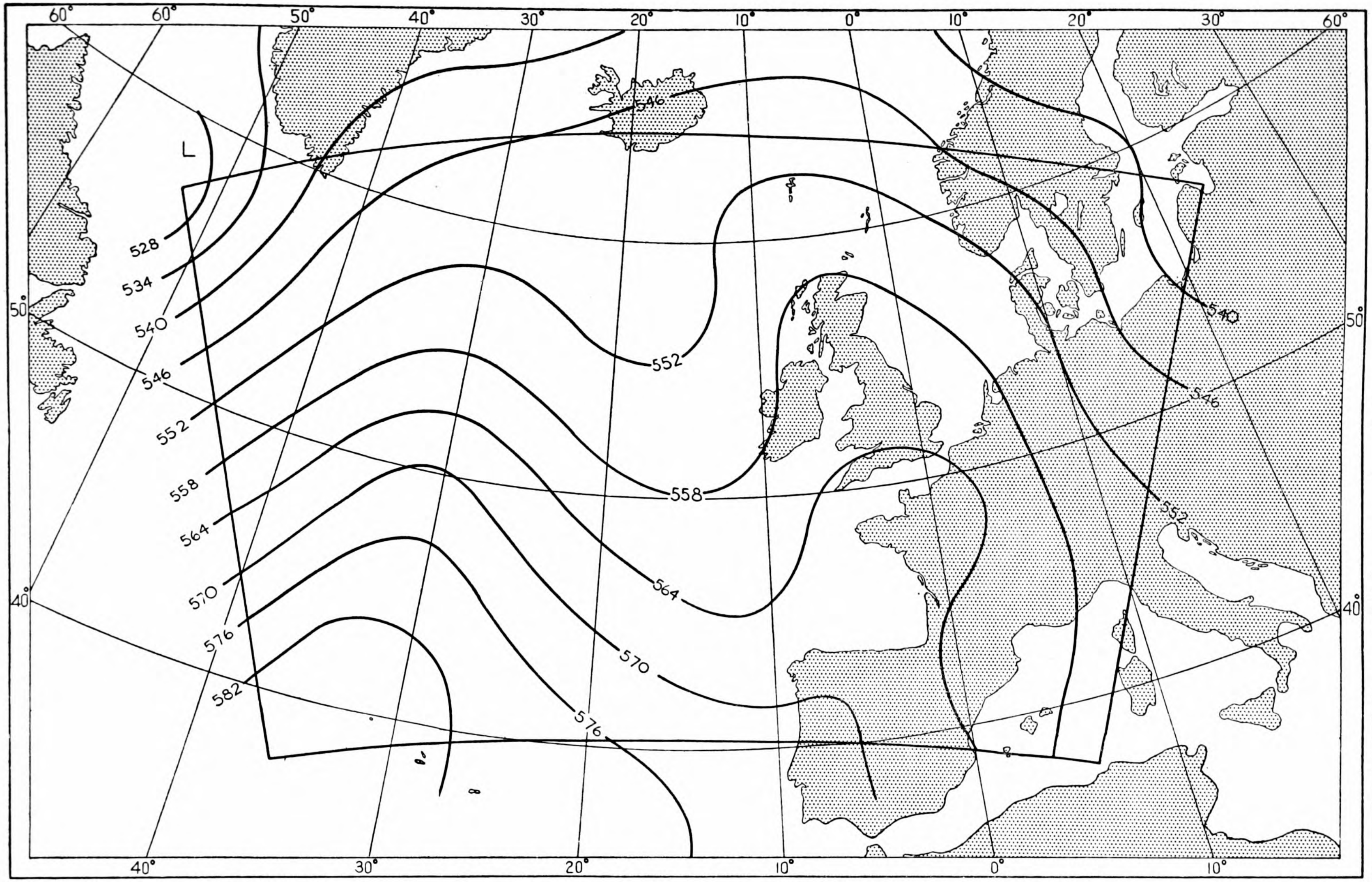

FIGURE 6(*f*). Numerical forecast for 0000 GMT, 23 April 1959, based on objective analysis of data for 0000 GMT, 22 April 1959: 500-millibar contours in decametres.

Verification data

Root mean square height error	61 m
Root mean square vector wind error	17 kt
Actual and forecast height change correlation coefficient ..	0·80

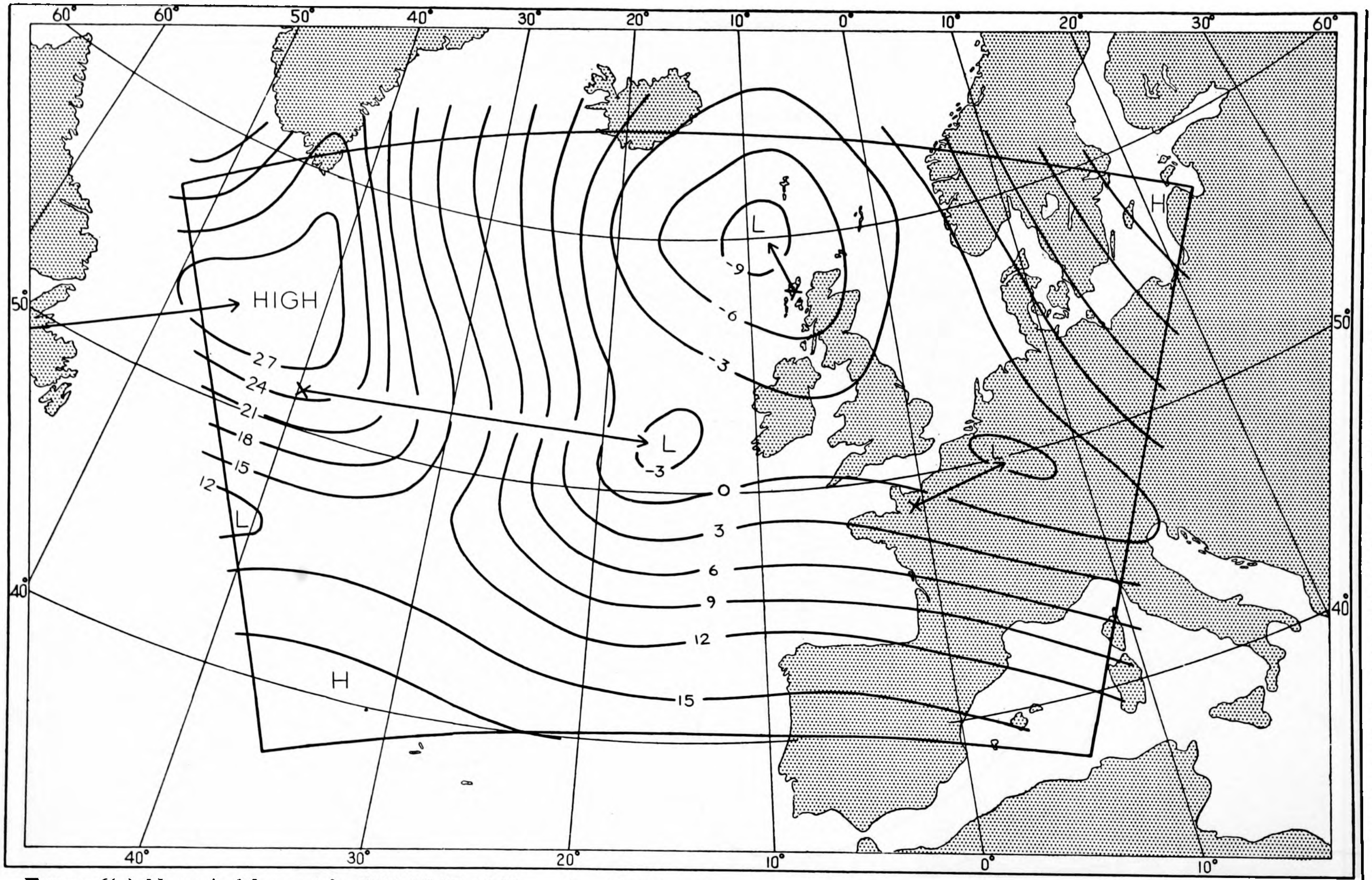

FIGURE 6(*g*). Numerical forecast for 0000 GMT, 13 November 1959, based on objective analysis of data for 0000 GMT, 12 November 1959: 1000-millibar contours in decametres.

Verification data

Root mean square height error	55 m
Root mean square vector wind error	31 kt
Actual and forecast height change correlation coefficient..	0·77

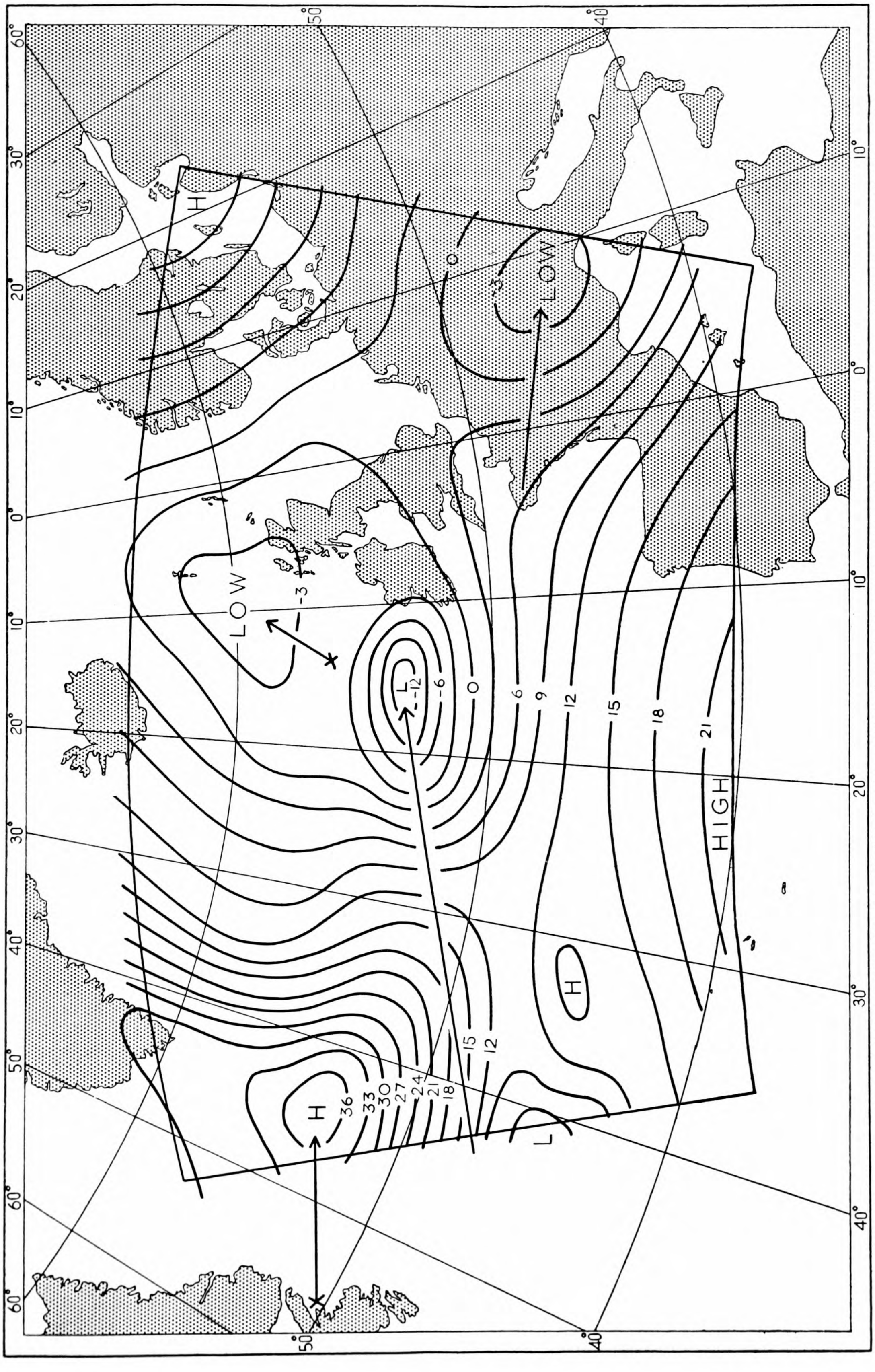

FIGURE 6(*h*). Numerical forecast for 0000 GMT, 13 November 1959, based on subjective analysis of data for 0000 GMT, 12 November 1959: 1000-millibar contours in decametres.

Verification data

Root mean square height error	58 m
Root mean square vector wind error	27 kt
Actual and forecast height change correlation coefficient . .	0·73

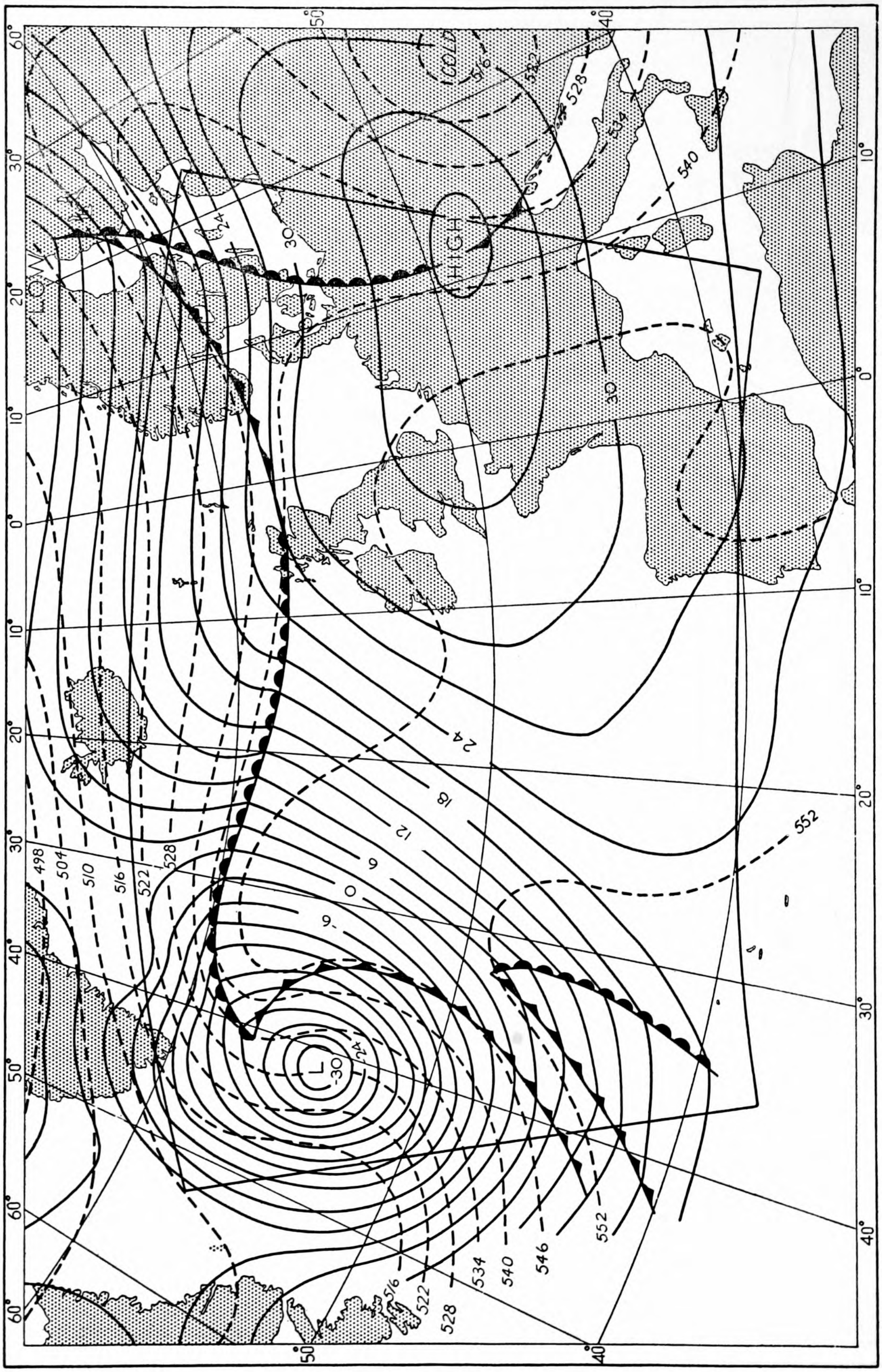

FIGURE 7(*a*). Actual chart for 0000 GMT, 17 February 1959: 1000-millibar contours and 500–1000 millibar thickness (broken lines) in decametres.

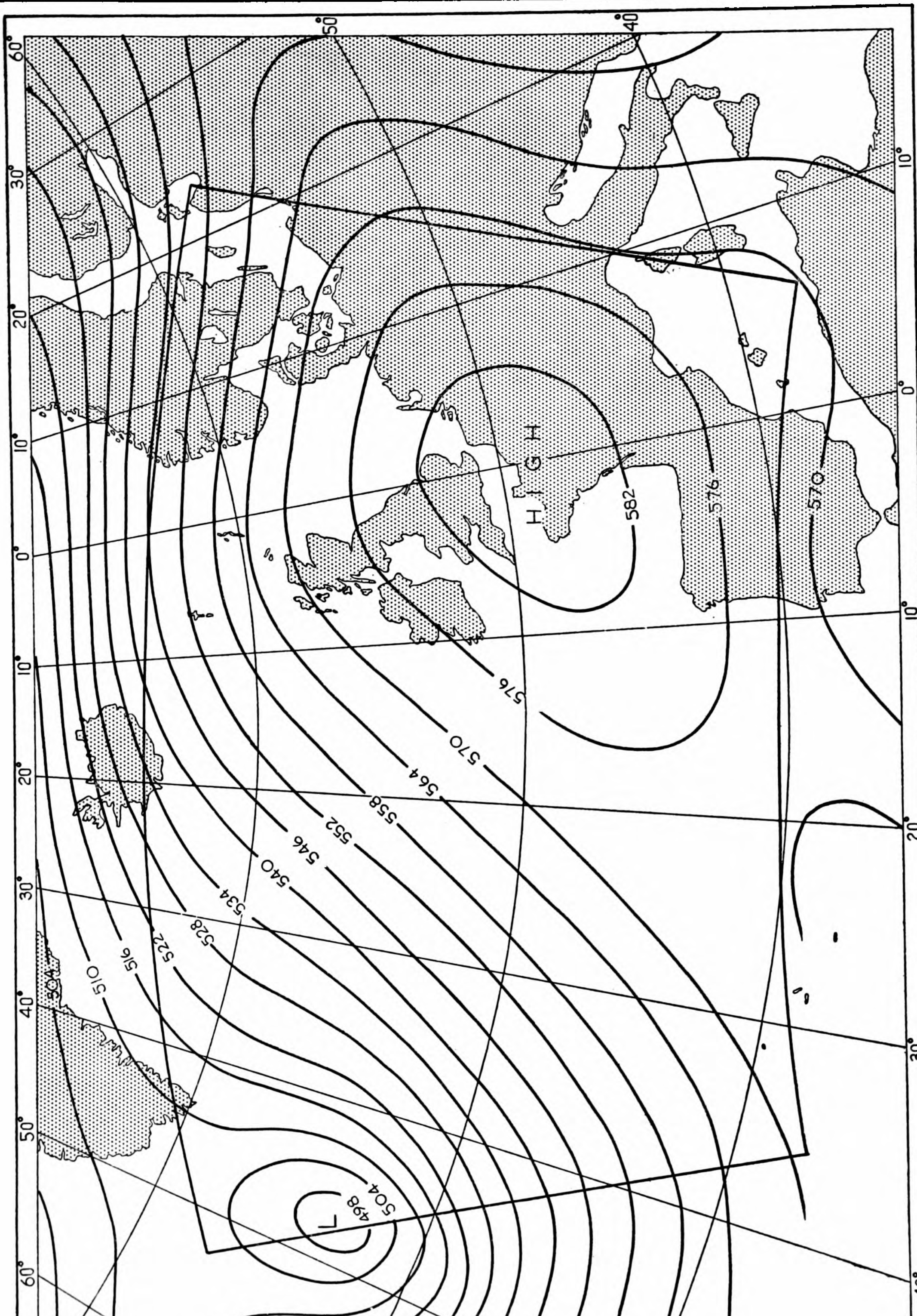

FIGURE 7(*b*). Actual chart for 0000 GMT, 17 February 1959: 500-millibar contours in decametres.

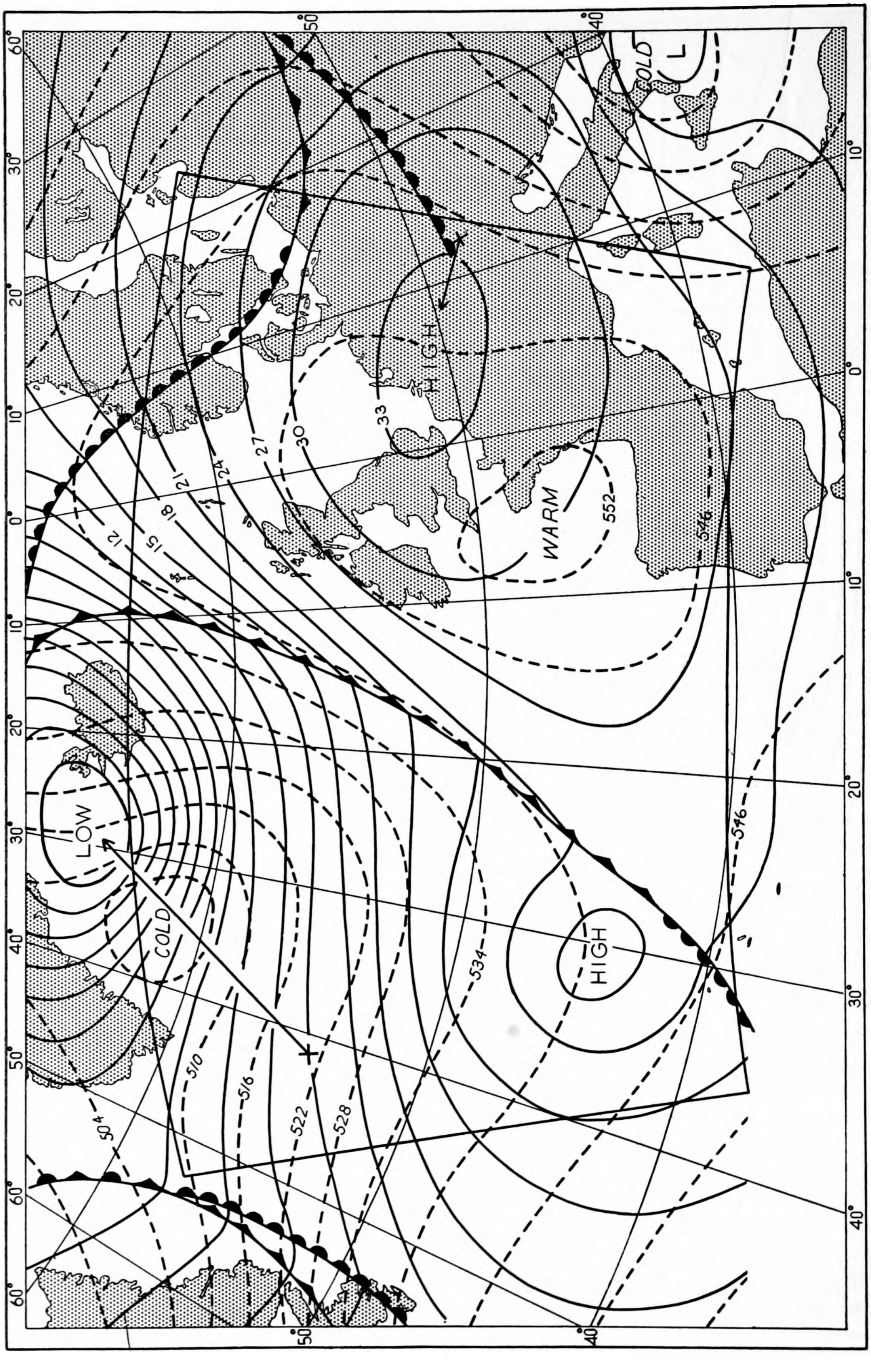

FIGURE 7(*c*). Actual chart for 0000 GMT, 18 February 1959: 1000-millibar contours and 500–1000 millibar thickness (broken lines) in decametres.

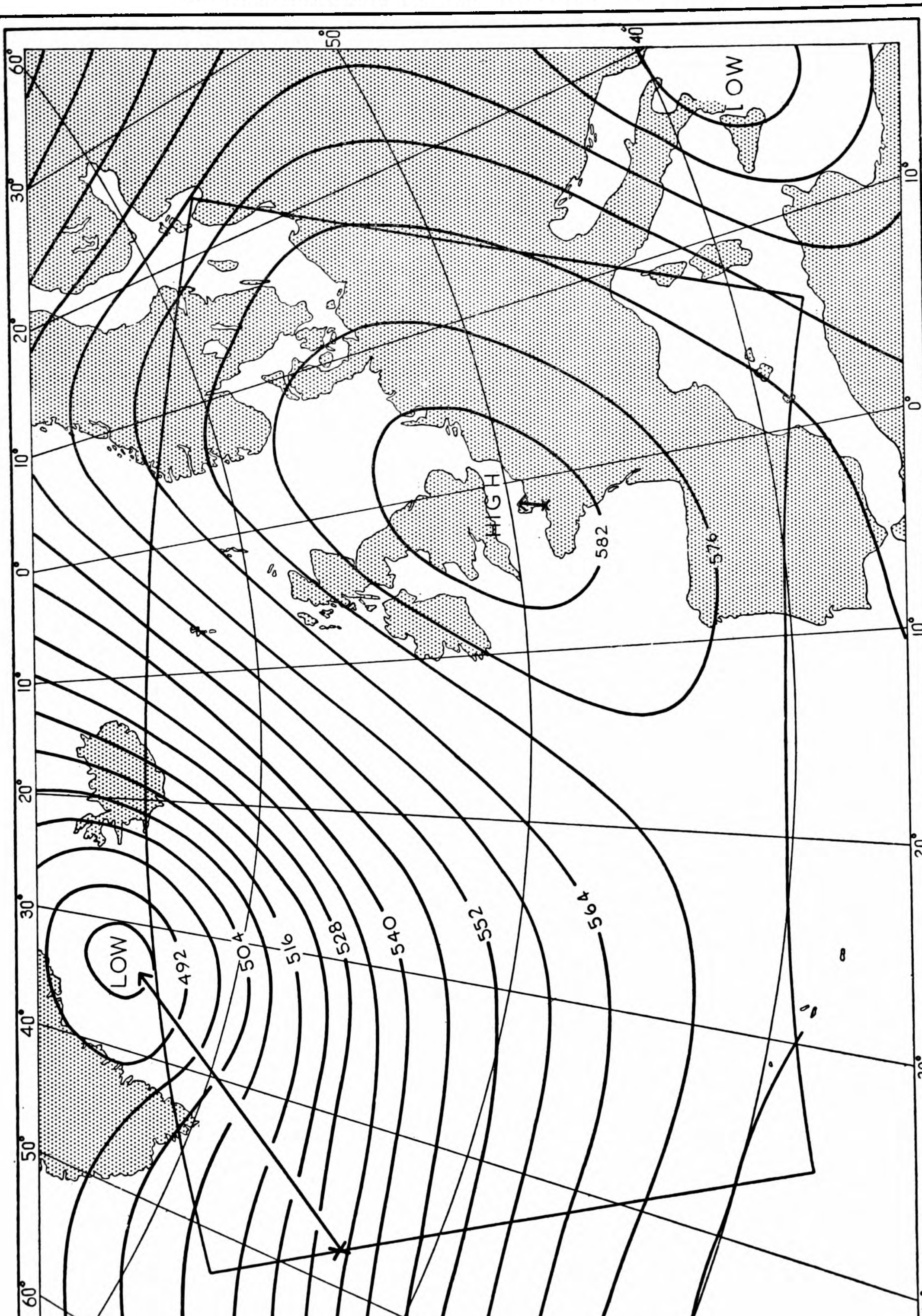

FIGURE 7(*d*). Actual chart for 0000 GMT, 18 February 1959: 500-millibar contours in decametres.

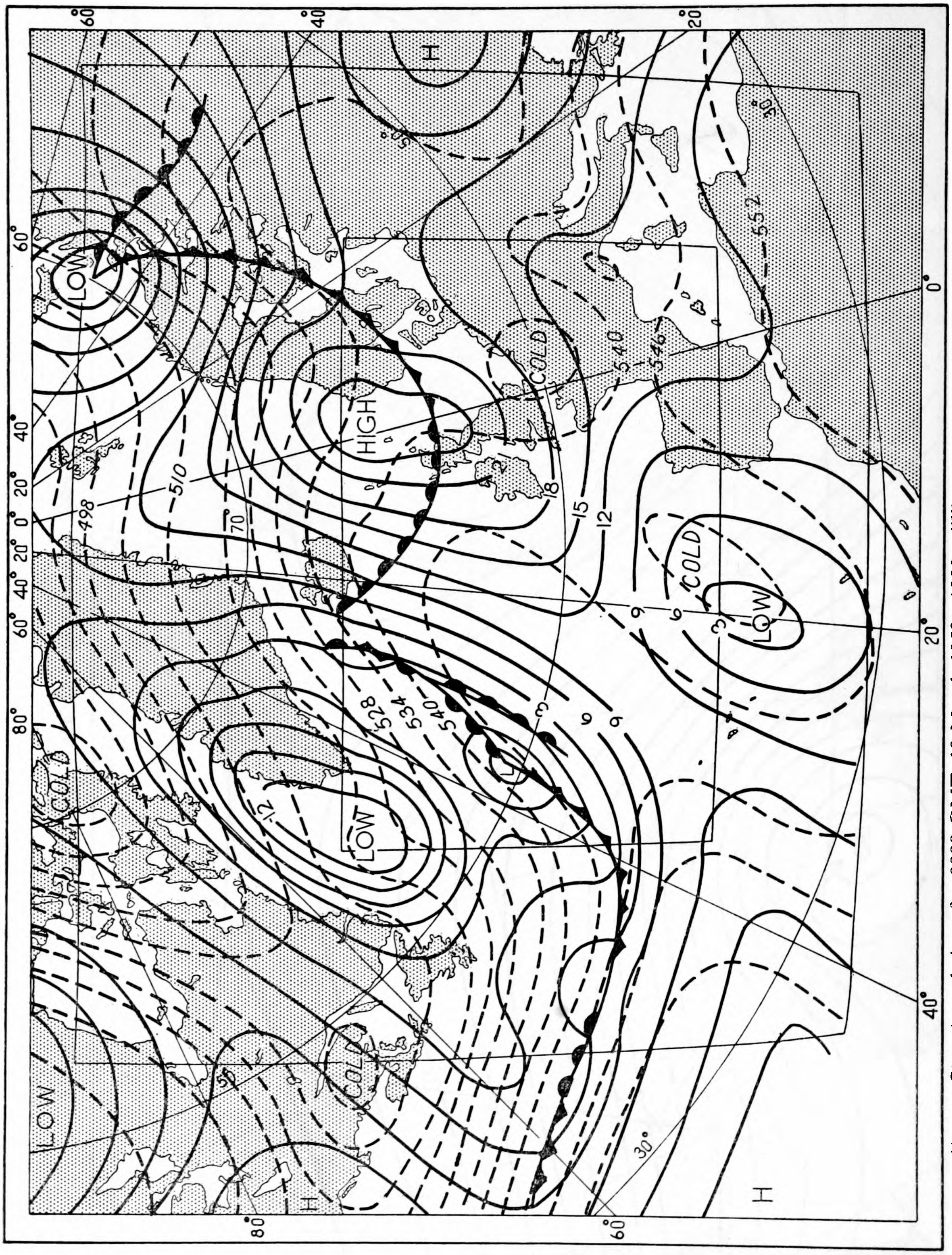

FIGURE 7(*e*). Actual chart for 0000 GMT, 19 March 1959: 1000-millibar contours and 500–1000 millibar thickness (broken lines) in decametres.

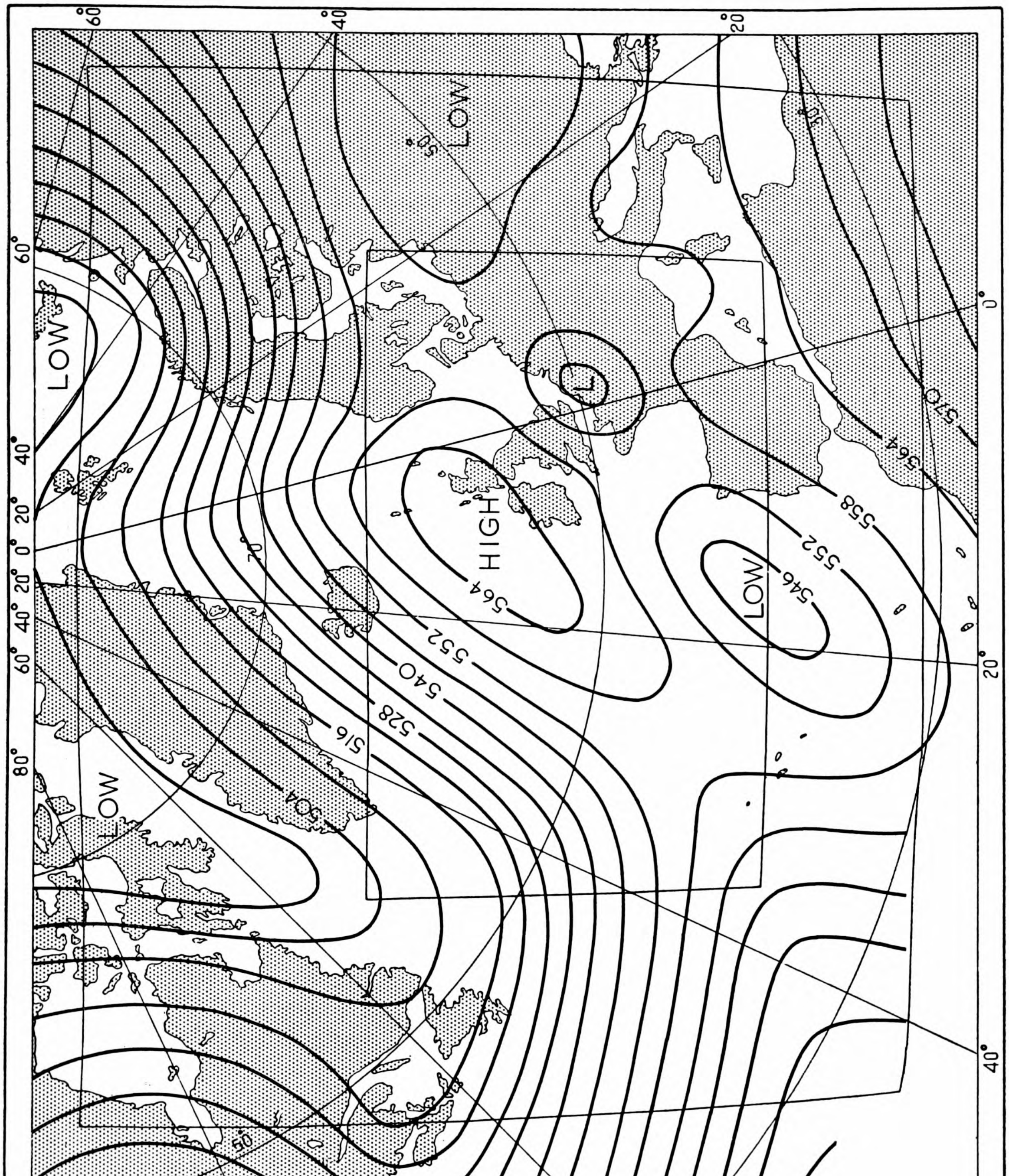

FIGURE 7(f). Actual chart for 0000 GMT, 19 March 1959: 500-millibar contours in decametres.

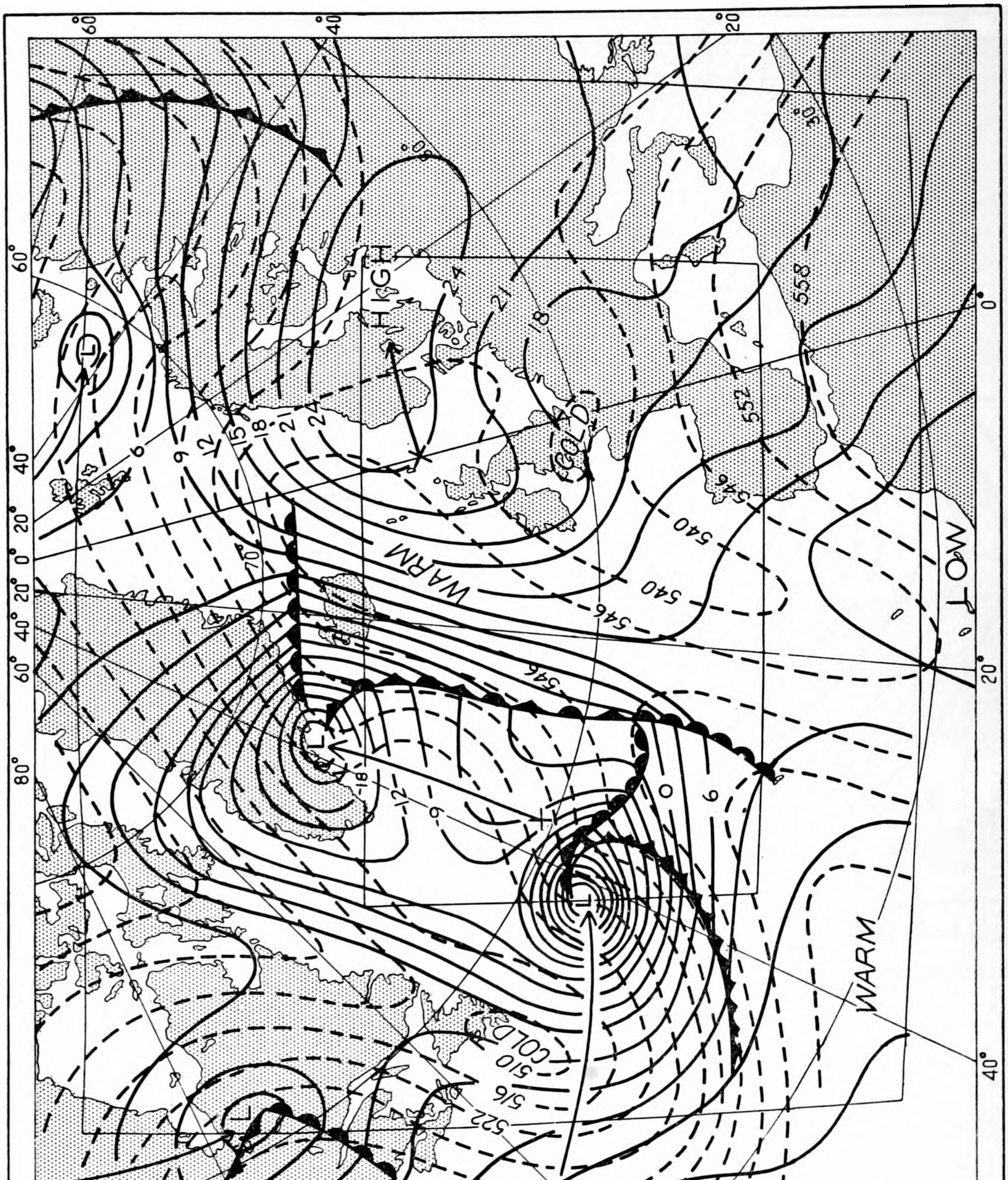

FIGURE 7(*g*). Actual chart for 0000 GMT, 20 March 1959: 1000-millibar contours and 500–1000 millibar thickness (broken lines) in decametres.

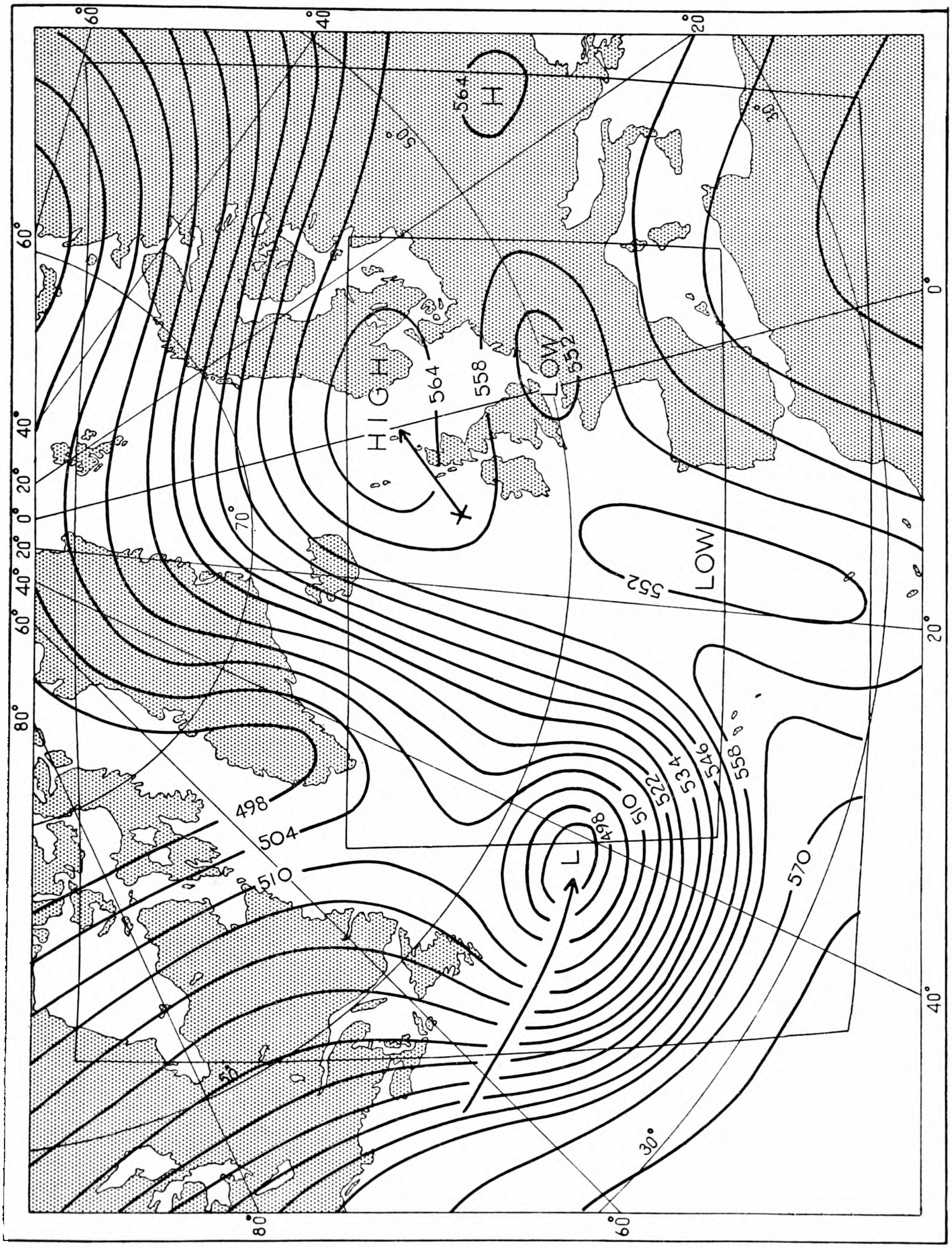

FIGURE 7(*h*). Actual chart for 0000 GMT, 20 March 1959: 500-millibar contours in decametres.

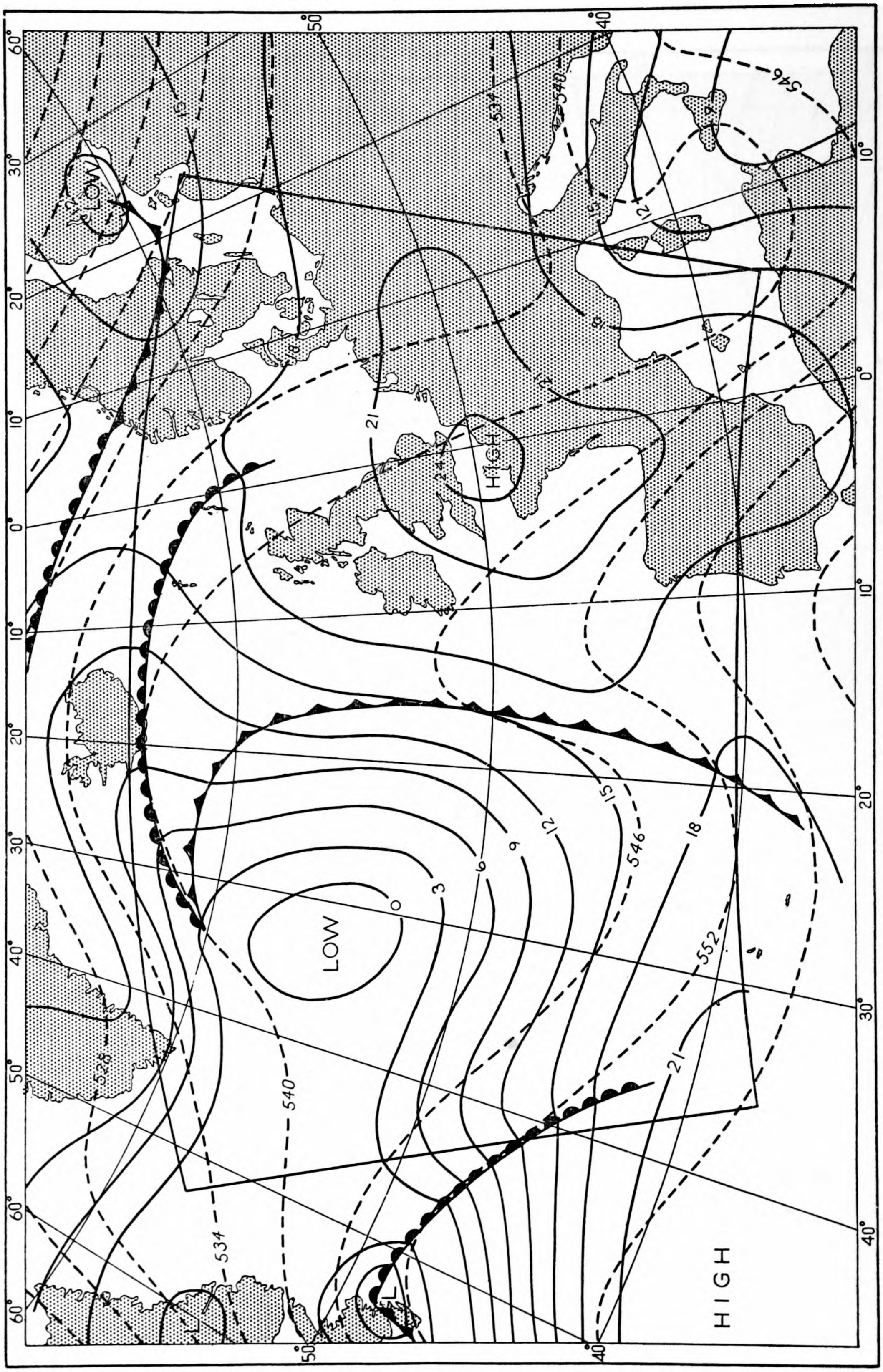

FIGURE 7(*i*). Actual chart for 0000 GMT, 22 April 1959: 1000-millibar contours and 500–1000 millibar thickness (broken lines) in decametres.

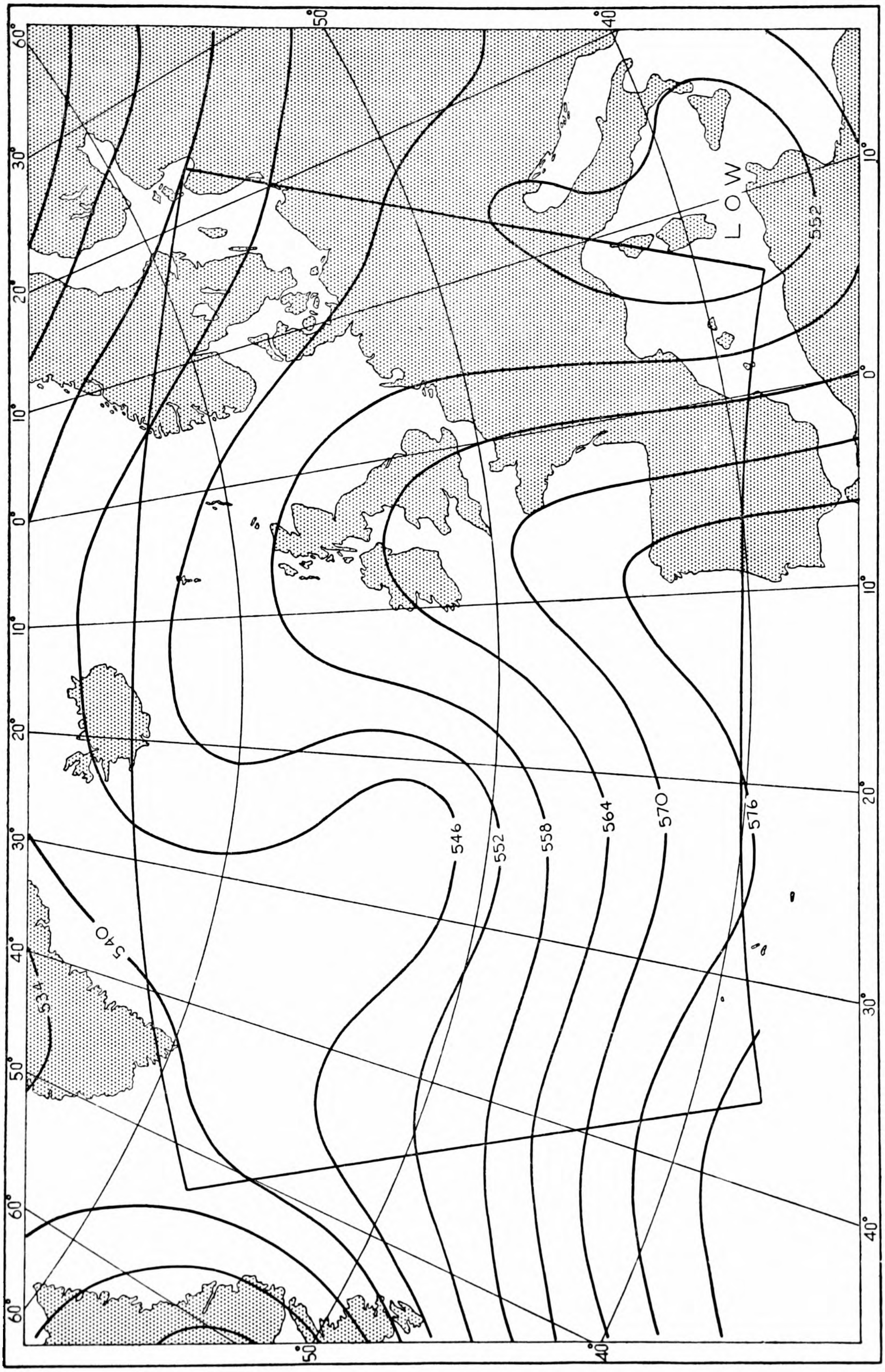

FIGURE 7(*j*). Actual chart for 0000 GMT, 22 April 1959: 500-millibar contours in decametres.

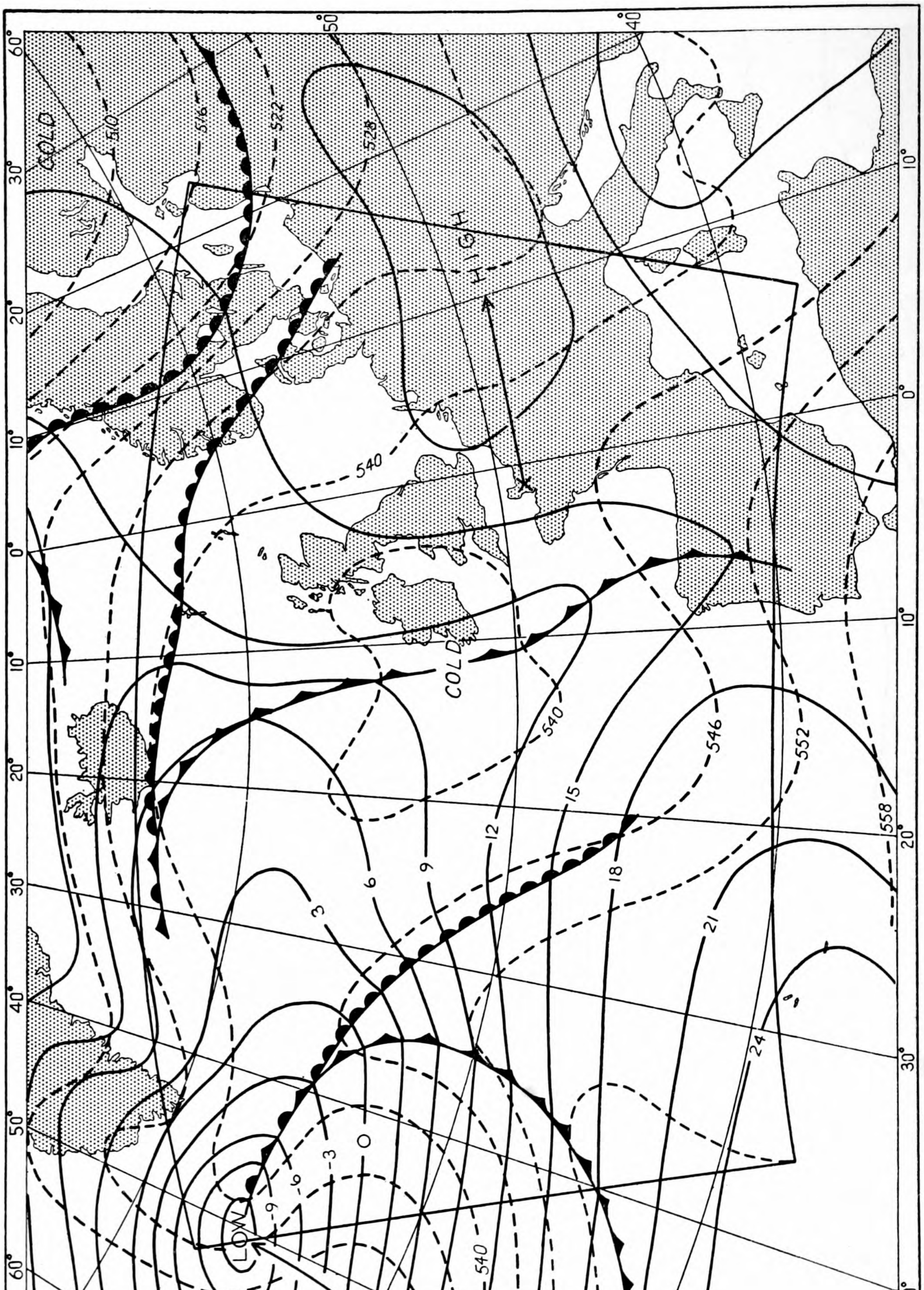

FIGURE 7(*k*). Actual chart for 0000 GMT, 23 April 1959: 1000-millibar contours and 500–1000 millibar thickness (broken lines) in decametres.

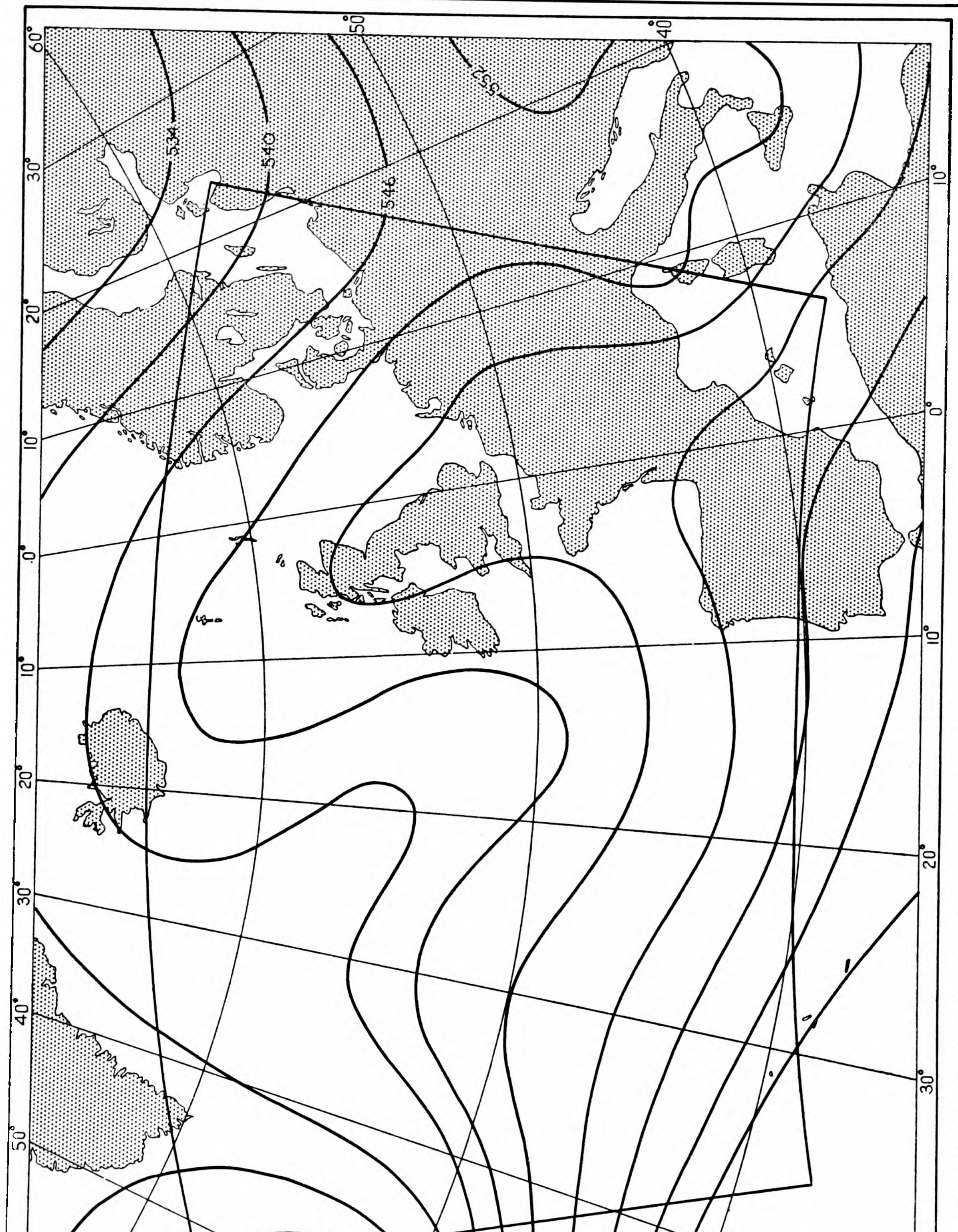

FIGURE 7(l). Actual chart for 0000 GMT, 23 April 1959: 500-millibar contours in decametres.

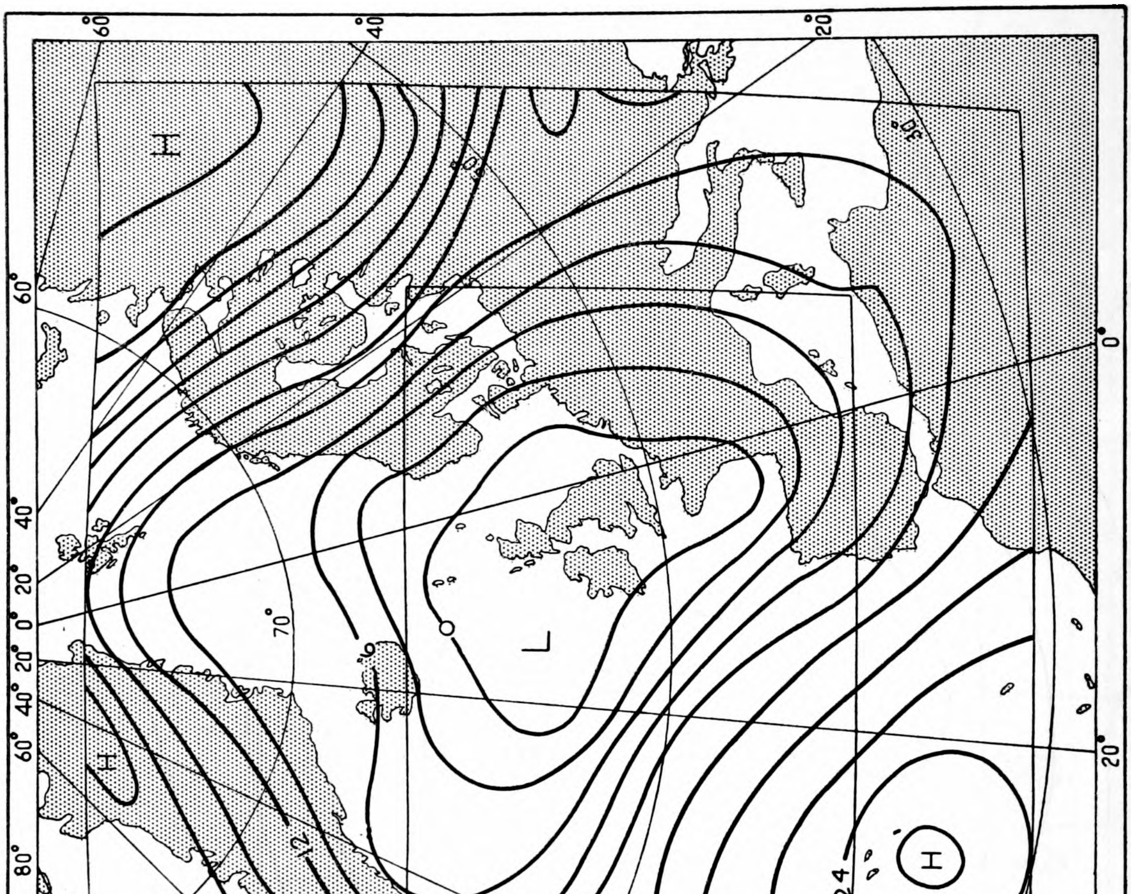

FIGURE 7(*m*). Subjective analysis for 0000 GMT, 12 November 1959: 1000-millibar contours in decametres.

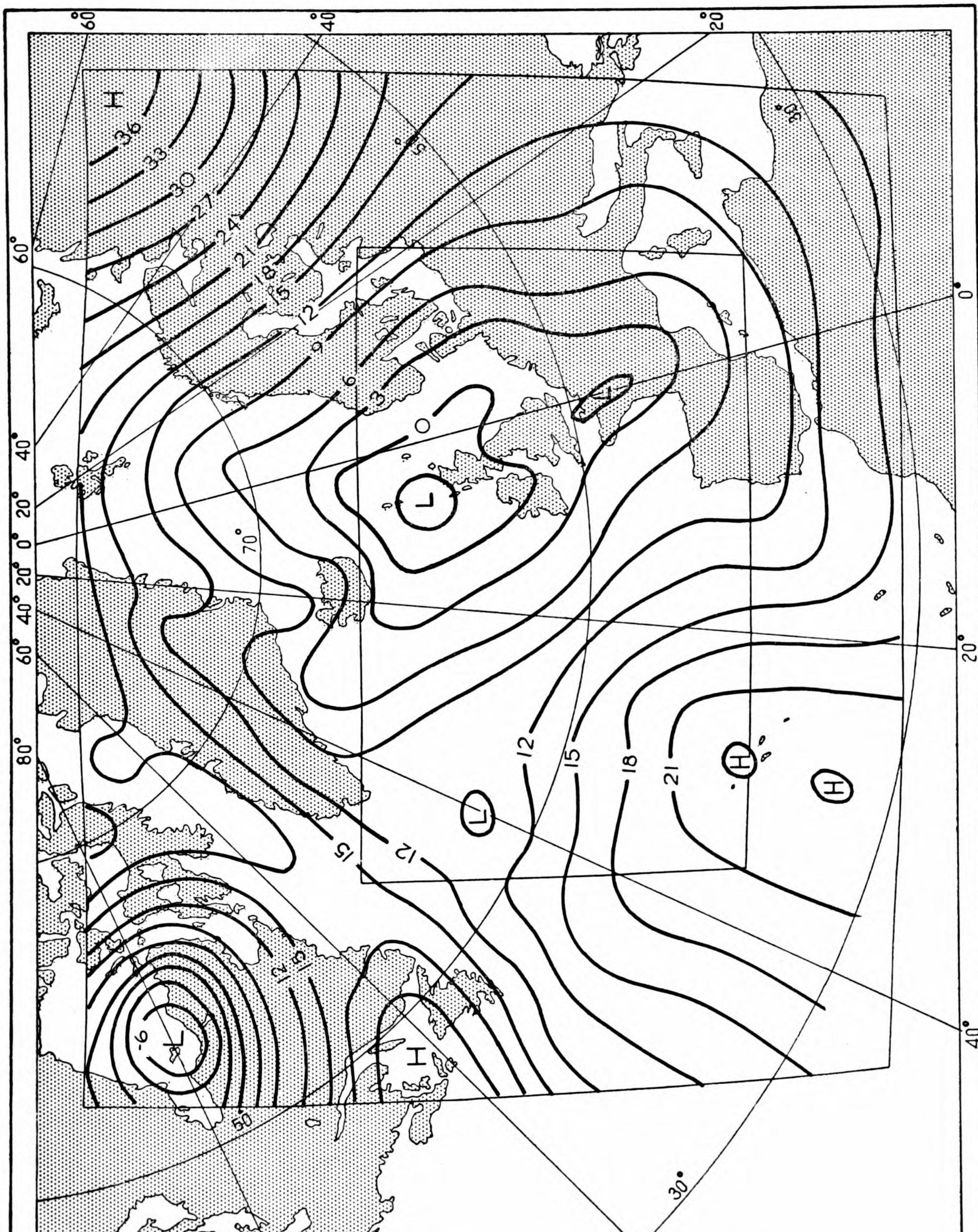

FIGURE 7(*n*). Objective analysis for 0000 GMT, 12 November 1959: 1000-millibar contours in decametres.

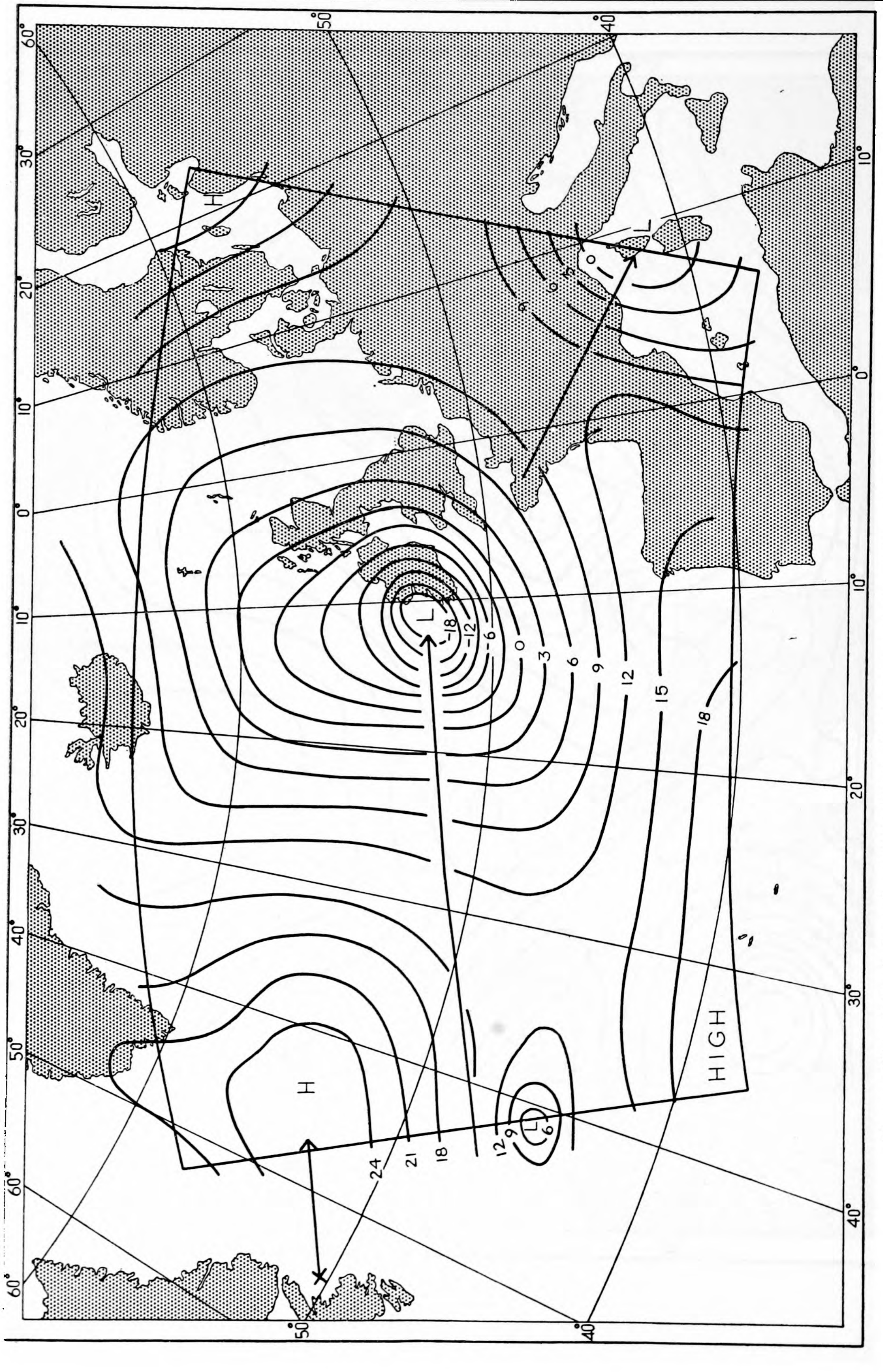

FIGURE 7(*p*). Actual chart for 0000 GMT, 13 November 1959: 1000-millibar contours in decametres.

24-hour forecast commencing from 0000 *GMT,* 22 *April* 1959

The analysed charts for 0000 GMT, 22 and 23 April 1959, and the numerical forecasts are given. The statistics relating to this forecast are among the best obtained except for the 24-hour thickness changes. The main features of the situation at 0000 GMT, 22 April, are the ridge–trough pair in the eastern Atlantic at 500 millibars associated with a depression with centre near 55°N 30°E and a high-pressure cell to the south of Great Britain and a cold anticyclone over central and eastern Europe. The forecast position of the trough at 500 millibars is only a little too far east, while the ridge stretching over Great Britain to Iceland is excellently positioned, if a little too broad. The thickness forecast was excellent in general. The resulting forecast at 1000 millibars was extremely satisfactory.

24-hour forecast commencing from 0000 *GMT,* 12 *November* 1959

Table II shows that there is little to choose in the mean between forecasts which proceed from objective and subjective analyses. Examination of the individual forecasts showed that in several cases the forecast development differed in certain areas owing to the differences between the objective and subjective analyses, due mainly to the lack of observations contributing to the objective analysis. The numerical forecasts based on data referring to 0000 GMT, 12 November 1959, are an excellent illustration of the differences which may arise.

Figure 7 includes the 1000-millibar contour charts for 0000 GMT, 12 November 1959, as objectively analysed and as obtained from the interpolated grid-point values of the 500-millibar contour and 1000–500 millibar thickness charts. There are, of course, minor differences over the whole chart, but the important difference occurs near 50°N 40°W. The objective analysis in this region is based mainly upon the neighbouring weather ships and reveals a region of low pressure to the west of ocean weather station "Charlie". The subjective analysis reveals that the low-pressure system was further south and more extensive westwards, with a lower central pressure. The subjective analysis in this region was based upon history and a single ship observation at 46°N 50°W.

Figure 6 includes the 24-hour numerical forecasts based upon the objective, and the subjective, analyses. The most striking difference between the two forecasts is to the west of Ireland, where that based on the objective analysis shows a low-pressure system with a central depth of about –4 decametres, corresponding to a surface pressure of about 995 millibars. That based on the subjective analysis gives a surface low of –12 decametres (a surface pressure of about 985 millibars), with correspondingly stronger circulation and wind. The low-pressure system to the north-west of Scotland has also been better developed in the forecast based upon the subjective analysis, but on the other hand the anticyclone to the south of Greenland has been over-developed. The statistics for these forecasts do not reveal the larger differences in the detail of the forecasts and it would be dangerous to assume that similar statistics imply similar charts.

THE COMPUTED VERTICAL MOTIONS

In the model used in making the numerical forecasts it is assumed that the vertical motion of the air relative to the pressure surfaces, as measured by dp/dt, varies parabolically in the vertical and vanishes at the pressure levels 1000 and 200 millibars. The vertical motion is thus represented by a single parameter which for convenience in representation is chosen to be the maximum value of dp/dt, that at 600 millibars. Inspection of the charts shows that the computed vertical motions are generally in accord with those which would be inferred from the observations or from the synoptic pattern. An example is shown in Figure 8.

The computed vertical motions should be regarded as average values over a large area surrounding each grid point. Additionally, as shown elsewhere (Knighting[9]), the gradient of the contours of equal vertical motion may be very large so that the assessment of the vertical motion at a point may be a difficult task of interpolation. However, a simple preliminary experiment has been carried out to assess whether rainfall and computed vertical motion can be associated. It is presumed that the average vertical motion over a period of time is more likely to be related to the rainfall rather than the vertical motion at any instant. The mean computed vertical motion, as represented by the average at the times $t = 0$, 12 24 hours, was estimated at four stations and compared with the measurable rainfall between 0900 and 2100 GMT as reported at these stations for each of the 42 cases of the first experiment. The simple contingency tables are given in Table IV. The computed vertical motion at the time of origin of the forecast was also compared with rainfall reported in the six-hour period centred on that time and these are also given in Table IV.

TABLE IV. *Contingency tables of computed vertical motion and rainfall*

	Mean vertical motion over 24 hr			Vertical motion at initial time	
	Downward	Upward		Downward	Upward
	millibars per hour			*millibars per hour*	
Scilly					
(A)	10	11	(C)	7	8
(B)	9	12	(D)	15	22
Elmdon					
(A)	13	9	(C)	8	8
(B)	10	10	(D)	15	11
Tynemouth					
(A)	5	11	(C)	1	4
(B)	10	16	(D)	18	19
Stornoway					
(A)	14	14	(C)	8	12
(B)	5	9	(D)	7	15

(A): Measurable rainfall in period 0900–2100 GMT
(B): No measurable rainfall
(C): Rainfall observed in period of 6 hr
(D): No rainfall observed

It is possible for showers to develop in an airstream in which the computed vertical motion is downward and this may account for the measurable rainfall which occurred associated with downward motion. Nevertheless, Table IV shows that there is no simple association between computed vertical motion and rainfall at a given station.

It is reasonable to suppose that precipitation will not occur unless the vertical motion exceeds some critical value. Table V gives the number of occasions of reported rain associated with given vertical motion, summed over the four stations.

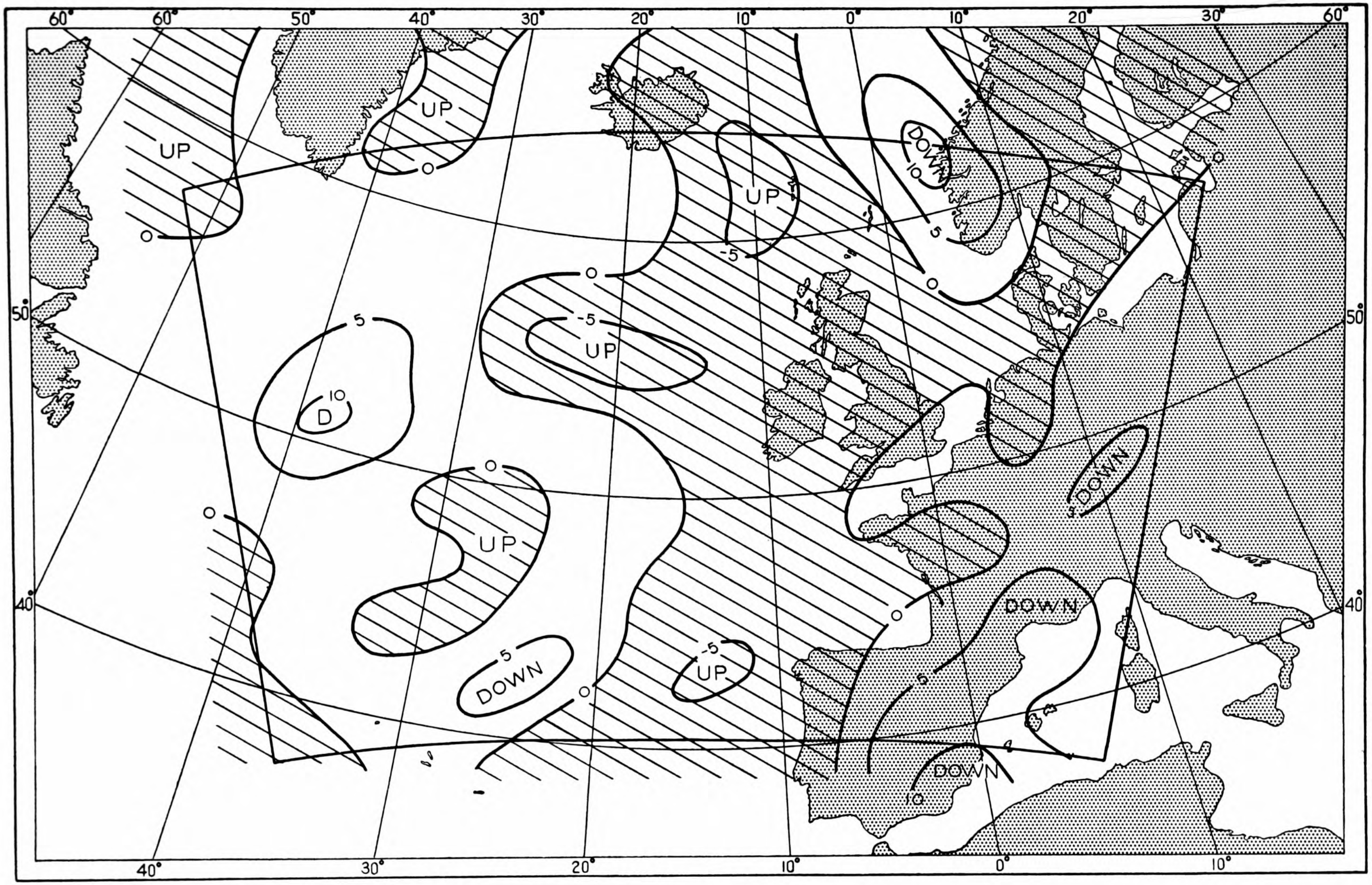

FIGURE 8. Vertical motion: $\frac{dp}{dt}$ at 600 millibars associated with a numerical forecast for 0000 GMT, 2 April 1959, based on an objective analysis for 0000 GMT, 1 April 1959.

TABLE V. *Mean vertical motion and occurrence of precipitation*

Vertical motion mb hr^{-1}	No. of reports of (*a*) precipitation	(*b*) no precipitation
Downward motion		
> 5	2	0
5 to 4	3	2
4 to 3	3	2
3 to 2	4	7
2 to 1	13	10
1 to 0	16	12
Upward motion		
0 to −1	15	15
−1 to −2	14	17
−2 to −3	12	11
−3 to −4	6	2
−4 to −5	0	0
< −5	0	1

Table V again shows no clear association of vertical motion with reported precipitation. It appears that either a more detailed knowledge of the profile of vertical motion is required in order to be able to relate vertical motion and precipitation or that account must be taken of the moisture in the atmosphere.

SUMMARY OF CONCLUSIONS

(i) It is possible to use the Sawyer–Bushby forecasting equations to obtain numerical forecasts at 1000 and 500 millibars which are statistically as good as those made by conventional methods with regard to 24-hour changes in contour height and to the gradients of the contour fields. However, the height errors of the numerical forecasts significantly exceeded those of the conventional forecasts.

(ii) The numerical forecasts of the 1000–500 millibar thickness field are superior, as measured by the computed statistics, to the corresponding conventional forecasts.

(iii) Although the objectively analysed charts do not agree with the conventionally analysed charts in detail, especially in the vicinity of deep depressions in areas of few observations, they serve as a basis for a numerical forecast which is statistically as good as that which proceeds from the subjective analyses.

(iv) Further investigation into methods of objective analysis is needed in order to improve the analysis, making it acceptable as an alternative to the conventional analysis.

(v) The main errors in the numerical forecasts arise from:

(*a*) Spurious anticyclogenesis which is a consequence of the assumption that the wind is geostrophic.

(*b*) The boundary conditions which it is necessary to assume in order to solve the equations.

(*c*) The neglect in the equations of the effect of topography.

(vi) There is no clear relation between vertical motion as computed by this model and precipitation observed at a given station.

Bibliography

1. SAWYER, J. S. and BUSHBY, F. H.; A baroclinic model atmosphere suitable for numerical integration. *J. Met., Lancaster, Pa.*, **10**, 1953, p. 54.
2. BUSHBY, F. H. and HINDS, M. K.; Further computations of 24-hr pressure changes based on a two-parameter model. *Quart. J.R. met. Soc., London*, **81**, 1955, p. 396.
3. JONES, D. E.; A note on the equation of mean motion as used in numerical prediction. (To be published.)
4. ARNASON, G. and CARSTENSEN, L. P.; The effects of vertical vorticity advection and turning of the vortex tubes in hemispheric forecasts with a two-level model. *Mon. Weath. Rev., Washington, D.C.*, **87**, 1959, p. 119.
5. BUSHBY, F. H. and HUCKLE, V.; Objective analysis in numerical forecasting. *Quart. J.R. met. Soc., London*, **83**, 1957, p. 232.
6. BERGGREN, R.; On the accuracy of 500 mb analysis with special reference to numerical forecasting. *Tellus, Stockholm*, **9**, 1957, p. 323.
7. SHUMAN, F. G.; Predictive consequences of certain physical inconsistencies in the geostrophic barotropic model. *Mon. Weath, Rev., Washington, D.C.*, **85**, 1957, p. 229.
8. KNIGHTING, E., JONES, D. E. and HINDS, M. K.; Numerical experiments in the integration of the meteorological equations of motion. *Quart. J.R. met. Soc., London*, **84**, 1958, p. 91.
9. KNIGHTING, E.; Some computations of vertical velocity profiles in the atmosphere. *Quart. J.R. met. Soc., London*, **86**, 1960, p. 318.

Appendix I

TABULATED RESULTS OF FIRST EXPERIMENT

1000-millibar contours verified against subjective analyses

		Numerical forecasts based on objective analyses					Numerical forecasts based on subjective analyses					CFO prebaratics				
		(*a*)	(*b*) m	(*c*)	(*d*) kt	(*e*)	(*a*)	(*b*) m	(*c*)	(*d*) kt	(*e*)	(*a*)	(*b*) m	(*c*)	(*d*) kt	(*e*)
Jan.	20	0·66	77	0·85	34	0·69	0·66	65	0·90	32	0·74	0·59	66	0·83	25	0·72
	21	0·46	85	0·85	22	0·85	0·51	77	0·85	22	0·85	0·46	72	0·77	25	0·71
	22	0·56	72	0·81	26	0·72	0·78	75	0·91	28	0·69	0·31	101	0·72	31	0·62
	27	0·69	64	0·87	25	0·55	0·81	59	0·90	29	0·57	0·69	68	0·92	20	0·71
	28	0·91	65	0·70	20	0·39	0·89	59	0·76	23	0·41	0·88	41	0·91	17	0·55
	29	0·88	71	0·88	18	0·70	0·83	74	0·83	19	0·67	0·94	28	0·94	15	0·79
Feb.	5	0·17	89	0·76	25	0·50	0·38	80	0·81	30	0·43	0·27	82	0·72	40	0·33
	10	0·76	112	0·78	36	0·39	0·77	108	0·81	37	0·41	0·75	77	0·87	29	0·61
	11	0·62	110	0·89	33	0·40	0·33	141	0·69	46	0·26	0·22	107	0·75	37	0·30
	12	0·71	115	0·80	27	0·54	0·76	106	0·85	33	0·47	0·81	64	0·89	25	0·65
	17	0·86	126	0·92	32	0·69	0·86	95	0·93	38	0·61	0·64	92	0·65	33	0·07
	18	0·68	93	0·87	21	0·69	0·70	82	0·83	22	0·62	0·65	68	0·70	22	0·41
	19	0·73	124	0·74	20	0·70	0·72	100	0·80	22	0·64	0·26	88	0·59	28	0·34
	24	0·58	59	0·92	23	0·52	0·52	76	0·92	29	0·38	0·59	74	0·85	28	0·43
	25	0·57	79	0·93	24	0·59	0·65	56	0·95	24	0·60	0·69	52	0·93	22	0·66
	26	0·36	101	0·84	34	0·50	0·38	90	0·83	43	0·44	0·61	71	0·89	30	0·64
Mar.	3	0·76	98	0·81	43	0·56	0·91	76	0·92	35	0·74	0·37	125	0·49	45	0·33
	4	0·66	92	0·81	33	0·71	0·87	73	0·93	31	0·83	0·91	61	0·88	27	0·76
	5	0·69	98	0·87	24	0·81	0·75	73	0·90	26	0·81	0·85	55	0·84	28	0·58
	10	0·71	74	0·93	24	0·69	0·67	82	0·90	26	0·65	0·90	42	0·95	16	0·83
	11	0·65	95	0·82	22	0·73	0·59	91	0·80	25	0·70	0·80	59	0·83	19	0·69
	12	0·80	61	0·85	23	0·72	0·76	73	0·87	30	0·64	0·88	47	0·89	21	0·76
	17	0·77	79	0·75	22	0·69	0·81	76	0·83	30	0·72	0·87	37	0·89	18	0·72
	19	0·27	115	0·83	26	0·49	0·37	110	0·85	31	0·35	0·52	70	0·92	22	0·63
	24	0·73	43	0·94	20	0·55	0·58	59	0·94	25	0·54	0·82	28	0·95	15	0·67
Apr.	1	0·64	81	0·83	19	0·62	0·59	72	0·78	24	0·58	0·65	35	0·96	13	0·83
	2	0·88	95	0·80	20	0·65	0·84	72	0·86	23	0·62	0·80	38	0·94	16	0·71
	7	0·77	73	0·95	23	0·65	0·73	77	0·92	29	0·53	0·82	39	0·96	17	0·73
	8	0·71	71	0·94	21	0·75	0·66	73	0·96	22	0·81	0·65	58	0·91	17	0·76
	9	0·57	111	0·82	22	0·66	0·49	135	0·79	25	0·61	0·87	41	0·92	16	0·73
	14	0·44	75	0·90	29	0·74	0·73	78	0·94	28	0·86	0·63	61	0·84	24	0·78
	15	0·26	94	0·73	30	0·57	0·25	92	0·85	28	0·70	0·72	50	0·87	19	0·78
	16	0·46	97	0·57	31	0·55	0·39	127	0·60	57	0·52	0·70	94	0·74	32	0·61
	21	0·86	52	0·86	17	0·63	0·78	53	0·90	19	0·62	0·89	25	0·94	12	0·80
	22	0·78	44	0·91	17	0·53	0·80	39	0·92	19	0·56	0·85	26	0·95	13	0·64
	23	0·29	50	0·86	22	0·40	0·23	62	0·85	25	0·41	0·56	37	0·89	19	0·51
	28	0·84	40	0·88	17	0·69	0·68	53	0·77	23	0·48	0·82	31	0·89	15	0·65
	29	0·84	40	0·81	21	0·61	0·79	46	0·77	24	0·61	0·67	71	0·62	22	0·52
May	5	0·79	34	0·81	17	0·67	0·87	28	0·89	17	0·68	0·59	43	0·63	19	0·45
	6	0·84	52	0·89	18	0·65	0·71	59	0·82	21	0·56	0·83	35	0·87	15	0·72
	7	0·65	70	0·86	20	0·62	0·63	51	0·89	20	0·89	0·19	73	0·67	38	0·28
	12	0·82	33	0·97	14	0·85	0·72	37	0·95	17	0·80	0·66	45	0·95	14	0·79
Mean correlations and root mean square errors (42 *cases*)																
		0·66	83	0·84	25	0·62	0·66	80	0·86	29	0·60	0·67	63	0·84	24	0·61

Column (*a*): Correlation coefficients between actual and forecast 24 hr height changes
(*b*): Root mean square height errors
(*c*): Correlation between actual and forecast heights
(*d*): Root mean square vector wind errors
(*e*): Stretch vector correlation between actual and forecast winds

	Numerical forecasts based on objective analyses					Numerical forecasts based on subjective analyses					CFO prebaratics				
	(*a*)	(*b*) m	(*c*)	(*d*) kt	(*e*)	(*a*)	(*b*) m	(*c*)	(*d*) kt	(*e*)	(*a*)	(*b*) m	(*c*)	(*d*) kt	(*e*)
Jan. 20	0·72	82	0·88	33	0·81	0·83	67	0·93	30	0·85	0·52	136	0·81	32	0·62
21	0·53	83	0·92	24	0·80	0·54	78	0·92	26	0·77	0·03	94	0·85	30	0·74
22	0·60	94	0·91	21	0·80	0·85	92	0·96	21	0·88	0·46	108	0·86	33	0·72
27	0·71	72	0·97	23	0·83	0·72	71	0·97	30	0·78	0·66	63	0·97	24	0·84
28	0·93	63	0·98	18	0·80	0·93	48	0·99	20	0·80	0·59	96	0·95	26	0·73
29	0·83	96	0·97	18	0·81	0·62	107	0·92	21	0·77	0·82	46	0·97	20	0·78
Feb. 5	0·42	103	0·85	27	0·70	0·48	95	0·84	32	0·67	0·76	80	0·88	26	0·78
10	0·58	101	0·94	38	0·62	0·60	100	0·95	35	0·67	0·56	83	0·96	36	0·68
11	0·63	91	0·94	30	0·66	0·68	114	0·90	39	0·66	0·51	90	0·92	41	0·39
12	0·50	83	0·97	22	0·84	0·49	95	0·95	32	0·70	0·57	75	0·96	26	0·76
17	0·87	143	0·97	30	0·81	0·95	78	0·99	25	0·87	0·55	115	0·89	37	0·53
18	0·90	95	0·97	20	0·89	0·92	82	0·96	22	0·85	0·88	98	0·87	38	0·50
19	0·95	87	0·98	15	0·93	0·92	72	0·97	18	0·87	—0·07	127	0·76	33	0·60
24	0·43	104	0·93	33	0·66	0·53	100	0·96	30	0·76	0·64	91	0·95	23	0·76
25	0·81	73	0·98	23	0·79	0·86	61	0·99	23	0·82	0·82	55	0·98	22	0·76
26	0·31	135	0·91	36	0·51	0·38	112	0·92	42	0·56	0·55	99	0·93	34	0·70
Mar. 3	0·63	106	0·89	36	0·73	0·84	71	0·96	32	0·83	0·43	99	0·89	38	0·66
4	0·65	89	0·93	28	0·86	0·88	71	0·97	24	0·92	0·80	89	0·89	27	0·85
5	0·75	95	0·92	28	0·81	0·68	90	0·89	32	0·79	0·74	79	0·90	26	0·86
10	0·63	77	0·97	25	0·84	0·57	88	0·95	28	0·81	0·76	58	0·97	20	0·90
11	0·82	85	0·95	22	0·86	0·85	78	0·95	24	0·85	0·66	92	0·90	29	0·73
12	0·86	72	0·95	22	0·82	0·82	92	0·97	28	0·80	0·94	54	0·97	21	0·84
17	0·87	72	0·85	27	0·74	0·88	84	0·86	35	0·77	0·86	62	0·89	24	0·80
19	0·30	145	0·83	37	0·62	0·29	145	0·84	41	0·55	0·77	72	0·94	30	0·74
24	0·94	49	0·98	18	0·88	0·92	47	0·97	23	0·84	0·91	48	0·97	20	0·85
Apr. 1	0·79	77	0·98	22	0·83	0·75	64	0·97	23	0·84	0·69	67	0·97	21	0·88
2	0·94	77	0·95	20	0·83	0·94	57	0·95	23	0·83	0·91	58	0·97	23	0·81
7	0·92	80	0·98	25	0·78	0·91	77	0·97	27	0·76	0·90	51	0·97	20	0·84
8	0·74	95	0·96	26	0·83	0·76	78	0·98	24	0·88	0·76	74	0·95	30	0·73
9	0·76	121	0·94	23	0·85	0·63	144	0·92	28	0·79	0·86	54	0·95	20	0·86
14	0·24	88	0·94	28	0·84	0·78	91	0·98	24	0·92	0·70	62	0·95	25	0·87
15	0·05	127	0·80	35	0·66	0·29	111	0·91	31	0·82	0·62	78	0·93	24	0·87
16	0·54	124	0·70	37	0·62	0·58	169	0·76	59	0·65	0·75	123	0·80	36	0·74
21	0·84	53	0·93	21	0·67	0·83	57	0·94	22	0·69	0·89	48	0·91	21	0·65
22	0·80	61	0·93	17	0·76	0·87	55	0·95	19	0·79	0·88	38	0·96	17	0·77
23	0·63	70	0·92	27	0·70	0·72	71	0·93	31	0·69	0·73	58	0·94	24	0·76
28	0·82	48	0·96	21	0·81	0·69	56	0·93	24	0·74	0·83	41	0·96	20	0·81
29	0·91	42	0·95	19	0·83	0·89	47	0·93	25	0·79	0·78	87	0·88	28	0·64
May 5	0·79	49	0·95	23	0·73	0·87	42	0·97	23	0·75	0·72	58	0·94	24	0·68
6	0·78	66	0·94	22	0·75	0·76	70	0·94	26	0·73	0·92	44	0·98	16	0·87
7	0·75	74	0·97	21	0·81	0·68	68	0·95	23	0·78	0·82	32	0·98	16	0·88
12	0·83	46	0·96	21	0·82	0·84	40	0·97	20	0·82	0·52	65	0·91	21	0·77
Mean correlations and root mean square errors (42 *cases*)															
	0·70	89	0·93	26	0·77	0·73	86	0·94	29	0·78	0·69	79	0·92	27	0·75

Column (*a*): Correlation coefficients between actual and forecast 24 hr height changes
(*b*): Root mean square height errors
(*c*): Correlation between actual and forecast heights
(*d*): Root mean square vector wind errors
(*e*): Stretch vector correlation between actual and forecast winds

	Numerical forecasts based on objective analyses					Numerical forecasts based on subjective analyses					CFO prebaratics				
	(*a*)	(*b*) m	(*c*)	(*d*) kt	(*e*)	(*a*)	(*b*) m	(*c*)	(*d*) kt	(*e*)	(*a*)	(*b*) m	(*c*)	(*d*) kt	(*e*)
Jan. 20	0·80	60	0·86	34	0·35	0·79	57	0·87	35	0·27	0·77	83	0·87	22	0·58
21	0·80	42	0·94	24	0·34	0·78	44	0·93	24	0·39	0·51	63	0·88	28	0·22
22	0·54	62	0·86	24	0·35	0·68	55	0·90	25	0·43	0·35	76	0·88	25	0·47
27	0·87	43	0·97	23	0·75	0·71	61	0·93	33	0·55	0·74	56	0·93	23	0·74
28	0·91	40	0·97	19	0·73	0·89	41	0·97	23	0·70	0·51	77	0·91	28	0·64
29	0·88	40	0·97	14	0·82	0·80	52	0·93	20	0·73	0·76	37	0·97	18	0·72
Feb. 5	0·61	74	0·47	29	0·34	0·80	58	0·72	28	0·60	0·81	70	0·68	41	0·45
10	0·76	78	0·88	31	0·53	0·75	76	0·89	32	0·57	0·83	63	0·88	31	0·53
11	0·77	74	0·84	38	0·37	0·77	82	0·85	40	0·48	0·58	91	0·77	43	0·21
12	0·84	64	0·95	24	0·76	0·79	71	0·93	35	0·67	0·83	51	0·95	22	0·76
17	0·78	68	0·86	32	0·44	0·81	61	0·88	31	0·46	0·42	100	0·71	31	0·32
18	0·95	35	0·96	19	0·79	0·93	42	0·94	21	0·73	0·87	79	0·77	33	0·41
19	0·87	52	0·96	18	0·81	0·82	55	0·95	21	0·73	0·19	84	0·76	26	0·47
24	0·63	68	0·88	28	0·61	0·70	69	0·89	26	0·60	0·45	85	0·89	32	0·47
25	0·92	33	0·97	17	0·79	0·89	35	0·97	21	0·75	0·84	40	0·95	20	0·64
26	0·69	68	0·89	26	0·63	0·63	72	0·87	35	0·46	0·76	70	0·91	26	0·69
Mar. 3	0·58	78	0·83	35	0·39	0·72	68	0·89	32	0·57	0·39	132	0·82	41	0·48
4	0·73	59	0·91	25	0·79	0·77	48	0·93	25	0·84	0·59	64	0·79	28	0·47
5	0·61	50	0·88	26	0·58	0·57	52	0·84	30	0·54	0·59	105	0·56	37	0·48
10	0·81	38	0·96	20	0·78	0·74	46	0·94	25	0·68	0·73	44	0·93	20	0·76
11	0·95	37	0·97	15	0·88	0·93	43	0·96	21	0·81	0·84	58	0·91	28	0·68
12	0·93	40	0·96	20	0·79	0·89	60	0·94	28	0·74	0·90	53	0·92	23	0·67
17	0·73	63	0·61	29	0·47	0·83	53	0·74	29	0·58	0·76	57	0·82	23	0·59
19	0·61	58	0·89	26	0·64	0·52	65	0·88	30	0·56	0·77	45	0·91	24	0·65
24	0·92	42	0·92	21	0·73	0·92	40	0·93	20	0·70	0·89	46	0·91	21	0·67
Apr. 1	0·69	46	0·96	22	0·67	0·69	49	0·95	26	0·64	0·64	56	0·92	20	0·69
2	0·93	39	0·96	19	0·77	0·92	45	0·94	21	0·74	0·92	44	0·93	21	0·74
7	0·82	64	0·86	27	0·48	0·84	61	0·88	28	0·47	0·93	30	0·96	15	0·74
8	0·72	57	0·89	25	0·65	0·82	42	0·92	23	0·68	0·47	69	0·79	29	0·18
9	0·78	36	0·91	20	0·65	0·80	37	0·91	23	0·58	0·71	38	0·90	19	0·68
14	0·50	53	0·87	27	0·52	0·72	54	0·91	26	0·73	0·45	54	0·94	20	0·77
15	0·38	71	0·75	25	0·59	0·62	54	0·86	25	0·71	0·78	44	0·94	23	0·79
16	0·74	72	0·77	28	0·52	0·81	94	0·84	34	0·58	0·80	64	0·79	26	0·65
21	0·70	42	0·86	21	0·52	0·76	39	0·88	20	0·56	0·67	43	0·88	18	0·55
22	0·61	43	0·85	19	0·47	0·76	40	0·90	20	0·59	0·85	30	0·93	16	0·62
23	0·82	41	0·90	23	0·61	0·87	39	0·92	27	0·58	0·83	45	0·92	21	0·73
28	0·91	26	0·97	17	0·78	0·81	36	0·95	22	0·67	0·78	45	0·95	19	0·69
29	0·86	38	0·94	21	0·72	0·89	36	0·94	26	0·66	0·69	54	0·90	30	0·52
May 5	0·72	39	0·95	18	0·62	0·76	38	0·95	21	0·62	0·82	33	0·97	16	0·69
6	0·71	39	0·94	17	0·75	0·71	40	0·94	21	0·62	0·85	51	0·96	15	0·82
7	0·79	31	0·96	18	0·67	0·70	39	0·94	20	0·60	0·47	67	0·84	36	0·50
12	0·71	30	0·88	17	0·43	0·65	32	0·86	17	0·45	0·21	45	0·72	17	0·40
Mean correlations and root mean square errors (42 *cases*)															
	0·76	53	0·89	24	0·62	0·78	54	0·90	26	0·61	0·68	64	0·87	26	0·58

Column (*a*): Correlation coefficients between actual and forecast 24 hr height changes
(*b*): Root mean square height errors
(*c*): Correlation between actual and forecast heights
(*d*): Root mean square vector wind errors
(*e*): Stretch vector correlation between actual and forecast winds

	Numerical forecasts based on objective analyses					Numerical forecasts based on subjective analyses					CFO prebaratics				
	(*a*)	(*b*) m	(*c*)	(*d*) kt	(*e*)	(*a*)	(*b*) m	(*c*)	(*d*) kt	(*e*)	(*a*)	(*b*) m	(*c*)	(*d*) kt	(*e*)
Jan. 20	0·65	71	0·89	31	0·76	0·72	60	0·92	30	0·80	0·63	60	0·86	22	0·77
21	0·48	78	0·89	22	0·84	0·58	69	0·88	22	0·83	0·49	63	0·82	23	0·76
22	0·69	66	0·90	23	0·78	0·75	73	0·92	27	0·71	0·26	97	0·75	30	0·64
27	0·72	57	0·89	22	0·62	0·77	62	0·87	31	0·49	0·63	67	0·94	17	0·79
28	0·93	61	0·75	16	0·61	0·92	55	0·82	20	0·61	0·90	37	0·94	13	0·73
29	0·90	56	0·90	14	0·75	0·86	59	0·85	16	0·68	0·92	28	0·93	13	0·75
Feb. 5	0·65	61	0·89	19	0·63	0·46	76	0·84	27	0·54	0·39	75	0·77	36	0·50
10	0·76	91	0·84	24	0·54	0·75	88	0·87	27	0·57	0·50	68	0·94	20	0·67
11	0·53	99	0·92	26	0·55	0·06	134	0·71	41	0·37	0·12	102	0·73	34	0·30
12	0·62	108	0·79	25	0·53	0·72	99	0·84	32	0·45	0·83	63	0·90	21	0·72
17	0·86	123	0·92	32	0·69	0·86	91	0·94	37	0·62	0·64	92	0·66	31	0·14
18	0·79	83	0·90	18	0·79	0·82	73	0·86	19	0·72	0·76	63	0·74	22	0·40
19	0·75	119	0·73	19	0·71	0·72	96	0·78	21	0·63	0·08	89	0·54	27	0·30
24	0·35	59	0·92	22	0·50	0·41	72	0·94	26	0·46	0·64	71	0·87	23	0·59
25	0·37	75	0·93	22	0·64	0·57	53	0·06	22	0·66	0·66	51	0·93	20	0·71
26	0·42	94	0·86	29	0·57	0·38	84	0·86	40	0·48	0·67	55	0·93	25	0·73
Mar. 3	0·77	94	0·83	40	0·61	0·91	75	0·93	34	0·76	0·38	122	0·51	42	0·36
4	0·62	94	0·79	35	0·65	0·86	77	0·91	34	0·78	0·88	64	0·86	25	0·78
5	0·74	91	0·91	23	0·83	0·76	67	0·93	27	0·82	0·87	53	0·82	25	0·59
10	0·75	71	0·93	23	0·73	0·70	80	0·90	26	0·45	0·91	41	0·95	14	0·86
11	0·77	79	0·89	19	0·80	0·71	45	0·87	22	0·79	0·87	58	0·89	15	0·80
12	0·84	49	0·88	18	0·79	0·78	65	0·90	28	0·67	0·92	45	0·92	17	0·78
17	0·75	64	0·84	18	0·77	0·74	70	0·85	31	0·68	0·81	32	0·92	15	0·79
19	0·34	93	0·86	23	0·49	0·53	88	0·90	24	0·53	0·54	53	0·91	24	0·39
24	0·73	38	0·97	18	0·61	0·58	58	0·96	24	0·62	0·76	27	0·95	14	0·67
Apr. 1	0·68	72	0·85	18	0·67	0·62	64	0·81	23	0·63	0·68	39	0·96	13	0·83
2	0·89	86	0·83	17	0·75	0·88	62	0·89	19	0·75	0·82	40	0·94	13	0·80
7	0·77	70	0·97	20	0·75	0·76	71	0·95	26	0·66	0·89	29	0·98	13	0·83
8	0·71	64	0·96	19	0·82	0·66	68	0·98	20	0·87	0·53	57	0·92	17	0·75
9	0·56	104	0·86	20	0·72	0·49	128	0·84	24	0·65	0·83	45	0·91	17	0·66
14	0·34	80	0·90	28	0·75	0·72	82	0·95	28	0·86	0·73	56	0·86	23	0·79
15	0·25	92	0·75	29	0·55	0·21	93	0·86	28	0·69	0·69	49	0·88	16	0·82
16	0·50	99	0·58	27	0·62	0·39	126	0·60	56	0·59	0·76	96	0·78	27	0·72
21	0·82	48	0·86	17	0·65	0·69	51	0·90	18	0·63	0·87	21	0·94	11	0·78
22	0·81	41	0·92	15	0·59	0·85	35	0·93	17	0·61	0·78	28	0·93	13	0·62
23	0·29	43	0·91	16	0·60	0·20	57	0·90	21	0·53	0·66	27	0·94	13	0·67
28	0·85	37	0·91	14	0·74	0·66	50	0·79	22	0·50	0·80	28	0·93	12	0·73
29	0·85	36	0·85	16	0·75	0·80	41	0·81	21	0·70	0·64	67	0·64	20	0·58
May 5	0·86	28	0·87	14	0·74	0·90	26	0·92	14	0·75	0·71	36	0·66	15	0·55
6	0·83	46	0·90	17	0·67	0·73	53	0·85	21	0·59	0·85	31	0·90	15	0·71
7	0·69	59	0·91	17	0·70	0·68	40	0·93	18	0·69	0·22	70	0·69	37	0·29
12	0·81	30	0·98	13	0·87	0·73	34	0·96	16	0·83	0·56	49	0·94	15	0·77
Mean correlations and root mean square errors (42 *cases*)															
	0·66	76	0·87	22	0·68	0·66	74	0·86	27	0·65	0·67	60	0·84	22	0·65

Column (*a*): Correlation coefficients between actual and forecast 24 hr height changes
(*b*): Root mean square height errors
(*c*): Correlation between actual and forecast heights
(*d*): Root mean square vector wind errors
(*e*): Stretch vector correlation between actual and forecast winds

	Numerical forecasts based on objective analyses					Numerical forecasts based on subjective analyses					CFO prebaratics				
	(a)	(b) m	(c)	(d) kt	(e)	(a)	(b) m	(c)	(d) kt	(e)	(a)	(b) m	(c)	(d) kt	(e)
Jan. 20	0·80	66	0·93	27	0·88	0·89	56	0·95	26	0·90	0·52	127	0·85	30	0·69
21	0·66	76	0·95	20	0·87	0·69	68	0·95	21	0·85	0·21	85	0·88	29	0·76
22	0·65	75	0·94	21	0·84	0·81	82	0·96	24	0·83	0·44	94	0·89	29	0·77
27	0·73	59	0·98	18	0·89	0·70	71	0·97	30	0·78	0·54	64	0·97	23	0·85
28	0·93	61	0·98	17	0·83	0·94	45	0·99	18	0·82	0·49	96	0·95	24	0·77
29	0·93	67	0·99	13	0·90	0·80	75	0·96	16	0·86	0·69	47	0·97	18	0·79
Feb. 5	0·61	58	0·93	18	0·76	0·48	93	0·81	31	0·70	0·70	89	0·80	30	0·70
10	0·71	75	0·97	26	0·81	0·70	76	0·98	25	0·83	0·41	82	0·96	30	0·76
11	0·57	76	0·97	24	0·76	0·56	115	0·90	40	0·63	0·18	80	0·93	31	0·63
12	0·36	74	0·97	19	0·87	0·58	87	0·96	29	0·75	0·65	61	0·97	22	0·81
17	0·80	130	0·97	30	0·82	0·92	76	0·98	31	0·78	0·37	99	0·90	34	0·56
18	0·92	83	0·98	18	0·91	0·93	72	0·97	19	0·88	0·86	99	0·87	37	0·50
19	0·96	78	0·98	15	0·93	0·93	63	0·97	18	0·88	−0·18	128	0·76	33	0·60
24	0·63	82	0·96	26	0·79	0·68	83	0·98	24	0·85	0·66	77	0·97	23	0·76
25	0·88	60	0·99	20	0·85	0·87	54	0·99	22	0·84	0·81	61	0·98	21	0·75
26	0·48	76	0·97	25	0·76	0·50	67	0·97	34	0·53	0·50	85	0·95	50	0·78
Mar. 3	0·69	91	0·92	34	0·73	0·86	60	0·95	33	0·80	0·47	81	0·92	31	0·71
4	0·73	78	0·95	28	0·86	0·91	64	0·97	25	0·91	0·79	96	0·88	28	0·84
5	0·83	73	0·96	22	0·90	0·71	74	0·92	26	0·87	0·69	84	0·89	26	0·87
10	0·70	65	0·98	20	0·89	0·64	76	0·97	24	0·84	0·74	55	0·97	18	0·91
11	0·88	71	0·98	18	0·91	0·89	68	0·97	22	0·89	0·72	83	0·94	26	0·78
12	0·89	50	0·98	16	0·90	0·83	82	0·98	26	0·84	0·92	56	0·98	18	0·86
17	0·89	57	0·89	23	0·80	0·86	82	0·85	36	0·77	0·83	60	0·91	23	0·79
19	0·63	92	0·94	22	0·83	0·65	91	0·95	25	0·80	0·80	44	0·97	21	0·78
24	0·96	45	0·99	16	0·91	0·93	50	0·97	23	0·84	0·92	41	0·97	18	0·84
Apr. 1	0·84	57	0·98	19	0·86	0·79	48	0·98	20	0·88	0·75	72	0·98	19	0·91
2	0·96	71	0·96	16	0·87	0·94	54	0·96	20	0·86	0·88	60	0·98	19	0·86
7	0·93	68	0·98	22	0·84	0·92	68	0·97	25	0·79	0·86	58	0·97	23	0·77
8	0·78	84	0·97	25	0·84	0·76	74	0·98	24	0·88	0·73	80	0·95	29	0·72
9	0·78	103	0·96	20	0·87	0·65	127	0·94	26	0·82	0·83	65	0·94	20	0·85
14	0·38	76	0·97	24	0·86	0·78	94	0·97	27	0·92	0·67	64	0·95	23	0·87
15	0·14	104	0·89	29	0·73	0·40	94	0·96	28	0·87	0·71	61	0·97	21	0·89
16	0·61	107	0·80	30	0·73	0·65	163	0·80	56	0·71	0·75	118	0·84	33	0·78
21	0·89	38	0·97	15	0·80	0·81	48	0·96	18	0·78	0·82	44	0·93	17	0·68
22	0·80	50	0·95	15	0·80	0·88	47	0·96	19	0·79	0·87	30	0·98	14	0·80
23	0·71	55	0·95	20	0·79	0·78	64	0·96	27	0·74	0·79	46	0·96	19	0·82
28	0·82	48	0·96	19	0·82	0·69	51	0·95	21	0·78	0·78	42	0·96	17	0·85
29	0·90	40	0·96	16	0·87	0·88	45	0·93	22	0·85	0·75	79	0·90	25	0·69
May 5	0·84	36	0·97	16	0·82	0·87	37	0·97	18	0·82	0·77	48	0·96	16	0·78
6	0·83	52	0·97	17	0·84	0·77	60	0·96	24	0·76	0·89	48	0·98	16	0·88
7	0·79	62	0·98	17	0·84	0·75	58	0·97	20	0·81	0·79	27	0·99	13	0·90
12	0·89	33	0·98	15	0·91	0·90	29	0·98	16	0·89	0·36	73	0·90	20	0·78
Mean correlation coefficients and root mean square errors (42 *cases*)															
	0·76	72	0·96	21	0·84	0·77	75	0·95	26	0·80	0·66	75	0·93	25	0·78

Column (*a*): Correlation coefficients between actual and forecast 24 hr height changes
(*b*): Root mean square height errors
(*c*): Correlation between actual and forecast heights
(*d*): Root mean square vector wind errors
(*e*): Stretch vector correlation between actual and forecast winds

	Numerical forecasts based on objective analyses					Numerical forecasts based on subjective analyses					CFO prebaratics				
	(*a*)	(*b*) m	(*c*)	(*d*) kt	(*e*)	(*a*)	(*b*) m	(*c*)	(*d*) kt	(*e*)	(*a*)	(*b*) m	(*c*)	(*d*) kt	(*e*)
Jan. 20	0·88	51	0·90	29	0·56	0·86	48	0·90	29	0·52	0·82	79	0·90	22	0·60
21	0·88	34	0·96	23	0·36	0·89	34	0·96	21	0·56	0·65	54	0·91	26	0·37
22	0·64	48	0·91	23	0·41	0·64	50	0·91	27	0·31	0·37	55	0·91	26	0·39
27	0·88	38	0·98	21	0·78	0·70	58	0·93	32	0·56	0·66	56	0·92	24	0·72
28	0·94	36	0·97	17	0·78	0·92	37	0·97	22	0·75	0·53	72	0·94	25	0·74
29	0·95	27	0·98	11	0·87	0·91	38	0·96	16	0·83	0·87	31	0·97	15	0·79
Feb. 5	0·83	41	0·67	19	0·56	0·90	44	0·73	26	0·62	0·78	79	0·52	42	0·37
10	0·58	56	0·95	24	0·70	0·57	56	0·95	28	0·68	0·46	59	0·90	29	0·55
11	0·76	60	0·92	28	0·58	0·72	76	0·89	36	0·53	0·31	81	0·83	36	0·31
12	0·84	58	0·96	22	0·79	0·77	72	0·93	36	0·63	0·87	39	0·97	18	0·82
17	0·83	54	0·89	28	0·56	0·87	48	0·91	28	0·53	0·33	97	0·68	30	0·29
18	0·96	34	0·96	18	0·82	0·94	43	0·93	20	0·76	0·84	83	0·75	34	0·36
19	0·88	54	0·96	17	0·81	0·84	55	0·96	21	0·75	0·28	77	0·81	24	0·57
24	0·86	49	0·94	23	0·74	0·87	55	0·93	24	0·64	0·60	75	0·93	29	0·57
25	0·94	32	0·98	15	0·84	0·89	38	0·97	21	0·76	0·84	44	0·95	20	0·66
26	0·51	57	0·92	28	0·56	0·46	67	0·88	37	0·39	0·67	55	0·93	25	0·73
Mar. 3	0·70	69	0·88	32	0·45	0·79	60	0·92	33	0·54	0·39	124	0·86	39	0·52
4	0·81	59	0·92	25	0·81	0·79	51	0·92	30	0·75	0·72	58	0·85	24	0·75
5	0·69	42	0·92	21	0·71	0·58	50	0·85	28	0·61	0·54	109	0·53	36	0·51
10	0·82	37	0·96	20	0·79	0·74	46	0·90	26	0·65	0·75	45	0·93	19	0·51
11	0·96	30	0·98	13	0·92	0·95	37	0·97	18	0·88	0·85	50	0·93	26	0·72
12	0·95	32	0·98	17	0·84	0·89	61	0·94	28	0·73	0·88	52	0·93	21	0·71
17	0·79	55	0·73	26	0·59	0·87	50	0·77	29	0·55	0·80	51	0·89	23	0·59
19	0·90	30	0·97	19	0·77	0·87	34	0·97	22	0·74	0·50	61	0·89	24	0·62
24	0·95	36	0·95	18	0·79	0·94	36	0·94	19	0·72	0·91	41	0·92	18	0·72
Apr. 1	0·69	41	0·97	19	0·74	0·64	49	0·96	25	0·70	0·68	54	0·94	19	0·72
2	0·92	35	0·97	16	0·83	0·92	43	0·94	20	0·78	0·91	45	0·92	20	0·75
7	0·91	45	0·93	21	0·72	0·93	41	0·94	22	0·70	0·89	39	0·94	17	0·68
8	0·81	50	0·91	23	0·72	0·87	40	0·92	21	0·76	0·56	74	0·78	30	0·10
9	0·84	31	0·93	18	0·70	0·82	36	0·93	22	0·60	0·72	41	0·89	18	0·70
14	0·70	41	0·93	22	0·58	0·80	53	0·90	27	0·67	0·73	43	0·97	18	0·78
15	0·65	49	0·87	22	0·61	0·74	45	0·89	26	0·67	0·84	40	0·95	22	0·84
16	0·82	61	0·87	23	0·63	0·88	98	0·84	33	0·61	0·79	60	0·81	27	0·61
21	0·69	39	0·89	18	0·61	0·76	37	0·90	19	0·62	0·57	39	0·91	16	0·59
22	0·59	35	0·90	15	0·60	0·72	36	0·91	19	0·62	0·86	21	0·96	13	0·69
23	0·89	32	0·94	19	0·71	0·88	38	0·92	25	0·65	0·90	39	0·95	18	0·81
28	0·91	26	0·97	16	0·79	0·80	34	0·95	21	0·70	0·72	48	0·94	18	0·69
29	0·85	36	0·85	16	0·75	0·91	33	0·95	24	0·72	0·72	46	0·93	26	0·61
May 5	0·75	31	0·97	14	0·72	0·78	34	0·96	19	0·70	0·71	36	0·66	15	0·55
6	0·79	32	0·96	16	0·74	0·75	35	0·95	20	0·64	0·87	51	0·95	18	0·70
7	0·80	20	0·96	17	0·67	0·73	39	0·94	20	0·60	0·48	69	0·82	37	0·56
12	0·81	30	0·98	13	0·87	0·74	26	0·92	15	0·64	0·02	47	0·71	17	0·40
Mean correlations and root mean square errors (42 *cases*)															
	0·81	43	0·93	21	0·70	0·81	49	0·92	25	0·65	0·67	61	0·87	25	0·60

Column (*a*): Correlation coefficients between actual and forecast 24 hr height changes
(*b*): Root mean square height errors
(*c*): Correlation between actual and forecast heights
(*d*): Root mean square vector wind errors
(*e*): Stretch vector correlation between actual and forecast winds

	1000 mb contours				500–1000 mb thickness contours				500 mb contours			
	(*a*) m	(*b*)	(*c*) kt	(*d*)	(*a*) m	(*b*)	(*c*) kt	(*d*)	(*a*) m	(*b*)	(*c*) kt	(*d*)
Jan. 20	86	0·76	34	0·54	88	0·71	34	0·06	125	0·82	41	0·50
21	48	0·88	26	0·73	73	0·85	24	0·15	82	0·87	30	0·64
22	91	0·72	31	0·49	67	0·81	26	0·08	108	0·84	35	0·59
27	76	0·85	28	0·39	76	0·86	35	0·42	73	0·95	35	0·62
28	76	0·84	22	0·38	69	0·88	27	0·54	90	0·94	30	0·65
29	83	0·41	30	−0·07	57	0·91	25	0·44	85	0·92	30	0·49
Feb. 5	76	0·80	27	0·39	106	0·36	36	0·19	96	0·81	34	0·54
10	115	0·77	79	0·17	109	0·71	78	0·21	95	0·93	42	0·49
11	97	0·81	44	0·19	112	0·56	44	−0·01	92	0·92	42	0·44
12	66	0·91	32	0·43	86	0·86	35	0·44	65	0·97	32	0·64
17	121	0·67	42	0·80	108	0·61	40	0·01	129	0·84	45	0·40
18	52	0·91	19	0·67	85	0·77	29	0·38	108	0·90	29	0·74
19	70	0·75	26	0·40	84	0·74	24	0·56	102	0·86	27	0·73
24	68	0·85	29	0·22	75	0·80	32	0·24	101	0·90	38	0·42
25	44	0·94	22	0·60	70	0·84	23	0·56	79	0·94	29	0·67
26	86	0·83	38	0·24	91	0·78	29	0·34	111	0·91	37	0·41
Mar. 3	130	0·54	49	0·03	73	0·85	30	0·27	111	0·88	47	0·45
4	90	0·73	39	0·53	74	0·81	27	0·55	117	0·85	39	0·71
5	83	0·72	32	0·63	63	0·80	31	0·37	116	0·79	44	0·57
10	90	0·83	23	0·68	72	0·85	27	0·54	83	0·92	33	0·70
11	78	0·74	27	0·43	110	0·63	38	0·09	108	0·85	37	0·53
12	87	0·54	35	0·23	89	0·55	32	0·22	125	0·77	43	0·31
17	74	0·54	35	0·14	61	0·81	31	0·48	122	0·57	49	0·22
19	77	0·85	30	0·31	96	0·40	38	−0·13	113	0·84	40	0·55
24	45	0·87	23	0·51	63	0·90	26	0·39	108	0·78	41	0·38
Apr. 1	46	0·90	18	0·67	96	0·74	30	0·35	76	0·95	28	0·72
2	59	0·76	24	0·36	76	0·76	32	0·11	127	0·81	41	0·42
7	62	0·89	25	0·34	69	0·77	30	0·10	112	0·87	458	0·33
8	76	0·84	23	0·55	58	0·81	23	0·54	112	0·88	39	0·49
9	69	0·79	25	0·43	46	0·91	23	0·60	101	0·85	37	0·55
14	58	0·86	32	0·63	68	0·79	25	0·63	67	0·94	31	0·79
15	75	0·81	27	0·65	106	0·33	41	−0·10	110	0·87	29	0·83
16	95	0·38	32	0·48	54	0·81	23	0·25	152	0·46	48	0·37
21	50	0·72	22	0·39	52	0·77	27	0·05	82	0·73	33	0·21
22	43	0·85	19	0·49	66	0·71	31	0·06	71	0·83	32	0·27
23	41	0·86	19	0·53	53	0·87	23	0·53	81	0·86	36	0·36
28	51	0·62	23	0·34	71	0·76	36	0·13	68	0·87	32	0·52
29	78	0·26	30	0·08	50	0·91	22	0·42	107	0·69	41	0·19
May 5	54	0·40	23	0·30	57	0·90	24	0·41	76	0·86	30	0·46
6	63	0·56	24	0·34	48	0·93	20	0·60	81	0·85	33	0·49
7	54	0·86	18	0·63	39	0·78	16	0·46	56	0·94	25	0·72
12	54	0·90	18	0·63	106	0·60	33	0·28	73	0·88	26	0·64
Mean correlations and root mean square errors (42 *cases*)												
	75	0·75	31	0·41	78	0·76	32	0·31	100	0·85	37	0·52

Column (*a*): Root mean square height errors
(*b*): Correlation between actual and persistence heights
(*c*): Root mean square vector wind errors
(*d*): Stretch vector correlation between actual and persistence winds

Appendix II

TABULATED RESULTS OF SECOND EXPERIMENT

1000–millibar contours verified against subjective analyses

	Numerical forecasts based on objective analyses					Numerical forecasts based on subjective analyses					CFO prebaratics				
	(*a*)	(*b*) m	(*c*)	(*d*) kt	(*e*)	(*a*)	(*b*) m	(*c*)	(*d*) kt	(*e*)	(*a*)	(*b*) m	(*c*)	(*d*) kt	(*e*)
June 30	0·65	55	0·80	22	0·56	0·72	62	0·86	25	0·59	0·71	59	0·83	19	0·70
July 1	0·68	44	0·90	22	0·55	0·70	60	0·93	24	0·60	0·74	38	0·91	18	0·66
2	0·24	50	0·92	18	0·72	0·42	47	0·94	19	0·77	0·80	26	0·95	15	0·80
7	0·68	37	0·81	14	0·55	0·70	35	0·82	15	0·57	0·78	28	0·82	14	0·51
8	0·67	36	0·89	17	0·53	0·59	35	0·86	19	0·41	0·50	33	0·84	17	0·45
9	0·73	37	0·91	16	0·61	0·70	33	0·88	18	0·50	0·61	30	0·85	16	0·50
14	0·91	21	0·95	12	0·69	0·86	25	0·93	17	0·57	0·87	28	0·92	13	0·63
15	0·77	25	0·94	14	0·71	0·73	27	0·94	15	0·69	0·57	29	0·92	14	0·67
16	0·66	24	0·95	13	0·73	0·62	30	0·95	14	0·75	0·64	30	0·96	12	0·77
21	0·62	36	0·90	15	0·56	0·52	38	0·87	17	0·53	0·72	21	0·94	13	0·67
22	0·62	40	0·89	14	0·61	0·62	35	0·91	16	0·64	0·61	27	0·91	13	0·61
23	0·60	30	0·89	15	0·55	0·34	34	0·83	18	0·45	0·66	25	0·89	16	0·45
28	0·24	41	0·79	15	0·55	0·09	47	0·75	15	0·52	0·56	27	0·87	15	0·38
29	0·78	30	0·93	12	0·60	0·75	29	0·93	14	0·59	0·76	24	0·93	12	0·50
30	0·57	33	0·82	17	0·34	0·57	35	0·85	17	0·42	0·70	28	0·84	13	0·55
Aug. 11	0·53	32	0·84	13	0·55	0·56	30	0·89	13	0·62	0·38	31	0·80	11	0·61
12	0·56	41	0·65	18	0·49	0·71	37	0·73	17	0·59	0·53	40	0·67	18	0·57
13	0·81	39	0·79	25	0·45	0·79	40	0·78	26	0·48	0·74	44	0·77	26	0·47
18	0·70	59	0·87	15	0·71	0·71	55	0·91	18	0·70	0·88	29	0·83	13	0·70
19	0·75	64	0·87	15	0·66	0·61	57	0·85	18	0·59	0·75	40	0·78	19	0·43
20	0·76	35	0·92	15	0·63	0·70	31	0·93	16	0·64	0·77	26	0·92	15	0·65
25	0·76	41	0·71	14	0·65	0·72	44	0·72	16	0·64	0·77	46	0·69	15	0·57
26	0·68	30	0·76	13	0·69	0·67	32	0·75	16	0·58	0·73	30	0·81	12	0·74
27	0·43	41	0·73	19	0·51	0·36	44	0·69	19	0·56	0·49	36	0·80	17	0·61
Sept. 2	0·52	45	0·66	17	0·51	0·63	41	0·75	17	0·63	0·86	36	0·92	13	0·75
3	0·70	48	0·83	15	0·79	0·71	50	0·83	19	0·69	0·53	49	0·77	21	0·61
8	0·82	22	0·96	13	0·78	0·63	28	0·91	16	0·64	0·61	30	0·91	14	0·66
9	0·64	30	0·96	13	0·79	0·68	29	0·96	15	0·75	0·75	28	0·95	12	0·77
10	0·69	38	0·82	14	0·57	0·45	53	0·81	19	0·48	0·89	29	0·83	12	0·60
29	0·63	70	0·84	23	0·61	0·53	73	0·85	24	0·64	0·59	52	0·83	22	0·66
30	0·82	55	0·91	21	0·60	0·80	59	0·89	26	0·60	0·58	73	0·76	28	0·16
Oct. 1	0·54	52	0·91	11	0·73	0·57	51	0·93	21	0·73	0·88	28	0·97	13	0·88
6	0·56	53	0·88	21	0·52	0·54	51	0·86	23	0·48	0·24	53	0·81	23	0·41
7	0·59	75	0·82	27	0·60	0·31	106	0·61	34	0·42	0·69	58	0·87	26	0·66
8	0·76	90	0·84	29	0·58	0·90	58	0·93	28	0·74	0·63	78	0·77	27	0·56
13	0·89	58	0·91	17	0·76	0·90	53	0·92	20	0·72	0·83	68	0·88	23	0·55
14	0·85	40	0·91	18	0·47	0·70	48	0·88	20	0·43	0·85	41	0·93	15	0·54
15	0·27	74	0·83	18	0·50	0·37	62	0·89	20	0·57	0·60	37	0·89	17	0·52
20	0·57	76	0·89	26	0·47	0·55	80	0·92	31	0·50	0·77	55	0·91	23	0·57
21	0·81	70	0·95	21	0·66	0·78	76	0·95	23	0·67	0·82	43	0·96	16	0·79
22	0·85	47	0·96	18	0·77	0·67	53	0·94	27	0·66	0·78	46	0·94	20	0·68
27	0·88	60	0·96	21	0·85	0·78	84	0·89	31	0·71	0·88	64	0·93	28	0·65
28	0·50	110	0·86	38	0·29	0·34	129	0·80	44	0·34	0·95	54	0·89	24	0·48
29	0·79	45	0·94	20	0·62	0·76	48	0·92	25	0·56	0·75	42	0·92	16	0·71
Nov. 3	0·85	76	0·93	21	0·78	0·64	75	0·85	30	0·63	0·85	43	0·91	19	0·76
4	0·62	101	0·84	23	0·66	0·58	73	0·78	27	0·58	0·84	39	0·90	18	0·71
5	0·33	116	0·46	32	0·09	0·41	100	0·45	44	0·05	0·84	42	0·92	20	0·67
10	0·62	47	0·88	17	0·58	0·54	60	0·87	19	0·52	0·65	39	0·91	17	0·49
11	0·34	52	0·86	19	0·57	0·18	61	0·84	22	0·49	0·77	29	0·93	15	0·72
12	0·73	58	0·84	27	0·55	0·77	55	0·85	31	0·58	0·23	85	0·48	33	0·18
Mean correlations and root mean square errors (50 cases)															
	0·65	55	0·86	19	0·60	0·61	57	0·85	23	0·58	0·70	43	0·86	18	0·60

Column (*a*): Correlation coefficients between actual and forecast 24 hr height changes; (*b*): Root mean square height errors; (*c*): Correlation between actual and forecast heights; (*d*): Root mean square vector wind errors; (*e*): Stretch vector correlation between actual and forecast winds

	Numerical forecasts based on objective analyses					Numerical forecasts based on subjective analyses					CFO prebaratics				
	(*a*)	(*b*)	(*c*)	(*d*)	(*e*)	(*a*)	(*b*)	(*c*)	(*d*)	(*e*)	(*a*)	(*b*)	(*c*)	(*d*)	(*e*)
		m		kt			m		kt			m		kt	
June 30	0·66	71	0·91	25	0·68	0·78	67	0·94	25	0·74	0·66	69	0·93	24	0·72
July 1	0·82	45	0·97	20	0·75	0·79	67	0·96	25	0·94	0·91	39	0·98	16	0·82
2	0·68	50	0·99	17	0·79	0·78	45	0·98	16	0·86	0·78	28	0·99	15	0·85
7	0·90	43	0·96	13	0·87	0·91	37	0·97	15	0·85	0·87	43	0·95	17	0·77
8	0·91	43	0·98	13	0·89	0·91	38	0·98	14	0·87	0·85	29	0·97	19	0·78
9	0·74	47	0·95	18	0·76	0·75	42	0·95	19	0·75	0·56	40	0·94	20	0·73
14	0·82	32	0·97	13	0·65	0·84	27	0·97	14	0·70	0·74	36	0·96	15	0·58
15	0·78	44	0·97	15	0·74	0·89	30	0·98	12	0·84	0·64	54	0·96	16	0·74
16	0·72	38	0·97	16	0·85	0·80	32	0·98	14	0·88	0·86	33	0·99	12	0·91
21	0·86	42	0·97	14	0·79	0·86	40	0·97	15	0·77	0·56	47	0·92	16	0·73
22	0·64	51	0·96	15	0·79	0·77	47	0·97	12	0·88	0·65	49	0·95	15	0·82
23	0·75	38	0·97	15	0·77	0·71	38	0·95	17	0·72	0·64	46	0·98	18	0·61
28	0·62	34	0·96	13	0·90	0·59	36	0·95	16	0·85	0·73	29	0·96	16	0·85
29	0·86	33	0·96	14	0·88	0·81	36	0·95	14	0·88	0·69	41	0·93	17	0·78
30	0·73	40	0·92	14	0·86	0·71	45	0·92	15	0·85	0·78	36	0·92	18	0·67
Aug. 11	0·73	26	0·98	12	0·87	0·65	32	0·98	15	0·82	0·33	39	0·96	16	0·78
12	0·47	47	0·95	19	0·76	0·66	44	0·96	17	0·80	0·35	48	0·94	16	0·84
13	0·80	43	0·96	20	0·80	0·79	42	0·96	21	0·78	0·45	97	0·82	67	0·38
18	0·68	72	0·94	15	0·85	0·84	59	0·96	15	0·88	0·48	55	0·88	18	0·78
19	0·82	71	0·95	15	0·83	0·77	56	0·95	16	0·82	0·85	29	0·96	14	0·87
20	0·89	46	0·97	16	0·81	0·87	33	0·98	17	0·83	0·78	42	0·94	20	0·69
25	0·66	48	0·66	17	0·85	0·79	39	0·98	18	0·88	0·44	53	0·95	19	0·82
26	0·89	37	0·95	13	0·88	0·86	37	0·95	16	0·84	0·77	48	0·94	17	0·82
27	0·86	33	0·97	13	0·83	0·77	39	0·96	17	0·75	0·79	45	0·93	18	0·71
Sept. 2	0·39	55	0·87	17	0·67	0·59	48	0·93	17	0·73	0·83	34	0·98	15	0·80
3	0·64	42	0·92	16	0·77	0·65	46	0·90	20	0·73	0·35	53	0·88	21	0·61
8	0·88	36	0·95	14	0·88	0·81	41	0·92	18	0·78	0·84	38	0·94	17	0·81
9	0·93	43	0·97	13	0·90	0·93	34	0·98	17	0·86	0·83	44	0·93	15	0·88
10	0·80	48	0·93	19	0·70	0·72	60	0·93	22	0·69	0·78	51	0·92	22	0·63
29	0·82	94	0·94	26	0·80	0·81	93	0·94	26	0·81	0·61	83	0·88	29	0·75
30	0·54	79	0·94	24	0·79	0·61	84	0·90	29	0·73	0·44	68	0·92	23	0·80
Oct. 1	0·35	74	0·93	24	0·73	0·62	54	0·97	22	0·79	0·23	82	0·94	27	0·75
6	0·65	52	0·96	18	0·78	0·64	53	0·95	21	0·73	0·23	59	0·92	22	0·72
7	0·41	95	0·91	28	0·79	0·14	127	0·83	34	0·64	0·39	81	0·89	31	0·69
8	0·82	86	0·97	22	0·88	0·91	41	0·98	21	0·92	0·74	55	0·95	24	0·85
13	0·83	68	0·96	17	0·85	0·87	59	0·95	19	0·85	0·70	91	0·89	30	0·58
14	0·74	68	0·95	17	0·81	0·72	63	0·94	26	0·72	0·85	35	0·98	17	0·81
15	0·57	94	0·95	21	0·79	0·83	60	0·98	18	0·89	0·86	35	0·98	17	0·87
20	0·71	110	0·93	32	0·72	0·78	108	0·97	36	0·77	0·85	79	0·96	31	0·74
21	0·86	84	0·98	21	0·84	0·83	87	0·98	23	0·85	0·86	55	0·98	19	0·87
22	0·83	67	0·99	21	0·86	0·62	82	0·96	34	0·73	0·57	80	0·95	28	0·68
27	0·87	72	0·97	23	0·91	0·69	107	0·92	37	0·77	0·81	86	0·94	32	0·80
28	0·50	124	0·94	31	0·72	0·38	138	0·91	34	0·71	0·89	57	0·98	21	0·85
29	0·93	38	0·98	22	0·82	0·91	45	0·98	23	0·83	0·84	53	0·96	21	0·81
Nov. 3	0·96	52	0·98	20	0·91	0·83	92	0·92	40	0·72	0·89	72	0·91	24	0·81
4	0·76	124	0·93	28	0·84	0·86	76	0·95	30	0·81	0·85	66	0·96	28	0·80
5	0·72	148	0·86	34	0·63	0·87	95	0·92	28	0·76	0·91	67	0·94	26	0·79
10	0·75	42	0·99	17	0·89	0·69	57	0·98	19	0·85	0·70	48	0·98	18	0·87
11	–0·06	61	0·97	24	0·82	–0·06	67	0·97	27	0·78	0·73	44	0·99	19	0·89
12	0·87	70	0·97	27	0·78	0·78	79	0·92	37	0·67	0·23	126	0·81	48	0·32

Mean correlations and root mean square errors (*50 cases*)

	(*a*)	(*b*)	(*c*)	(*d*)	(*e*)	(*a*)	(*b*)	(*c*)	(*d*)	(*e*)	(*a*)	(*b*)	(*c*)	(*d*)	(*e*)
Mean	0·73	66	0·95	20	0·81	0·74	63	0·95	23	0·80	0·68	58	0·94	23	0·76

Column (*a*): Correlation coefficients between actual and forecast 24 hr height changes; (*b*): Root mean square height errors; (*c*): Correlation between actual and forecast heights; (*d*): Root mean square vector wind errors; (*e*): Stretch vector correlation between actual and forecast winds

	Numerical forecasts based on objective analyses					Numerical forecasts based on subjective analyses					CFO prebaratics				
	(*a*)	(*b*) m	(*c*)	(*d*) kt	(*e*)	(*a*)	(*b*) m	(*c*)	(*d*) kt	(*e*)	(*a*)	(*b*) m	(*c*)	(*d*) kt	(*e*)
June 30	0·62	41	0·89	23	0·44	0·63	43	0·88	25	0·46	0·74	37	0·94	18	0·64
July 1	0·65	38	0·89	19	0·40	0·66	41	0·88	22	0·50	0·76	42	0·93	16	0·54
2	0·60	36	0·95	15	0·29	0·54	38	0·94	18	0·32	0·83	23	0·97	14	0·48
7	0·91	25	0·97	11	0·89	0·89	27	0·97	13	0·85	0·87	41	0·95	15	0·82
8	0·82	34	0·96	18	0·80	0·82	35	0·95	20	0·77	0·75	39	0·93	24	0·67
9	0·89	26	0·95	14	0·84	0·83	34	0·92	18	0·80	0·79	35	0·93	18	0·77
14	0·76	25	0·94	12	0·75	0·77	27	0·93	16	0·64	0·77	27	0·93	15	0·64
15	0·66	41	0·92	15	0·64	0·59	39	0·93	14	0·68	0·70	45	0·92	16	0·56
16	0·72	41	0·90	18	0·63	0·79	35	0·91	16	0·74	0·79	35	0·95	14	0·80
21	0·84	28	0·92	15	0·71	0·86	25	0·95	13	0·78	0·61	46	0·89	16	0·69
22	0·80	23	0·95	12	0·67	0·72	30	0·92	15	0·62	0·63	65	0·85	19	0·63
23	0·74	30	0·95	15	0·64	0·74	30	0·93	16	0·61	0·41	55	0·84	21	0·42
28	0·52	30	0·90	14	0·78	0·50	34	0·89	15	0·75	0·58	32	0·89	15	0·78
29	0·59	31	0·92	14	0·79	0·57	32	0·90	14	0·77	0·48	33	0·89	17	0·65
30	0·79	27	0·92	14	0·79	0·75	32	0·89	16	0·75	0·72	32	0·91	17	0·69
Aug. 11	0·83	21	0·98	11	0·86	0·80	23	0·97	13	0·81	0·69	29	0·96	14	0·77
12	0·23	35	0·94	17	0·65	0·53	29	0·96	15	0·75	0·49	34	0·95	16	0·68
13	0·66	32	0·96	22	0·65	0·60	38	0·94	23	0·64	0·17	96	0·75	69	0·17
18	0·65	40	0·87	18	0·67	0·77	34	0·90	18	0·71	0·60	42	0·90	15	0·76
19	0·81	31	0·91	13	0·77	0·80	32	0·90	17	0·72	0·79	51	0·83	20	0·79
20	0·86	26	0·95	14	0·73	0·88	25	0·95	16	0·69	0·76	39	0·91	17	0·63
25	0·71	35	0·95	15	0·78	0·66	35	0·95	17	0·78	0·43	41	0·94	19	0·75
26	0·93	23	0·97	13	0·78	0·92	27	0·97	17	0·70	0·85	35	0·95	15	0·69
27	0·65	38	0·94	19	0·49	0·61	41	0·93	20	0·49	0·68	41	0·93	19	0·45
Sept. 2	0·55	31	0·93	15	0·54	0·75	26	0·96	15	0·69	0·78	30	0·96	14	0·67
3	0·88	24	0·97	11	0·83	0·86	39	0·92	16	0·76	0·60	37	0·92	18	0·57
8	0·84	34	0·82	15	0·71	0·89	28	0·89	15	0·76	0·86	30	0·84	15	0·66
9	0·90	34	0·88	13	0·77	0·91	28	0·90	15	0·75	0·81	40	0·78	14	0·68
10	0·86	25	0·93	12	0·65	0·83	29	0·92	16	0·58	0·80	32	0·92	18	0·47
29	0·85	42	0·93	20	0·72	0·78	54	0·84	29	0·55	0·39	65	0·79	28	0·53
30	0·78	46	0·83	21	0·65	0·82	46	0·82	24	0·64	0·62	62	0·77	26	0·67
Oct. 1	0·83	39	0·90	17	0·55	0·87	31	0·93	18	0·62	0·61	72	0·83	25	0·52
6	0·84	30	0·95	16	0·77	0·71	45	0·95	20	0·72	0·64	43	0·90	22	0·58
7	0·93	42	0·95	18	0·81	0·86	50	0·92	24	0·71	0·55	83	0·79	34	0·36
8	0·85	47	0·90	24	0·71	0·97	40	0·95	22	0·85	0·62	78	0·90	26	0·72
13	0·63	45	0·84	21	0·56	0·67	50	0·80	24	0·50	0·72	40	0·89	20	0·55
14	0·61	42	0·93	14	0·73	0·69	34	0·94	20	0·63	0·83	33	0·94	16	0·71
15	0·59	42	0·95	17	0·75	0·76	32	0·96	18	0·76	0·69	36	0·95	19	0·70
20	0·86	66	0·89	26	0·76	0·88	67	0·92	35	0·70	0·83	102	0·83	40	0·44
21	0·92	41	0·96	25	0·61	0·91	42	0·96	25	0·67	0·93	36	0·96	18	0·76
22	0·90	38	0·98	18	0·79	0·72	62	0·93	36	0·54	0·62	67	0·90	27	0·45
27	0·88	51	0·94	23	0·78	0·71	62	0·87	32	0·54	0·66	66	0·88	29	0·60
28	0·72	61	0·88	36	0·39	0·75	66	0·87	36	0·47	0·65	92	0·90	30	0·67
29	0·89	36	0·94	22	0·72	0·87	43	0·94	27	0·65	0·81	48	0·91	20	0·75
Nov. 3	0·96	44	0·95	19	0·84	0·89	69	0·85	41	0·55	0·82	64	0·79	23	0·68
4	0·87	55	0·90	25	0·72	0·87	53	0·91	30	0·72	0·90	66	0·90	25	0·71
5	0·87	61	0·90	29	0·61	0·85	62	0·89	44	0·52	0·86	59	0·88	28	0·58
10	0·75	39	0·97	17	0·85	0·86	30	0·98	16	0·87	0·82	34	0·98	17	0·82
11	–0·02	49	0·96	23	0·70	0·20	51	0·96	23	0·73	0·35	40	0·98	21	0·70
12	0·76	55	0·94	26	0·64	0·69	73	0·88	35	0·52	0·28	76	0·87	35	0·31
Mean correlations and root mean square errors (50 cases)															
	0·75	39	0·93	19	0·69	0·75	42	0·92	22	0·67	0·68	52	0·90	23	0·63

Column (*a*): Correlation coefficients between actual and forecast 24 hr height changes; (*b*): Root mean square height errors; (*c*): Correlation between actual and forecast heights; (*d*): Root mean square vector wind errors; (*e*): Stretch vector correlation between actual and forecast winds

		Numerical forecasts based on objective analyses					Numerical forecasts based on subjective analyses					CFO prebaratics				
		(*a*)	(*b*) m	(*c*)	(*d*) kt	(*e*)	(*a*)	(*b*) m	(*c*)	(*d*) kt	(*e*)	(*a*)	(*b*) m	(*c*)	(*d*) kt	(*e*)
June	30	0·59	49	0·84	20	0·56	0·62	61	0·87	25	0·56	0·70	55	0·84	17	0·69
July	1	0·68	41	0·92	19	0·59	0·71	61	0·93	23	0·61	0·71	36	0·91	15	0·69
	2	0·21	48	0·93	16	0·75	0·24	45	0·94	19	0·77	0·78	26	0·95	14	0·82
	7	0·64	35	0·83	12	0·65	0·63	34	0·83	14	0·63	0·78	25	0·85	12	0·60
	8	0·80	29	0·95	10	0·83	0·73	28	0·93	12	0·71	0·63	27	0·92	10	0·71
	9	0·76	27	0·95	10	0·82	0·77	22	0·94	13	0·74	0·54	29	0·92	11	0·68
	14	0·92	19	0·96	10	0·79	0·89	23	0·95	15	0·68	0·87	26	0·93	12	0·67
	15	0·85	19	0·96	11	0·80	0·85	23	0·96	11	0·82	0·57	26	0·94	10	0·78
	16	0·67	23	0·96	10	0·83	0·63	33	0·95	13	0·79	0·73	32	0·97	9	0·85
	21	0·83	27	0·95	10	0·77	0·76	29	0·92	14	0·66	0·79	18	0·95	9	0·77
	22	0·45	33	0·92	12	0·71	0·64	30	0·92	15	0·66	0·62	30	0·93	10	0·70
	23	0·63	20	0·94	10	0·79	0·41	28	0·87	14	0·62	0·56	30	0·90	12	0·61
	28	−0·02	40	0·80	12	0·72	−0·08	45	0·77	13	0·66	0·38	24	0·91	11	0·63
	29	0·74	28	0·94	9	0·76	0·77	27	0·94	13	0·64	0·71	21	0·94	9	0·62
	30	0·57	30	0·88	12	0·58	0·63	32	0·91	13	0·64	0·75	21	0·91	8	0·66
Aug.	11	0·63	29	0·88	12	0·60	0·62	28	0·91	13	0·57	0·45	27	0·85	12	0·55
	12	0·66	36	0·71	16	0·56	0·76	33	0·76	15	0·62	0·60	39	0·71	16	0·61
	13	0·79	40	0·83	18	0·68	0·83	36	0·86	18	0·71	0·66	46	0·75	21	0·61
	18	0·67	55	0·88	14	0·76	0·65	53	0·89	18	0·71	0·91	27	0·86	12	0·74
	19	0·70	52	0·87	13	0·70	0·57	50	0·84	17	0·63	0·80	47	0·80	16	0·53
	20	0·66	33	0·91	13	0·67	0·58	35	0·91	15	0·67	0·73	29	0·91	13	0·71
	25	0·74	38	0·75	12	0·74	0·68	42	0·75	15	0·68	0·75	44	0·73	12	0·70
	26	0·70	28	0·77	10	0·80	0·70	30	0·76	13	0·70	0·78	27	0·84	10	0·77
	27	0·59	28	0·84	10	0·81	0·44	35	0·75	14	0·69	0·59	24	0·91	12	0·72
Sept.	2	0·46	42	0·68	13	0·66	0·58	40	0·76	15	0·70	0·81	38	0·92	12	0·77
	3	0·73	37	0·85	12	0·82	0·74	41	0·85	17	0·74	0·48	46	0·79	18	0·66
	8	0·75	25	0·95	13	0·79	0·67	29	0·91	16	0·61	0·53	29	0·91	14	0·65
	9	0·52	30	0·97	12	0·84	0·50	31	0·97	13	0·82	0·63	31	0·96	11	0·82
	10	0·58	38	0·83	13	0·63	0·35	55	0·81	19	0·48	0·85	29	0·85	11	0·62
	29	0·58	60	0·89	16	0·68	0·40	70	0·86	22	0·62	0·48	41	0·87	16	0·70
	30	0·85	47	0·94	17	0·66	0·84	52	0·92	24	0·66	0·60	64	0·81	23	0·32
Oct.	1	0·54	47	0·92	17	0·78	0·53	50	0·94	20	0·75	0·91	23	0·98	12	0·89
	6	0·57	51	0·90	17	0·57	0·55	49	0·87	21	0·48	0·32	45	0·86	17	0·58
	7	0·60	63	0·87	21	0·71	0·28	95	0·66	28	0·53	0·71	47	0·90	22	0·69
	8	0·75	78	0·84	24	0·62	0·86	67	0·90	30	0·42	0·67	63	0·78	20	0·64
	13	0·83	61	0·90	19	0·68	0·86	54	0·92	22	0·67	0·81	65	0·90	20	0·66
	14	0·87	34	0·83	14	0·66	0·68	45	0·89	18	0·55	0·83	42	0·95	12	0·69
	15	0·35	68	0·87	16	0·60	0·55	54	0·92	18	0·66	0·58	35	0·91	14	0·65
	20	0·60	72	0·89	25	0·44	0·59	77	0·92	29	0·52	0·75	56	0·91	23	0·51
	21	0·81	66	0·95	19	0·73	0·77	72	0·95	21	0·76	0·82	47	0·96	13	0·85
	22	0·82	46	0·96	17	0·77	0·58	56	0·93	28	0·62	0·70	49	0·93	19	0·68
	27	0·88	54	0·97	21	0·84	0·81	66	0·94	25	0·82	0·91	55	0·94	23	0·72
	28	0·59	106	0·89	32	0·49	0·46	124	0·84	40	0·45	0·96	52	0·89	20	0·54
	29	0·72	50	0·94	20	0·59	0·73	48	0·93	24	0·60	0·74	40	0·91	14	0·76
Nov.	3	0·89	65	0·96	17	0·86	0·65	68	0·89	27	0·69	0·86	44	0·92	14	0·82
	4	0·49	96	0·85	22	0·68	0·50	68	0·79	27	0·56	0·84	32	0·93	16	0·75
	5	0·31	110	0·51	26	0·20	0·38	95	0·46	41	0·80	0·86	39	0·93	16	0·78
	10	0·69	41	0·90	16	0·60	0·62	52	0·89	18	0·55	0·72	31	0·94	14	0·60
	11	0·28	48	0·90	16	0·68	0·13	58	0·88	19	0·56	0·74	28	0·94	13	0·77
	12	0·77	52	0·88	22	0·65	0·82	49	0·89	28	0·65	0·17	83	0·47	30	0·21
Mean correlations and root mean square errors (50 *cases*)																
		0·65	50	0·88	16	0·69	0·61	53	0·87	21	0·63	0·69	40	0·88	15	0·68

Column (*a*): Correlation coefficients between actual and forecast 24 hr height changes; (*b*): Root mean square height errors; (*c*): Correlation between actual and forecast heights; (*d*): Root mean square vector wind errors; (*e*): Stretch vector correlation between actual and forecast winds

	Numerical forecasts based on objective analyses					Numerical forecasts based on subjective analyses					CFO prebaratics				
	(*a*)	(*b*) m	(*c*)	(*d*) kt	(*e*)	(*a*)	(*b*) m	(*c*)	(*d*) kt	(*e*)	(*a*)	(*b*) m	(*c*)	(*d*) kt	(*e*)
June 30	0·68	59	0·93	18	0·77	0·75	61	0·95	22	0·80	0·72	55	0·94	19	0·75
July 1	0·84	38	0·98	16	0·81	0·81	63	0·97	23	0·78	0·90	39	0·98	14	0·84
2	0·72	42	0·99	15	0·82	0·70	44	0·97	19	0·82	0·78	29	0·99	14	0·89
7	0·89	33	0·97	11	0·90	0·90	29	0·98	13	0·87	0·86	46	0·95	15	0·81
8	0·92	38	0·98	10	0·92	0·92	36	0·98	13	0·89	0·87	26	0·98	17	0·80
9	0·81	33	0·96	12	0·88	0·81	32	0·96	14	0·86	0·57	39	0·95	16	0·80
14	0·86	28	0·97	11	0·75	0·89	23	0·98	12	0·76	0·75	35	0·96	14	0·62
15	0·77	33	0·97	12	0·77	0·84	27	0·98	11	0·84	0·65	40	0·96	14	0·68
16	0·78	27	0·98	12	0·87	0·79	35	0·98	14	0·88	0·74	42	0·98	14	0·88
21	0·87	36	0·98	11	0·86	0·84	36	0·97	14	0·80	0·61	41	0·94	15	0·74
22	0·67	40	0·97	12	0·82	0·79	39	0·97	12	0·84	0·59	43	0·95	16	0·79
23	0·81	26	0·98	10	0·86	0·74	30	0·96	14	0·80	0·60	38	0·95	14	0·73
28	0·73	32	0·96	12	0·91	0·64	36	0·95	16	0·85	0·78	29	0·96	16	0·83
29	0·90	25	0·98	10	0·93	0·85	32	0·97	12	0·91	0·71	34	0·94	15	0·82
30	0·73	36	0·94	12	0·89	0·72	42	0·93	15	0·86	0·74	33	0·94	18	0·67
Aug. 11	0·77	22	0·99	10	0·91	0·69	29	0·98	14	0·85	0·33	37	0·96	15	0·80
12	0·54	30	0·98	14	0·82	0·65	32	0·97	16	0·80	0·37	40	0·97	14	0·85
13	0·75	37	0·97	16	0·85	0·71	39	0·96	19	0·80	0·43	98	0·82	66	0·38
18	0·81	53	0·97	11	0·89	0·84	45	0·97	14	0·91	0·59	47	0·93	14	0·83
19	0·84	52	0·98	10	0·91	0·63	43	0·96	13	0·88	0·69	35	0·95	13	0·88
20	0·86	42	0·98	14	0·83	0·81	37	0·98	17	0·81	0·77	39	0·95	18	0·71
25	0·73	38	0·97	13	0·91	0·77	36	0·98	18	0·89	0·22	62	0·93	20	0·81
26	0·88	34	0·96	11	0·92	0·84	35	0·96	16	0·84	0·75	46	0·95	16	0·84
27	0·90	25	0·98	10	0·89	0·82	31	0·97	14	0·82	0·83	41	0·94	16	0·75
Sept. 2	0·29	45	0·93	13	0·75	0·38	47	0·95	17	0·72	0·64	43	0·98	16	0·80
3	0·47	34	0·94	12	0·84	0·60	41	0·90	18	0·75	0·25	47	0·91	18	0·69
8	0·89	31	0·96	12	0·90	0·84	37	0·94	16	0·81	0·84	34	0·94	15	0·82
9	0·89	38	0·97	13	0·89	0·89	36	0·97	18	0·84	0·76	48	0·92	16	0·88
10	0·82	38	0·96	14	0·84	0·76	52	0·96	17	0·83	0·77	45	0·95	18	0·75
29	0·88	68	0·97	17	0·88	0·73	77	0·96	23	0·85	0·56	65	0·90	24	0·79
30	0·67	57	0·97	18	0·85	0·72	65	0·93	26	0·78	0·53	59	0·92	19	0·85
Oct. 1	0·52	48	0·97	17	0·81	0·67	42	0·98	19	0·83	0·16	93	0·94	26	0·77
6	0·69	41	0·97	13	0·88	0·74	46	0·97	17	0·81	0·08	54	0·94	18	0·82
7	0·51	55	0·96	15	0·86	0·07	95	0·88	27	0·66	0·39	63	0·93	22	0·77
8	0·80	57	0·98	16	0·91	0·80	59	0·98	24	0·91	0·50	48	0·96	17	0·90
13	0·79	54	0·96	14	0·85	0·82	52	0·94	21	0·82	0·56	105	0·87	28	0·59
14	0·79	49	0·97	15	0·83	0·73	53	0·95	25	0·74	0·79	44	0·98	16	0·81
15	0·59	83	0·95	18	0·80	0·74	62	0·98	20	0·86	0·84	34	0·98	15	0·87
20	0·70	96	0·94	28	0·76	0·78	111	0·78	36	0·79	0·85	87	0·96	29	0·75
21	0·77	77	0·98	19	0·86	0·78	78	0·98	22	0·87	0·84	59	0·98	17	0·90
22	0·81	67	0·99	21	0·86	0·59	84	0·96	34	0·72	0·63	72	0·96	25	0·73
27	0·89	60	0·99	19	0·94	0·70	92	0·95	33	0·82	0·74	84	0·95	31	0·80
28	0·60	119	0·96	26	0·81	0·53	133	0·93	32	0·74	0·91	54	0·98	20	0·85
29	0·74	40	0·91	14	0·76	0·89	48	0·98	23	0·83	0·81	53	0·96	21	0·81
Nov. 3	0·97	44	0·98	18	0·93	0·85	88	0·94	36	0·79	0·88	74	0·91	23	0·83
4	0·78	108	0·94	25	0·88	0·86	69	0·95	28	0·84	0·88	72	0·96	25	0·84
5	0·77	117	0·91	25	0·75	0·89	67	0·95	22	0·82	0·94	57	0·95	23	0·82
10	0·84	32	0·99	15	0·90	0·80	48	0·98	17	0·87	0·77	42	0·98	16	0·88
11	−0·13	49	0·99	16	0·90	−0·16	58	0·98	20	0·87	0·71	41	0·99	16	0·90
12	0·90	51	0·98	18	0·89	0·80	69	0·93	31	0·74	0·25	111	0·83	41	0·41
Mean correlations and root mean square errors (50 *cases*)															
	0·75	53	0·97	15	0·86	0·73	57	0·96	21	0·82	0·65	56	0·95	21	0·78

Column (*a*): Correlation coefficients between actual and forecast 24 hr height changes; (*b*): Root mean square height errors; (*c*): Correlation between actual and forecast heights; (*d*): Root mean square vector wind errors; (*e*): Stretch vector correlation between actual and forecast winds

	Numerical forecasts based on objective analyses					Numerical forecasts based on subjective analyses					CFO prebaratics				
	(*a*)	(*b*) m	(*c*)	(*d*) kt	(*e*)	(*a*)	(*b*) m	(*c*)	(*d*) kt	(*e*)	(*a*)	(*b*) m	(*c*)	(*d*) kt	(*e*)
June 30	0·76	29	0·93	16	0·66	0·72	35	0·91	21	0·63	0·77	33	0·92	17	0·55
July 1	0·61	36	0·90	17	0·37	0·66	37	0·89	22	0·49	0·71	45	0·92	17	0·44
2	0·63	28	0·97	13	0·49	0·55	33	0·94	17	0·44	0·80	24	0·97	13	0·54
7	0·91	23	0·98	10	0·90	0·89	27	0·97	13	0·85	0·87	46	0·95	14	0·83
8	0·88	26	0·97	11	0·91	0·84	31	0·95	13	0·89	0·81	29	0·96	18	0·78
9	0·86	27	0·85	13	0·87	0·77	37	0·91	17	0·81	0·72	32	0·94	17	0·79
14	0·80	23	0·95	10	0·82	0·81	26	0·93	13	0·72	0·80	28	0·93	13	0·69
15	0·73	29	0·92	12	0·68	0·73	30	0·91	12	0·69	0·77	34	0·94	13	0·57
16	0·66	32	0·91	13	0·61	0·56	36	0·90	16	0·61	0·63	38	0·94	14	0·75
21	0·85	26	0·93	12	0·83	0·83	26	0·94	13	0·78	0·75	39	0·93	14	0·75
22	0·85	19	0·96	11	0·73	0·82	27	0·92	14	0·64	0·69	64	0·83	19	0·64
23	0·78	22	0·95	10	0·72	0·75	25	0·93	12	0·67	0·36	53	0·87	17	0·50
28	0·69	25	0·94	13	0·82	0·61	32	0·90	15	0·74	0·78	26	0·93	13	0·84
29	0·67	26	0·93	10	0·86	0·69	28	0·92	12	0·83	0·58	27	0·92	13	0·76
30	0·85	20	0·95	10	0·87	0·75	29	0·90	15	0·76	0·73	26	0·93	16	0·72
Aug. 11	0·85	18	0·98	10	0·88	0·81	22	0·97	12	0·85	0·68	29	0·96	14	0·77
12	0·66	23	0·98	13	0·78	0·78	19	0·98	12	0·82	0·78	22	0·98	12	0·79
13	0·88	19	0·98	11	0·87	0·84	26	0·97	14	0·83	0·20	100	0·74	69	0·14
18	0·78	28	0·91	15	0·72	0·84	29	0·91	16	0·75	0·65	39	0·93	13	0·77
19	0·75	29	0·92	12	0·80	0·76	31	0·90	16	0·75	0·76	56	0·78	21	0·77
20	0·84	26	0·95	13	0·77	0·84	28	0·94	16	0·69	0·74	40	0·91	16	0·65
25	0·81	23	0·98	10	0·90	0·69	29	0·96	14	0·86	0·05	45	0·92	21	0·71
26	0·95	18	0·99	9	0·87	0·84	22	0·98	14	0·77	0·87	31	0·96	13	0·77
27	0·83	25	0·97	12	0·74	0·81	29	0·96	14	0·69	0·77	35	0·94	14	0·56
Sept. 2	0·60	24	0·97	10	0·72	0·51	33	0·94	16	0·61	0·45	35	0·93	16	0·52
3	0·89	23	0·97	11	0·79	0·89	37	0·91	19	0·63	0·74	34	0·94	16	0·64
8	0·86	30	0·86	13	0·76	0·91	24	0·92	13	0·80	0·87	26	0·87	14	0·67
9	0·90	31	0·89	12	0·82	0·89	29	0·88	17	0·69	0·76	42	0·75	13	0·68
10	0·84	23	0·95	10	0·76	0·77	31	0·91	16	0·60	0·82	27	0·94	15	0·65
29	0·91	25	0·95	16	0·78	0·82	42	0·87	25	0·61	0·47	57	0·83	25	0·58
30	0·83	34	0·88	19	0·71	0·85	39	0·85	24	0·64	0·55	66	0·77	25	0·69
Oct. 1	0·91	26	0·94	13	0·72	0·87	32	0·93	17	0·68	0·64	85	0·83	25	0·48
6	0·87	26	0·97	13	0·83	0·79	44	0·97	17	0·82	0·68	36	0·93	18	0·69
7	0·88	32	0·96	15	0·78	0·79	43	0·93	23	0·71	0·38	88	0·77	32	0·23
8	0·84	43	0·93	20	0·79	0·93	58	0·90	27	0·81	0·62	84	0·94	23	0·81
13	0·74	38	0·87	18	0·64	0·79	44	0·84	22	0·59	0·69	50	0·86	18	0·58
14	0·74	29	0·95	14	0·73	0·75	29	0·95	19	0·65	0·87	31	0·94	16	0·73
15	0·82	25	0·97	12	0·84	0·78	30	0·96	18	0·76	0·61	44	0·94	18	0·67
20	0·87	56	0·92	24	0·78	0·87	69	0·92	35	0·71	0·83	111	0·81	38	0·44
21	0·94	33	0·97	20	0·74	0·93	39	0·97	23	0·72	0·93	35	0·96	16	0·77
22	0·84	44	0·98	20	0·74	0·64	65	0·92	37	0·50	0·62	60	0·92	24	0·52
27	0·91	44	0·95	22	0·79	0·77	59	0·89	30	0·57	0·68	64	0·88	27	0·60
28	0·75	58	0·89	31	0·50	0·78	66	0·86	35	0·49	0·68	90	0·91	27	0·73
29	0·90	36	0·95	22	0·71	0·86	46	0·94	27	0·63	0·80	43	0·93	19	0·77
Nov. 3	0·96	42	0·95	17	0·88	0·90	67	0·86	39	0·61	0·83	60	0·80	21	0·68
4	0·87	48	0·91	22	0·78	0·86	55	0·91	31	0·71	0·90	72	0·91	24	0·72
5	0·89	44	0·94	23	0·73	0·83	60	0·90	41	0·59	0·85	54	0·90	24	0·61
10	0·83	33	0·98	15	0·87	0·90	29	0·98	16	0·87	0·89	30	0·98	16	0·84
11	0·20	40	0·97	17	0·82	0·47	45	0·97	20	0·80	0·44	38	0·98	18	0·75
12	0·84	41	0·97	20	0·79	0·79	59	0·92	30	0·66	0·29	73	0·88	33	0·30
Mean correlations and root mean square errors (*50 cases*)															
	0·81	32	0·94	15	0·77	0·78	40	0·92	21	0·70	0·68	52	0·90	22	0·65

Column (*a*): Correlation coefficients between actual and forecast 24 hr height changes; (*b*): Root mean square height errors; (*c*): Correlation between actual and forecast heights; (*d*): Root mean square vector wind errors; (*e*): Stretch vector correlation between actual and forecast winds

	1000 mb contours				500–1000 mb thickness contours				500 mb contours			
	(*a*) m	(*b*)	(*c*) kt	(*d*)	(*a*) m	(*b*)	(*c*) kt	(*d*)	(*a*) m	(*b*)	(*c*) kt	(*d*)
June 30	71	0·62	28	0·35	50	0·84	23	0·50	94	0·83	31	0·54
July 1	52	0·82	26	0·45	46	0·88	22	0·36	71	0·90	30	0·55
2	43	0·90	20	0·64	40	0·92	17	0·41	43	0·97	21	0·71
7	39	0·70	18	0·37	58	0·85	23	0·54	76	0·84	24	0·61
8	31	0·79	19	0·35	57	0·85	24	0·63	54	0·90	21	0·71
9	37	0·75	22	0·24	53	0·87	26	0·56	44	0·93	22	0·67
14	49	0·73	20	0·33	36	0·88	17	0·58	52	0·90	20	0·47
15	41	0·88	16	0·60	52	0·83	19	0·46	70	0·92	18	0·63
16	27	0·94	14	0·72	57	0·79	21	0·47	51	0·94	19	0·76
21	32	0·88	15	0·58	40	0·87	19	0·48	52	0·90	22	0·50
22	27	0·93	13	0·66	35	0·87	17	0·47	45	0·93	19	0·67
23	30	0·85	18	0·39	44	0·84	19	0·35	47	0·91	23	0·47
28	32	0·81	16	0·36	35	0·89	15	0·76	43	0·92	18	0·81
29	36	0·82	15	0·43	39	0·87	18	0·63	58	0·86	24	0·67
30	39	0·77	18	0·23	43	0·82	19	0·61	56	0·85	24	0·57
Aug. 11	33	0·89	14	0·51	34	0·93	16	0·72	41	0·96	15	0·81
12	46	0·49	19	0·39	31	0·96	14	0·74	52	0·93	21	0·69
13	60	0·31	33	0·03	42	0·92	25	0·51	60	0·89	29	0·56
18	39	0·79	19	0·53	47	0·84	18	0·65	47	0·93	19	0·80
19	43	0·73	17	0·56	51	0·77	21	0·48	55	0·87	23	0·64
20	34	0·81	19	0·39	46	0·80	22	0·34	60	0·86	28	0·45
25	63	0·57	19	0·49	41	0·93	18	0·71	55	0·96	18	0·86
26	40	0·62	16	0·56	61	0·83	20	0·54	73	0·84	23	0·73
27	42	0·74	20	0·47	48	0·90	19	0·55	53	0·90	18	0·76
Sept. 2	51	0·63	20	0·44	36	0·90	18	0·40	58	0·87	22	0·54
3	61	0·64	25	0·34	49	0·85	20	0·37	52	0·87	23	0·46
8	35	0·86	18	0·48	56	0·59	24	0·35	73	0·80	28	0·47
9	29	0·92	15	0·66	65	0·36	24	0·21	78	0·78	28	0·49
10	53	0·67	19	0·29	48	0·72	19	0·29	79	0·77	29	0·29
29	62	0·73	29	0·37	60	0·85	24	0·65	87	0·85	34	0·69
30	89	0·68	31	0·36	57	0·78	27	0·43	69	0·92	29	0·75
Oct. 1	53	0·89	25	0·50	59	0·71	24	0·29	55	0·95	28	0·69
6	48	0·85	26	0·31	56	0·82	28	0·39	57	0·93	24	0·70
7	70	0·73	32	0·44	96	0·69	36	0·15	84	0·89	36	0·56
8	78	0·74	30	0·60	89	0·72	35	0·37	81	0·90	33	0·72
13	65	0·71	32	0·11	59	0·83	24	0·13	83	0·84	37	0·28
14	48	0·84	24	0·23	37	0·91	19	0·52	55	0·93	27	0·58
15	52	0·85	18	0·44	47	0·92	20	0·62	77	0·92	27	0·65
20	76	0·82	30	0·22	118	0·53	44	0·03	119	0·86	44	0·34
21	74	0·88	25	0·47	95	0·72	38	0·18	102	0·92	35	0·62
22	65	0·88	27	0·44	82	0·87	32	0·20	82	0·95	31	0·62
27	136	0·67	42	0·30	85	0·74	35	0·32	156	0·84	49	0·52
28	108	0·78	37	0·30	78	0·79	32	0·51	112	0·90	37	0·69
29	58	0·85	23	0·53	75	0·76	28	0·53	100	0·87	28	0·70
Nov. 3	74	0·69	26	0·53	117	0·42	44	−0·09	152	0·62	50	0·19
4	71	0·69	28	0·46	107	0·53	37	0·25	100	0·85	37	0·57
5	65	0·71	24	0·49	121	0·56	41	0·14	148	0·70	46	0·36
10	50	0·94	17	0·61	58	0·94	23	0·65	69	0·97	23	0·80
11	44	0·85	20	0·47	26	0·99	15	0·86	50	0·98	21	0·85
12	67	0·67	31	0·29	67	0·90	32	0·38	103	0·89	40	0·54
Mean correlations and root mean square errors (50 *cases*)												
	57	0·77	23	0·43	63	0·80	25	0·44	78	0·88	29	0·61

Column (*a*): Root mean square height errors; (*b*): Correlation between actual and persistence heights; (*c*): Root mean square vector wind errors; (*d*): Stretch vector correlation between actual and persistence winds

Printed in England under the authority of Her Majesty's Stationery Office
by James Townsend & Sons Ltd.

Wt. 2314-BM 4098 K 10

Published by
HER MAJESTY'S STATIONERY OFFICE

To be purchased from
York House, Kingsway, London W.C.2
423 Oxford Street, London W.1
13A Castle Street, Edinburgh 2
109 St. Mary Street, Cardiff
39 King Street, Manchester 2
50 Fairfax Street, Bristol 1
2 Edmund Street, Birmingham 3
80 Chichester Street, Belfast 1
or through any bookseller

Printed in England

S.O. Code No 40-164-5